Electronic Supplementary Material (ESI) for Organic & Biomolecular Chemistry.

Supplementary Information

Bactericidal urea crown ethers target phosphatidylethanolamine membrane lipids

Sarah R. Herschede,[a] Hassan Gneid,[a] Taylor Dent,[a] Ellen B. Jaeger,[a] Louise B. Lawson[b] and Nathalie Busschaert*[a]

[a] Department of Chemistry, Tulane University, New Orleans, Louisiana 70118, United States. Email: nbusschaert@tulane.edu
[b] Department of Microbiology and Immunology, Tulane University School of Medicine, New Orleans, Louisiana 70112, United States

Table of Contents

S1. General

Compound names are those generated by Chemdraw 16.0.1.4 following IUPAC nomenclature. Solvents, reagents and inorganic salt were purchased by Sigma Aldrich, TCI, or Alpha Aesar and used without further purification. Reactions were performed under an inert Ar atmosphere in oven-dried glassware. Flash column chromatography was carried out using SiliaFlash P60 (40-63 µm, 230-400 mesh). Thin-layer chromatography was carried out using silica gel TLC plates with fluorescent indicator, visualized under UV light (254 nm) or by staining with ninhydrin or permanganate solutions. ^{1}H NMR and ^{13}C NMR spectra were collected on a Bruker 500 MHz NMR, Varian Unity Inova 400 MHz or a Bruker Avance 300 MHz spectrometer. ^{13}C NMR spectra were collected proton decoupled. Mestrenova was used for NMR visualization. Chemical shifts (δ) are reported in parts per million (ppm) and calibrated to the residual solvent peak in $CDCl_3$ (δ = 7.26 (^{1}H) and 77.2 ppm (^{13}C)) or DMSO-d_6 (δ = 2.50 (^{1}H) and 39.5 ppm (^{13}C)). Coupling constants (*J*) are given in Hertz (Hz). The following abbreviations are used for spin multiplicity: s = singlet, d = doublet, h = heptet, m = multiplet, br. = broad. Infrared (IR) spectra were recorded on a Nexus 670 Avatar FTIR spectrometer; only selected maximum absorbances (ν_{max}) of the most intense peaks are reported (cm^{-1}). Low resolution electron spray ionization (ESI) mass spectra were recorded on a Bruker micrOTOF. Elemental analysis was conducted by *Midwest Laboratories, Inc*. The lipids POPE (1-palmitoyl-2-oleoyl-sn-glycero-3-phosphoethanolamine), POPC (1-palmitoyl-2-oleoyl-glycero-3-phosphocholine), DOPE (1,2-dioleoyl-sn-glycero-3-phosphoethanolamine), DOPC (1,2-dioleoyl-sn-glycero-3-phosphocholine), 18:1-6:0 NBD-PE (1-oleoyl-2-(6-((7-nitro-2-1,3-benzoxadiazol-4-yl)amino)hexanoyl)-sn-glycero-3-phosphoethanolamine) and 18:1-6:0 NBD-PC (1-oleoyl-2-(6-((7-nitro-2-1,3-benzoxadiazol-4-yl)amino)hexanoyl)-sn-glycero-3-phosphocholine) were purchased from *Avanti Polar Lipids, Inc*. Molecular modelling was performed using the Molecular Operating Environment (MOE) software version 2018.01. Fluorescence spectra and kinetic studies were performed on an Agilent Cary Eclipse fluorescence spectrophotometer equipped with stirring function and Peltier temperature controller. 3 mL macrocuvettes were used and all solutions were stirred using a cuvette stir bar (Sigma-Aldrich #Z363545). Bacterial growth curves and images were obtained using a BioTek Cytation 5 Cell Imaging Multi-Mode Reader.

S2. Synthesis and characterization

1-(2,3,5,6,8,9,11,12,14,15-decahydrobenzo[*b*][1,4,7,10,13,16]hexaoxacyclo-octadecin-18-yl)-3-(4-(trifluoromethyl)phenyl)urea (1a).

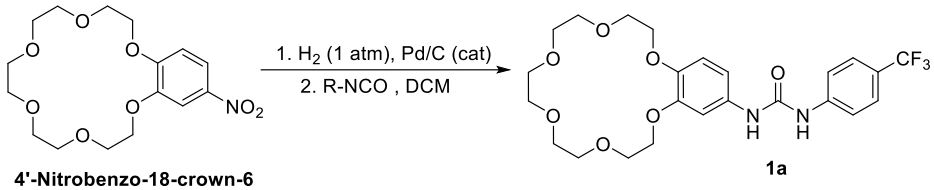

4'-Nitrobenzo-18-crown-6 (300 mg, 0.84 mmol, 1 eq) was dissolved in MeOH (5 mL) and a catalytic amount of Pd/C was added. The mixture was degassed, put under a hydrogen atmosphere (1 atm H_2) and allowed to stir for 12 h at room temperature. The solution was filtered over Celite to remove Pd/C, washed with MeOH and subsequently concentrated using a rotary evaporator. The resulting pale pink liquid which was dried overnight under high vacuum to remove all residual MeOH. To the obtained dried aniline was added DCM (5 mL) and 1-isocyanato-4-(trifluoromethyl)benzene (467 mg, 2.5 mmol, 3 eq) and the mixture was refluxed for 3 days under Ar atmosphere. The crude mixture was concentrated *in vacuo* and the obtained pale pink oil was subsequently purified by column chromatography (silica, solvent gradient of 0% to 10% MeOH in DCM) to yield **1a** as an off-white solid (410 mg, 0.796 mmol, 95% yield). ^{1}H NMR (300 MHz, $CDCl_3$, 298 K, ppm) δ 8.40 (br. s, 1H, N-*H*), 7.95 (br. s, 1H, N-*H*), 7.57 (d, *J* = 8.5 Hz, 2H, Ar-*H*), 7.46 (d, *J* = 8.5 Hz, 2H, Ar-*H*), 6.99 (d, *J* = 2.4 Hz, 1H, Ar-*H*), 6.71 (m, 1H, Ar-*H*), 6.57 (d, *J* = 8.6 Hz, 1H, Ar-*H*), 4.06 – 3.95 (m, 4H, 2xCH_2), 3.88 – 3.79 (m, 4H, 2xCH_2), 3.78 – 3.66 (m, 12H, 6xCH_2). ^{13}C NMR (101 MHz, $CDCl_3$, 298 K, ppm) δ 153.6, 148.5, 144.3, 142.8, 132.6, 126.1 (q, $^3J_{CF}$ = 3.9 Hz), 124.5 (q, $^1J_{CF}$ = 271.4 Hz), 123.8 (q, $^2J_{CF}$ = 32.6 Hz), 118.4, 113.8, 113.0, 106.7, 70.8, 70.7, 70.6, 70.5, 70.4 (presumable 2xC), 69.7, 69.5, 68.9, 68.2. IR (neat): *ν* (cm^{-1}) = 3317, 3295, 2911, 2875, 2875, 1648, 1603, 1554, 1514, 1409, 1329, 1242, 1236, 1183, 1130, 1110, 1108, 1070, 841. MS (ESI) *m/z* = 537 $[M+Na]^+$. Elemental analysis calcd for $C_{24}H_{29}F_3N_2O_7$: C 56.03, H 5.68, N 5.44, found: C 55.42, H 5.69, N 5.25.

1-(2-(1,4,7,10,13-pentaoxa-16-azacyclooctadecan-16-yl)-2-oxoethyl)-3-(4(trifluoromethyl)-phenyl)urea (1b).

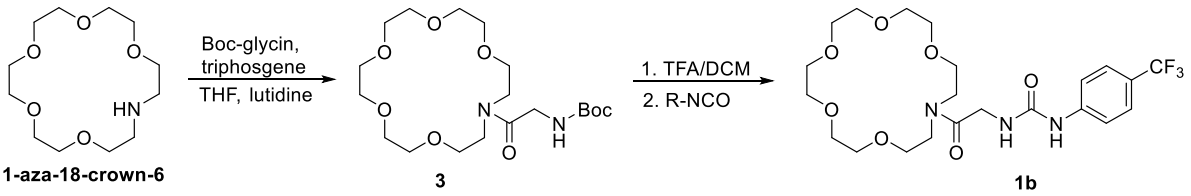

Boc-protected crown ether analog **3** was synthesized from **1-aza-18-crown-6** (170.9 mg, 0.65 mmol, 1 eq) according to a modified literature procedure.[1] The obtained Boc-protected intermediate **3** was dissolved in 30 mL 1:2 TFA:DCM and stirred at room temperature overnight. The reaction mixture was concentrated using a rotary evaporator to remove the solvents and left to dry under high vacuum for 24 hours. 1-isocyanato-4-(trifluoromethyl)benzene (0.3 mL, 2.1 mmol, 3.2 eq) was added to the Boc-deprotected oil in 95:5 DCM:pyridine (10 mL) and the resulting mixture was refluxed overnight. This crude mixture was concentrated *in vacuo* and the oily product was subsequently purified by column chromatography (silica, solvent gradient of 0% to 10% MeOH in DCM) to yield **1b** as a pale

yellow/brown oil (96.9 mg, 0.19 mmol, 29% yield) ^{1}H NMR (300 MHz, $CDCl_3$, 298 K, ppm) δ 8.74 (br. s, 1H, N-*H*), 7.42 (d, *J* = 8.5 Hz, 2H, Ar-*H*), 7.31 (d, *J* = 8.5 Hz, 2H, Ar-*H*), 6.86 (br. s, 1H, N-*H*), 4.19 (d, *J* = 4.7 Hz, 2H, CH_2), 3.77 – 3.54 (m, 24H, 12xCH_2).^{13}C NMR (101 MHz, $CDCl_3$, 298 K, ppm) δ 171.2, 156.1, 143.2, 125.8 (q, $^{3}J_{CF}$ = 3.4 Hz), 124.6 (q, $^{1}J_{CF}$ = 270.9 Hz), 123.3 (q, $^{2}J_{CF}$= 32.5 Hz), 118.1, 70.8 (2 peaks), 70.4, 70.2 (multiple C's), 70.1 (2 peaks), 69.7 (2 peaks), 48.7, 47.1, 42.1. IR (neat): *v* (cm^{-1}) = 3750,3628, 3301, 3009, 2868, 2360, 2341, 1652, 1557, 1324, 1216, 1112. MS (ESI) *m/z* = 530 [M+Na]$^{+}$. Elemental analysis calcd for $C_{22}H_{32}F_3N_3O_7$: C 52.07, H 6.36, N 8.28, found: C 51.83, H 6.26, N 8.10.

1-(3,4-dimethoxyphenyl)-3-(4-(trifluoromethyl)phenyl)urea (2a). 1-Isocyanato-4-(trifluoromethyl)benzene (150 µL, 1.0 mmol, 4.4 eq) and 2,4-(dimethoxy)aniline (36.6 mg, 0.24 mmol, 1 eq) were dissolved in DCM (3 mL) and the resulting mixture was stirred overnight. The resulting precipitate was filtered and washed with DCM to yield **2a** as a white solid (74.8 mg, 0.22 mmol, 92% yield). ^{1}H NMR (400 MHz, DMSO-d_6, 298 K, ppm) δ 9.02 (s, 1H, N-*H*), 8.64 (s, 1H, N-*H*), 7.70 – 7.58 (m, 4H, Ar-*H*), 7.21 (s, 1H, Ar-*H*), 6.92 – 6.85 (m, 2H, Ar-*H*), 3.74 (s, 3H, CH_3), 3.71 (s, 3H, CH_3). ^{13}C NMR (101 MHz, DMSO-d_6, 298 K, ppm) δ 152.4, 148.8, 144.3, 143.6, 133.8, 126.1 (q, $^{3}J_{CF}$ = 4.0 Hz), 124.6 (q, $^{1}J_{CF}$ = 270.7 Hz), 121.6 (q, $^{2}J_{CF}$ = 32.2 Hz), 117.8, 112.4, 110.5, 104.1, 55.8, 55.4. IR (neat): *v* (cm^{-1}) = 3321, 2935, 2857, 1705, 1650, 1512, 1322, 1122, 1158, 1021, 1068. MS (ESI) *m/z* = 341 [M+H]$^{+}$. Elemental analysis calcd for $C_{16}H_{15}F_3N_2O_3$: C 56.47, H 4.44, N 8.23, found: C 56.26, H 4.46, N 8.49.

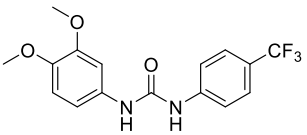

1-(2-ethylhexyl)-3-(4-(trifluoromethyl)phenyl)urea (2b). 4-(Trifluoromethyl)aniline (300 µL, 2.4 mmol, 1 eq) and 2-ethylhexyl isocyanate (1 mL, 5.7 mmol, 2.4 eq) were added to 10 mL DCM and refluxed for 3 days. The crude mixture was concentrated using a rotary evaporator and the obtained oil was subsequently purified by column chromatography (silica, 10% MeOH in DCM) to yield **2b** as a colourless oil (720 mg, 2.27 mmol, 95% yield). ^{1}H NMR (400 MHz, $CDCl_3$, 298 K, ppm) δ 7.76 (br. s, 1H, N-*H*), 7.45 (d, *J* = 8.6 Hz, 2H, Ar-*H*), 7.38 (d, *J* = 8.6 Hz, 2H, Ar-*H*), 5.57 (br. s, 1H, N-*H*), 3.25 – 3.06 (m, 2H, CH_2), 1.38 (h, *J* = 6.0 Hz, 1H, CH), 1.30 – 1.17 (m, 8H, 4xCH_2), 0.91 – 0.75 (m, 6H, 2xCH_3) .^{13}C NMR (101 MHz, $CDCl_3$, 298 K, ppm) δ 156.3, 142.4, 126.4 (q, $^{3}J_{CF}$ = 3.9 Hz), 124.7 (q, $^{2}J_{CF}$ = 32.8 Hz), 124.3 (q, $^{1}J_{CF}$ = 271.4 Hz), 118.8, 43.3, 39.7, 31.0, 29.0, 24.2, 23.1, 14.1, 10.9. IR (neat): *v* (cm^{-1}) = 3344, 2960, 2930, 1651, 1601, 1559, 1560, 1320, 1183, 1158, 1070, 1015, 839. MS (ESI) *m/z* = 317 [M+H]$^{+}$. Elemental analysis calcd for $C_{16}H_{23}F_3N_2O_7$: C 60.74, H 7.33, N 8.85, found: C 60.70, H 7.28, N 8.92.

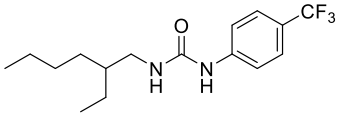

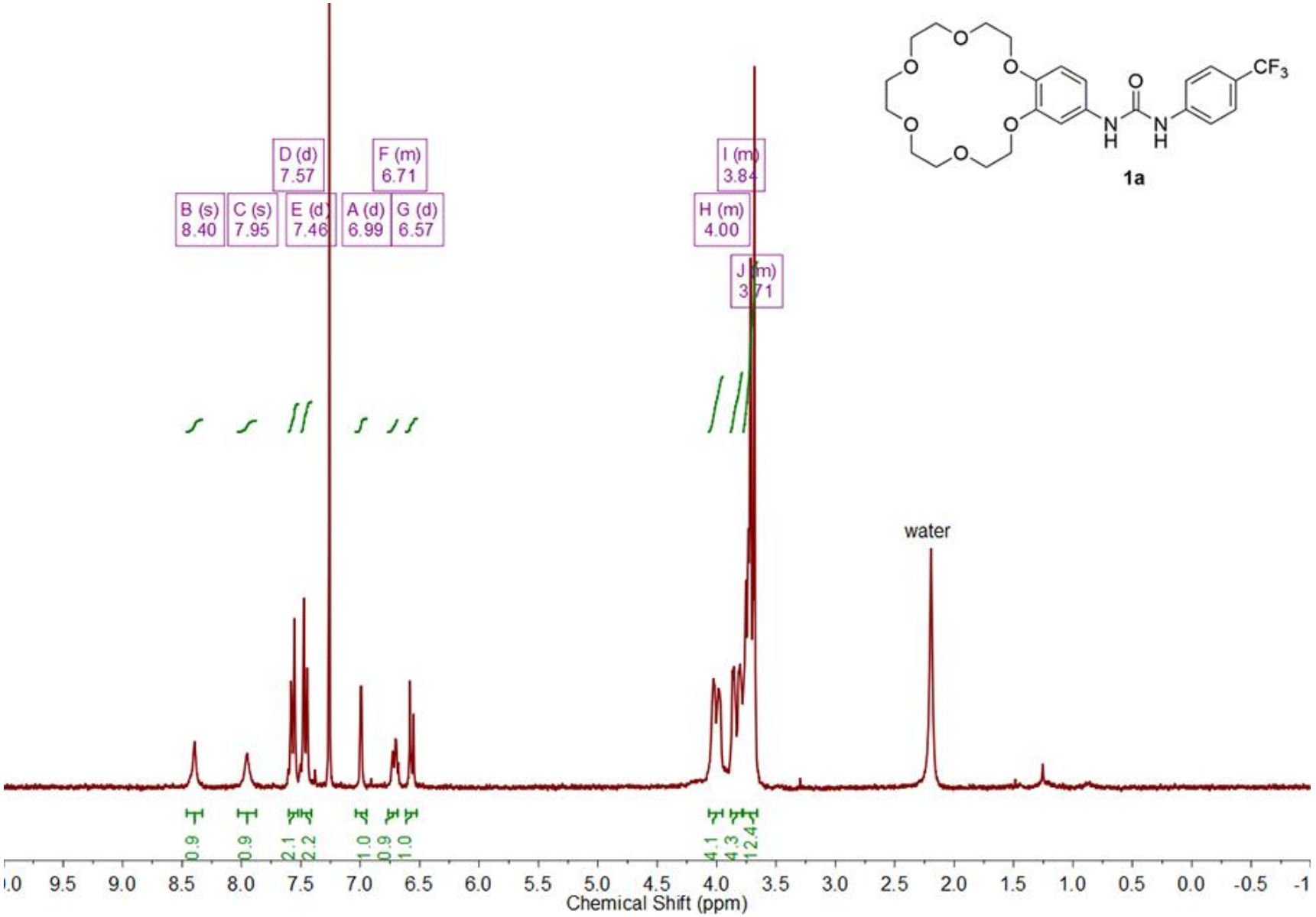

Figure S1. ^{1}H NMR (300 MHz) spectrum of compound **1a** in $CDCl_3$ at 298K.

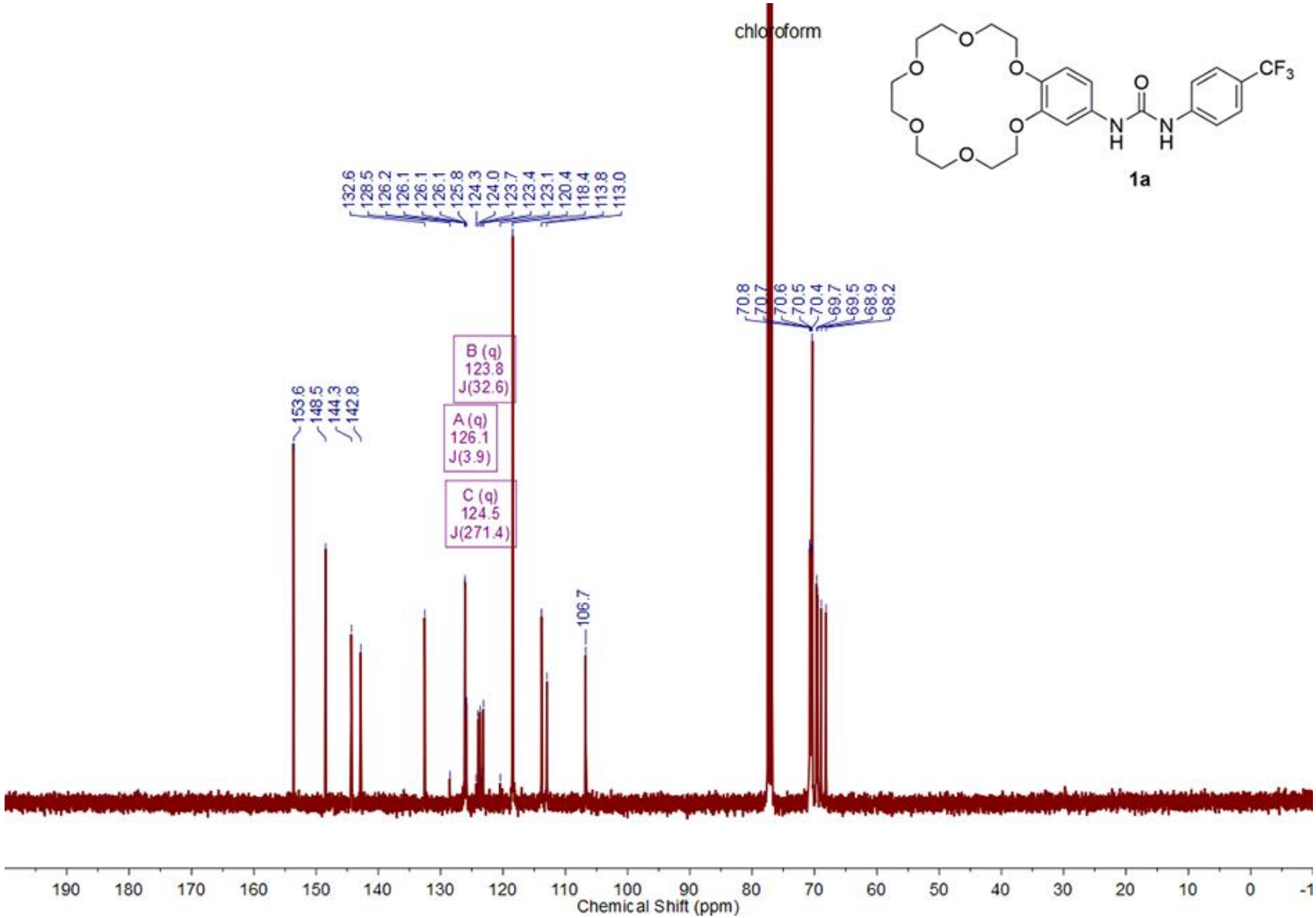

Figure S2. ^{13}C NMR (101 MHz) spectrum of compound **1a** in $CDCl_3$ at 298K.

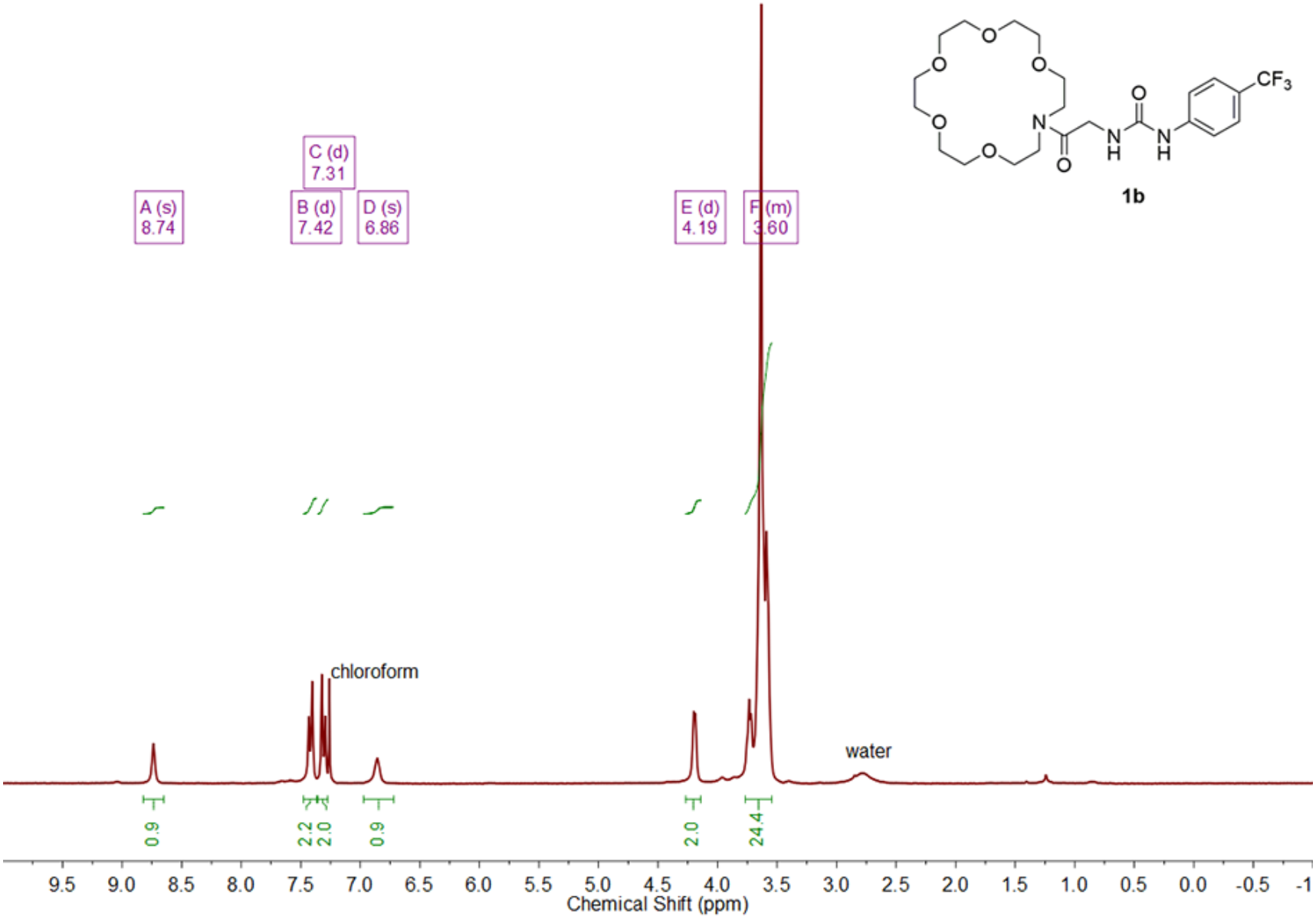

Figure S3. ^{1}H NMR (300 MHz) spectrum of compound **1b** in $CDCl_3$ at 298K.

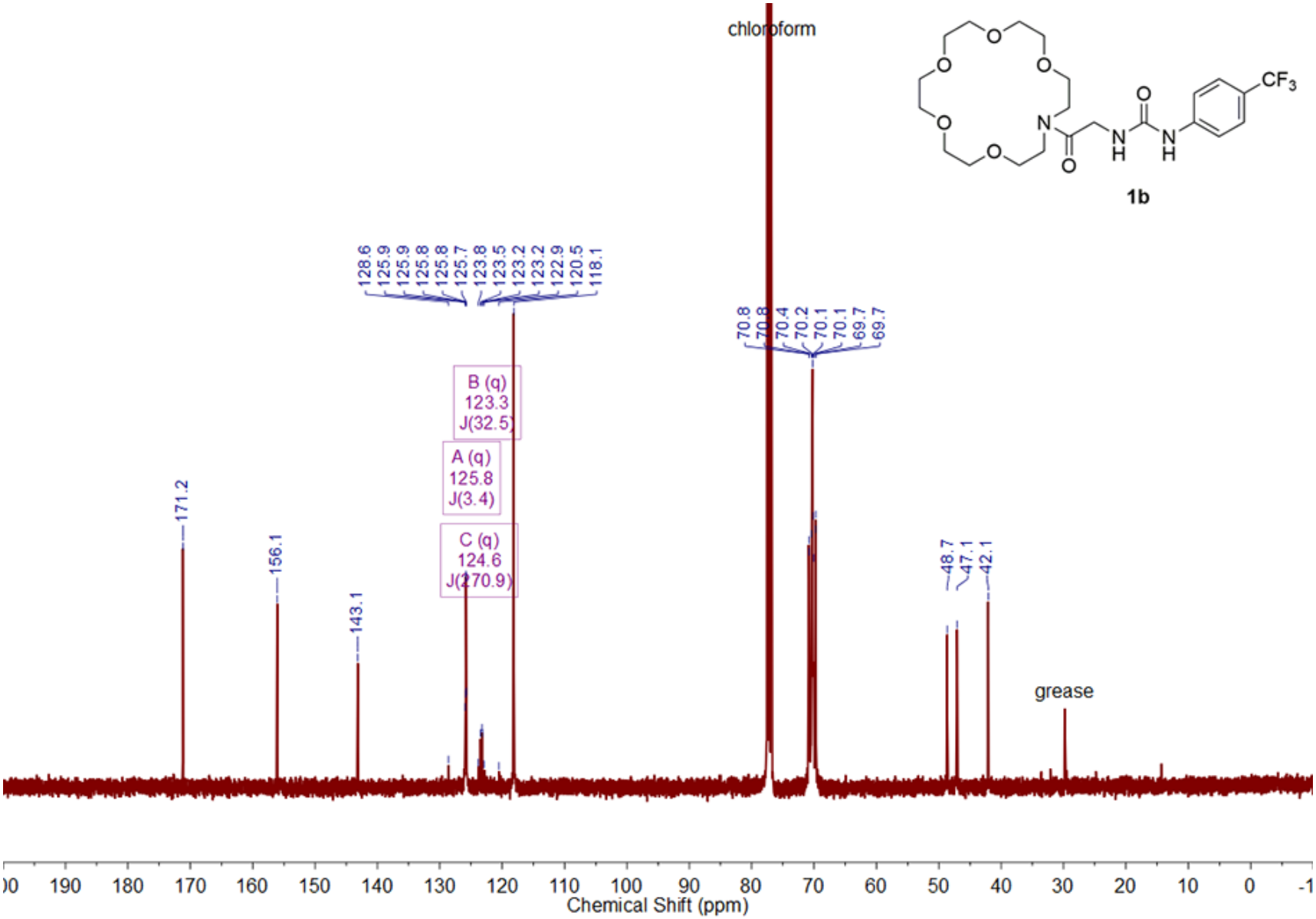

Figure S4. ^{13}C NMR (101 MHz) spectrum of compound **1b** in $CDCl_3$ at 298K.

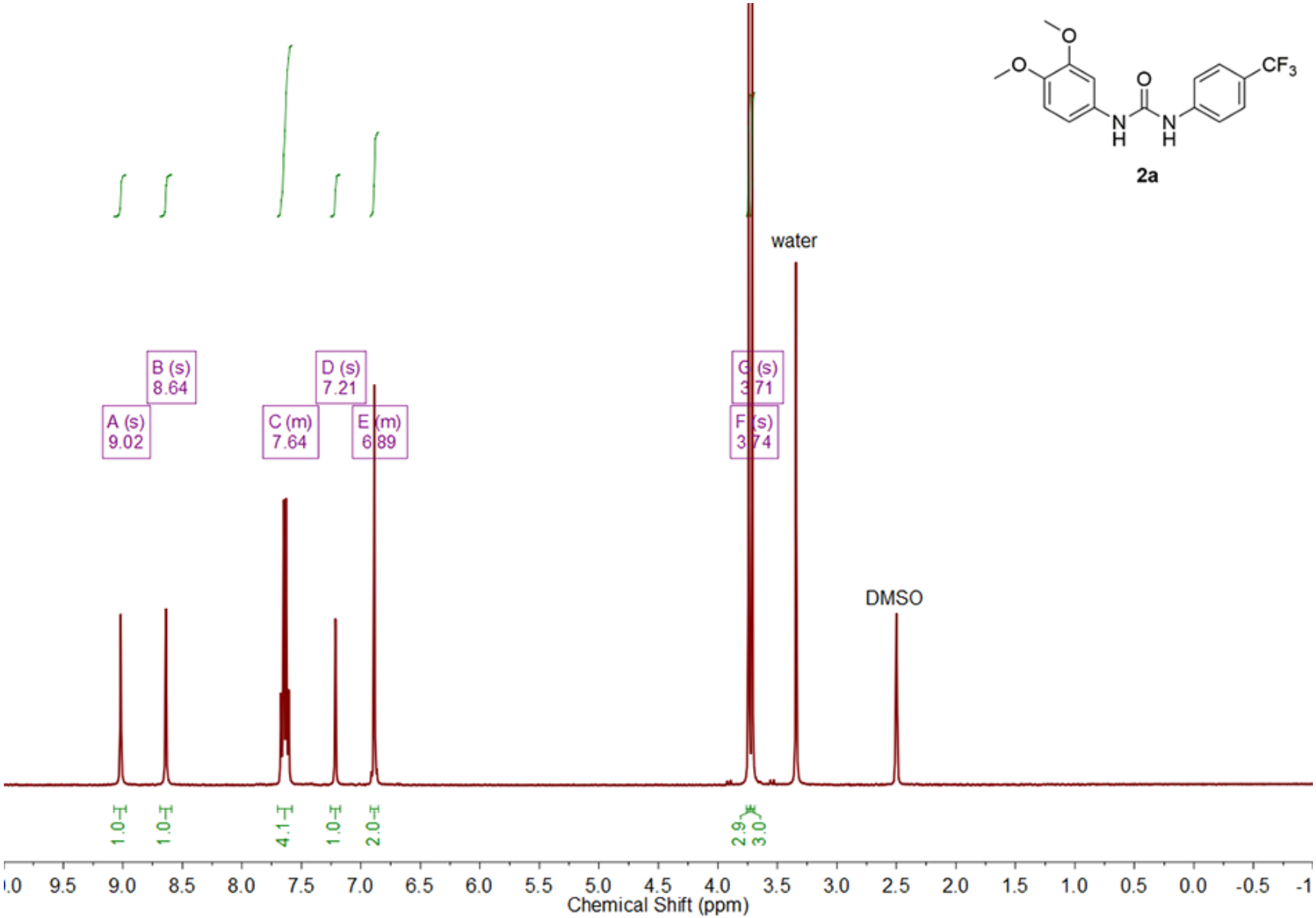

Figure S5. ^{1}H NMR (400 MHz) spectrum of compound **2a** in DMSO-d_6 at 298K.

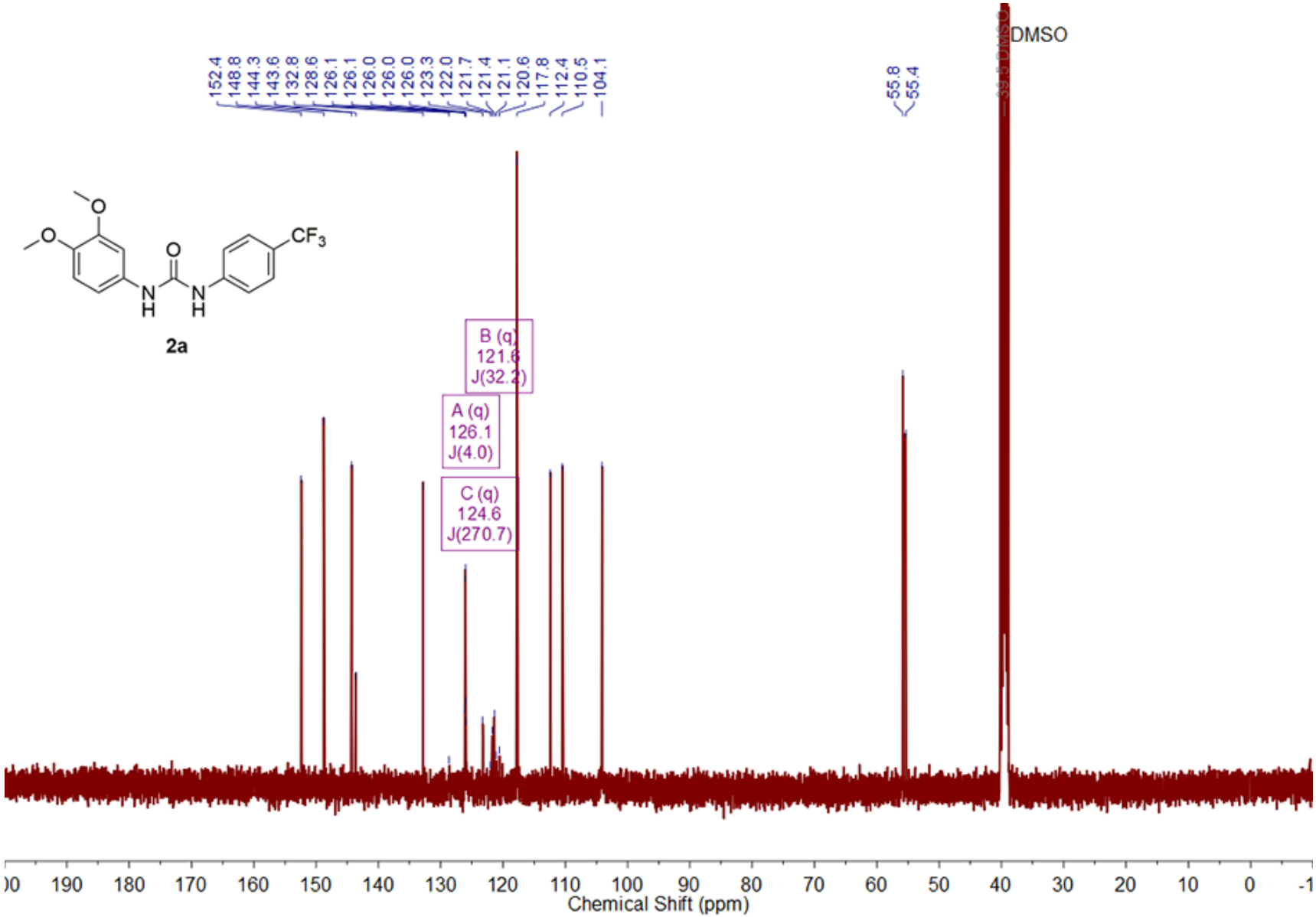

Figure S6. ^{13}C NMR (101 MHz) spectrum of compound 2**a** in DMSO-d_6 at 298K.

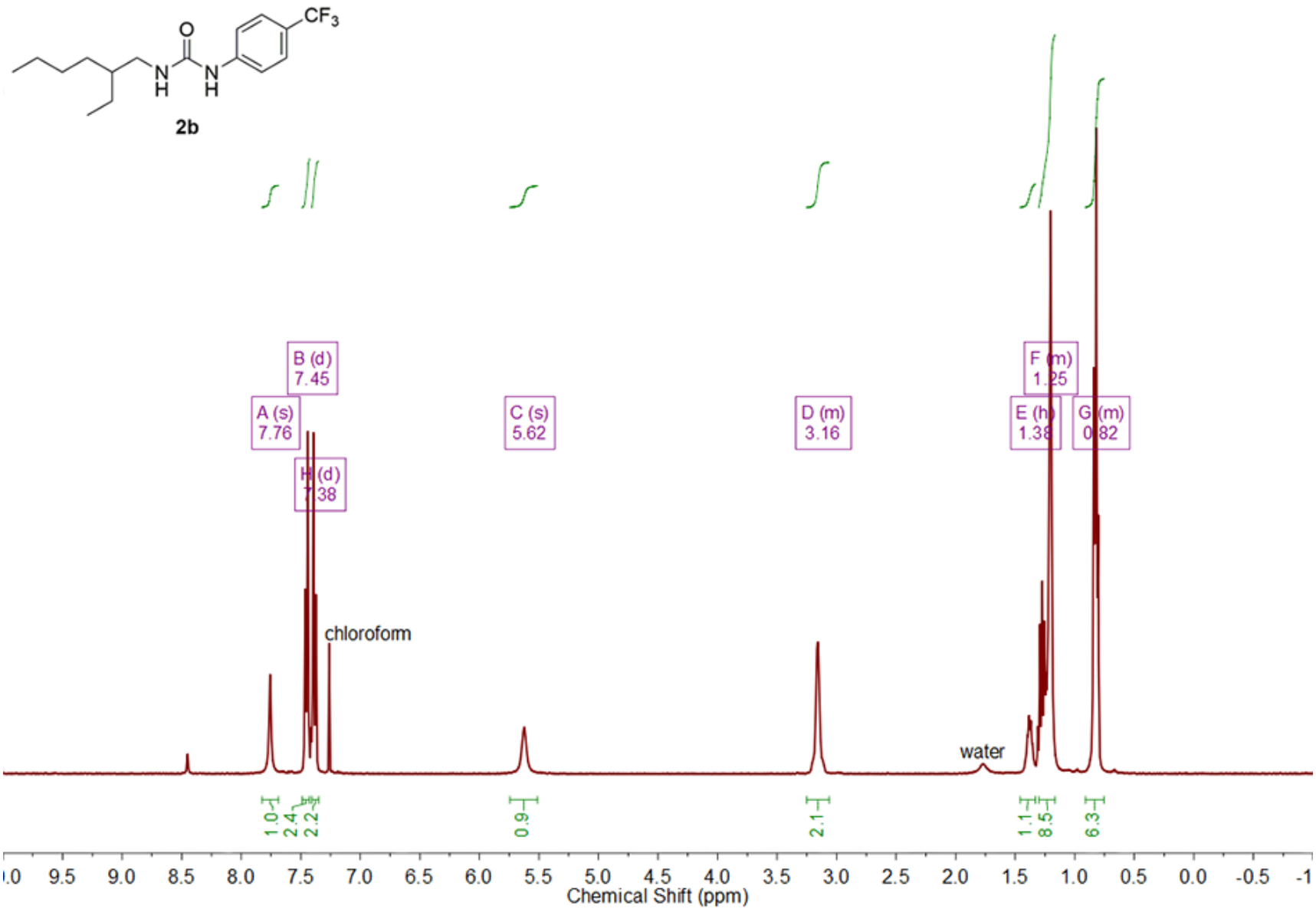

Figure S7. ^{1}H NMR spectrum of compound **2b** in $CDCl_3$ at 298K.

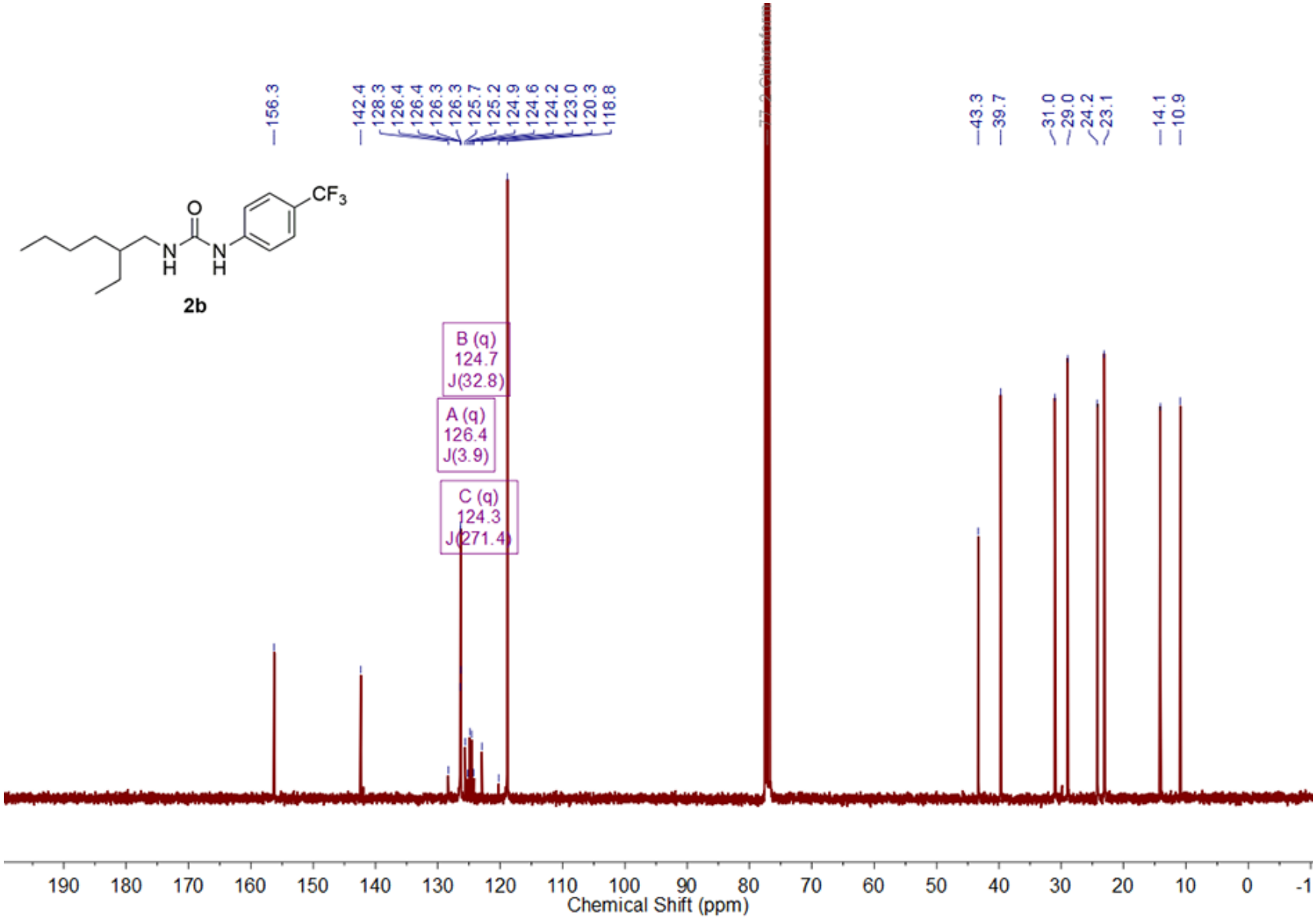

Figure S8. ^{13}C NMR spectrum of compound **2b** in $CDCl_3$ at 298K.

S3. ^{1}H NMR titrations in organic solvents

^{1}H NMR titrations were performed using a Bruker 500 MHz or Bruker 300 MHz instrument. A ternary mixture consisting of 0.5% Milli-Q H_2O, 24.5% DMSO-d_6 and 75% $CDCl_3$ was used to ensure adequate solubility of both the host and the guest in the same solvent system. Both host and guest were dried under high vacuum for 12 hours before each titration. Titrations were performed using a 5 mM solution of host as the starting point, to which aliquots of a solution containing 35 mM guest and 5 mM host were added using a Hamilton gas-tight syringe (this procedure ensures that the host concentration remains constant throughout the titration). The ^{1}H NMR spectrum was obtained upon each addition. The instrument was locked to DMSO, but data was referenced to $CDCl_3$ (δ = 7.26 ppm). In the case of the urea-containing compounds (**1a, 1b, 2a, 2b**), the ureas were used as the host and the lipids were used as guest. The downfield shift in the urea N-H peaks was determined using MestreNova, and these values were used to calculate association constants (K_a) using the online tool BindFit[2] assuming a 1:1 stoichiometry for binding. For the crown ether, the binding event could only be studied using the lipid (POPE) as the host and 18-crown-6 as the guest. In this case, the upfield shift of the POPE-NH_3^+ peak was determined using MestreNova, and these values were used to calculate association constants (K_a) using the online tool BindFit. All titrations were repeated a minimum of 3 times, and association constants are given as the average of these 3 repeats with errors representing standard deviations. Lipids purchased from *Avanti Polar Lipids, Inc* were used in powder form for all titrations: POPC (catalog# 850457) & POPE (catalog# 850757). The results are shown in **Figure S9 - Figure S18.**

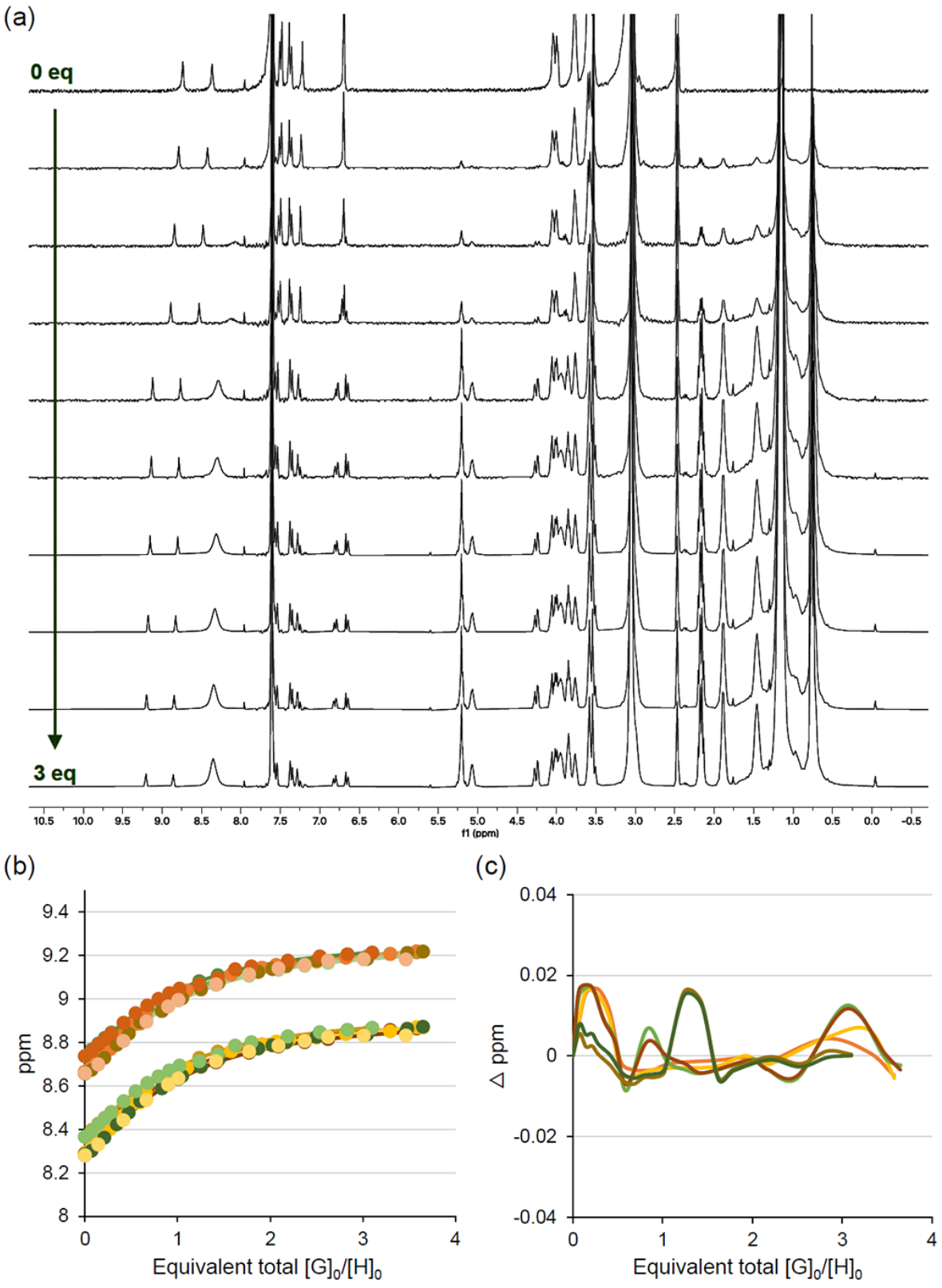

Figure S9. ^{1}H NMR titration of **1a** with POPE in 0.5% Milli-Q H_2O:24.5% DMSO-d_6:75% $CDCl_3$ at 298 K. (a) Stack plot of selected spectra of a representative titration. (b) Fitplot for the urea NHs at δ_A = 8.37 ppm and δ_B= 8.74 ppm using global analysis and 1:1 binding stoichiometry. Data from 3 independent repeats are overlaid. (c) Plot of the residuals for urea NHs at δ_A = 8.37 ppm and δ_B= 8.74 ppm using global analysis and 1:1 binding stoichiometry. Data from 3 independent repeats are overlaid.

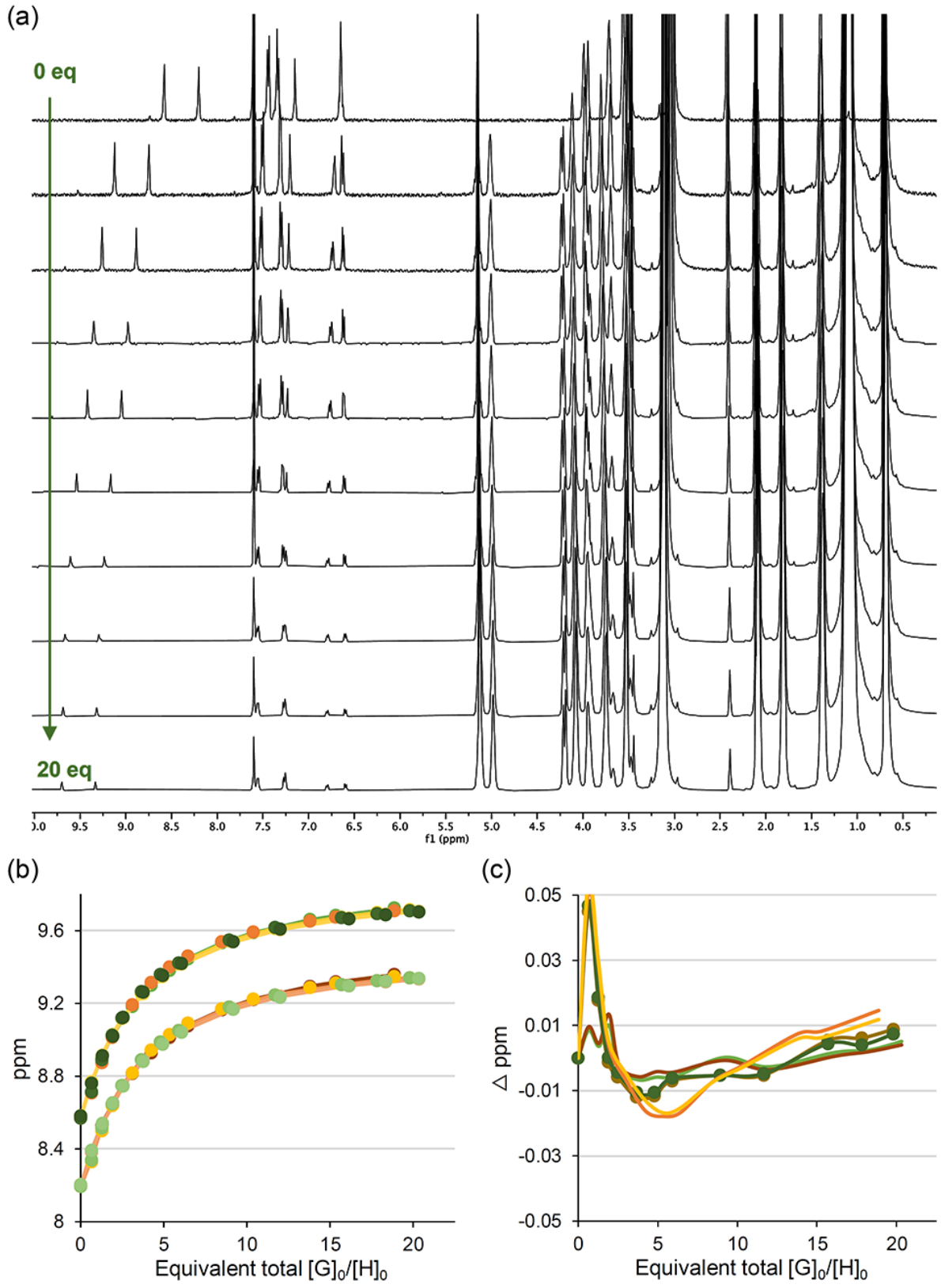

Figure S10. ^{1}H NMR titration of **1a** with POPC in 0.5% Milli-Q H_2O:24.5% DMSO-d_6:75% $CDCl_3$ at 298 K. (a) Stack plot of selected spectra of a representative titration. (b) Fitplot for the urea NHs at δ_A = 8.37 ppm and δ_B= 8.74 ppm using global analysis and 1:1 binding stoichiometry. Data from 3 independent repeats are overlaid. (c) Plot of the residuals for urea NHs at δ_A = 8.37 ppm and δ_B= 8.74 ppm using global analysis and 1:1 binding stoichiometry. Data from 3 independent repeats are overlaid.

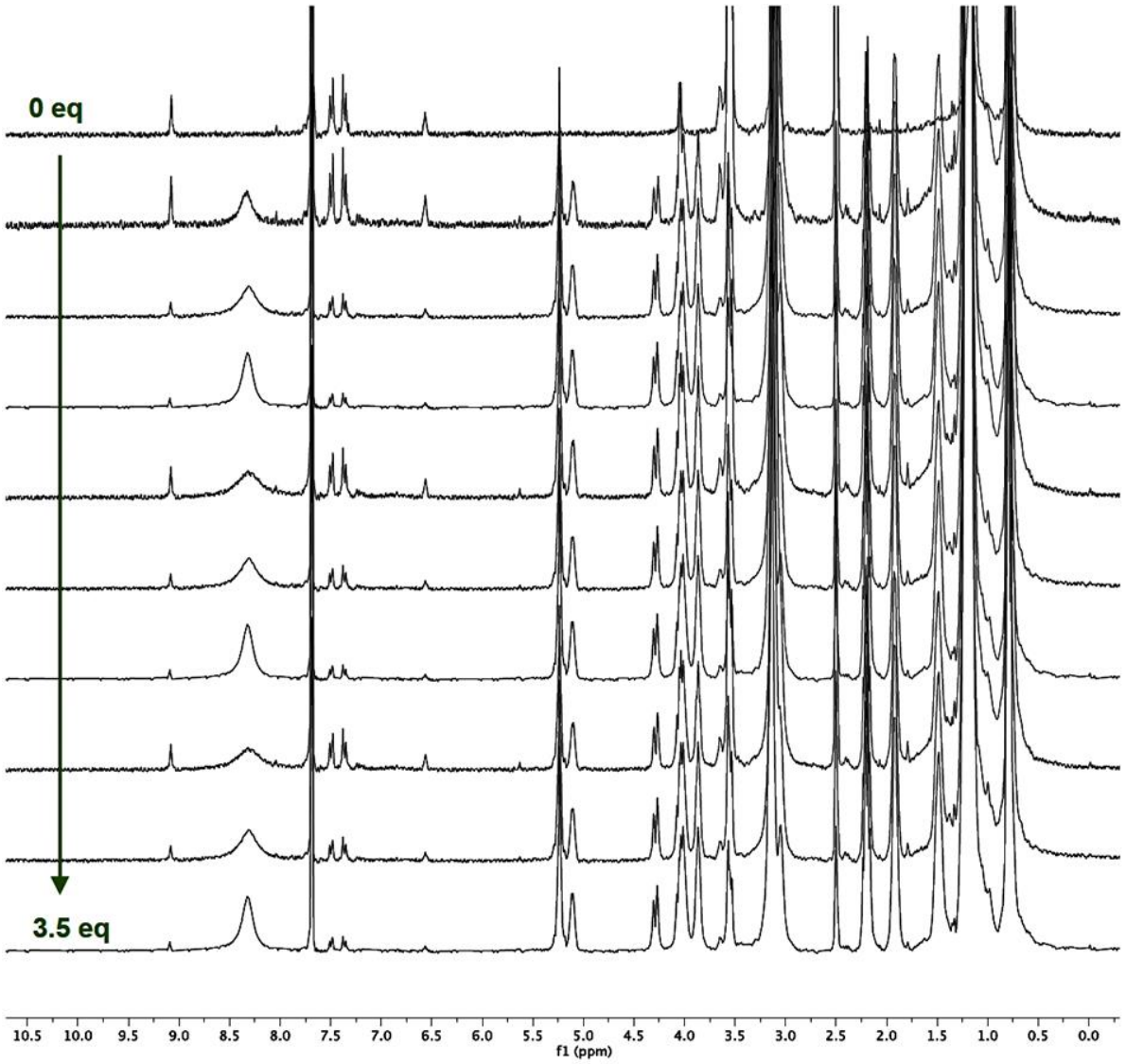

Figure S11. Stack plot of the ^{1}H NMR titration of **1b** with POPE in 0.5% Milli-Q H_2O:24.5% DMSO-d_6:75% $CDCl_3$ at 298 K. The change in chemical shift for the urea NHs is < 0.1 ppm, and we assume no binding event takes place (K_a < 10 M^{-1}).

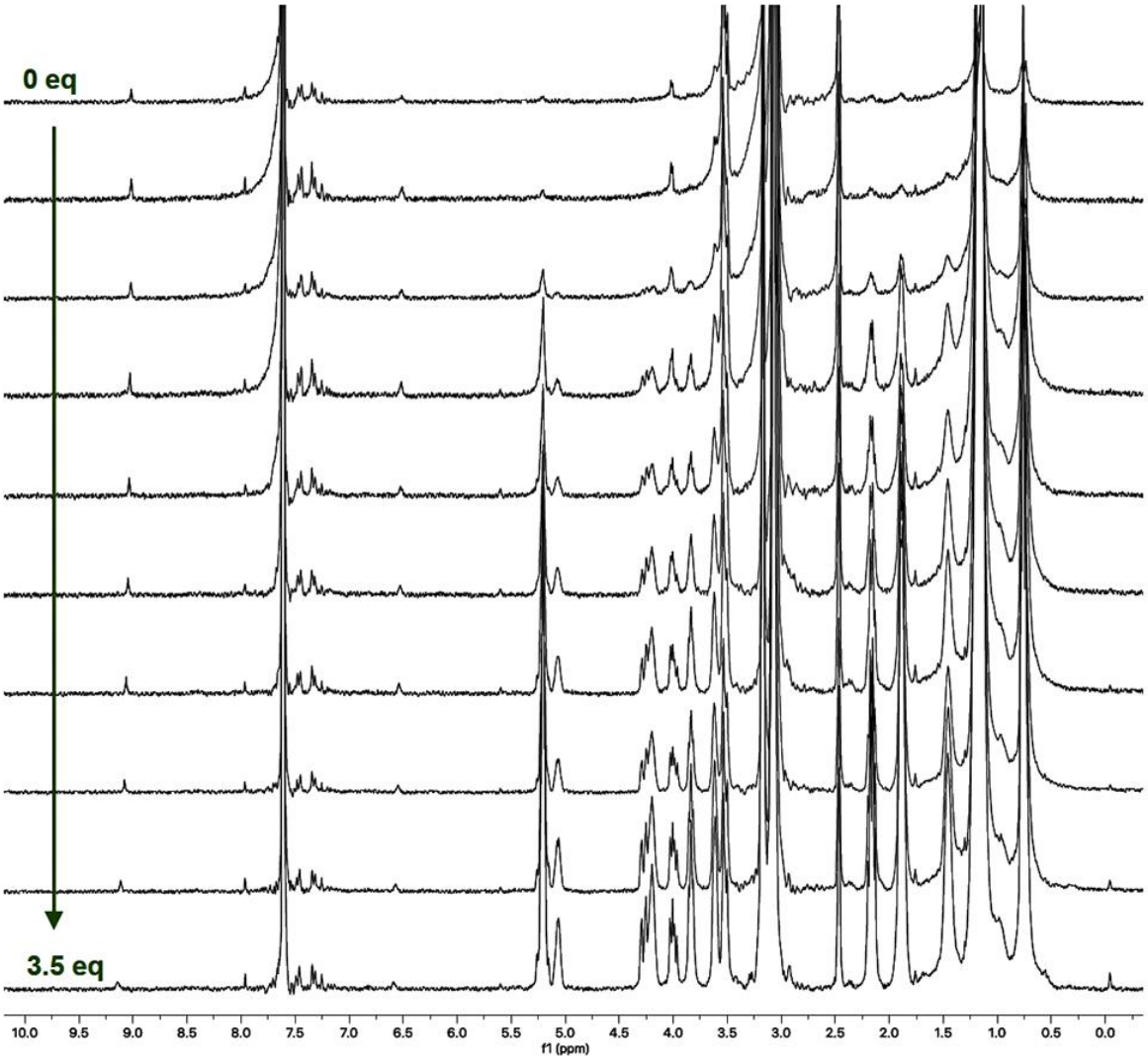

Figure S12. Stack plot of the ^{1}H NMR titration of **1b** with POPC in 0.5% Milli-Q H_2O:24.5% DMSO-d_6:75% $CDCl_3$ at 298 K. The change in chemical shift for the urea NHs is < 0.1 ppm, and we assume no binding event takes place (K_a < 10 M^{-1}).

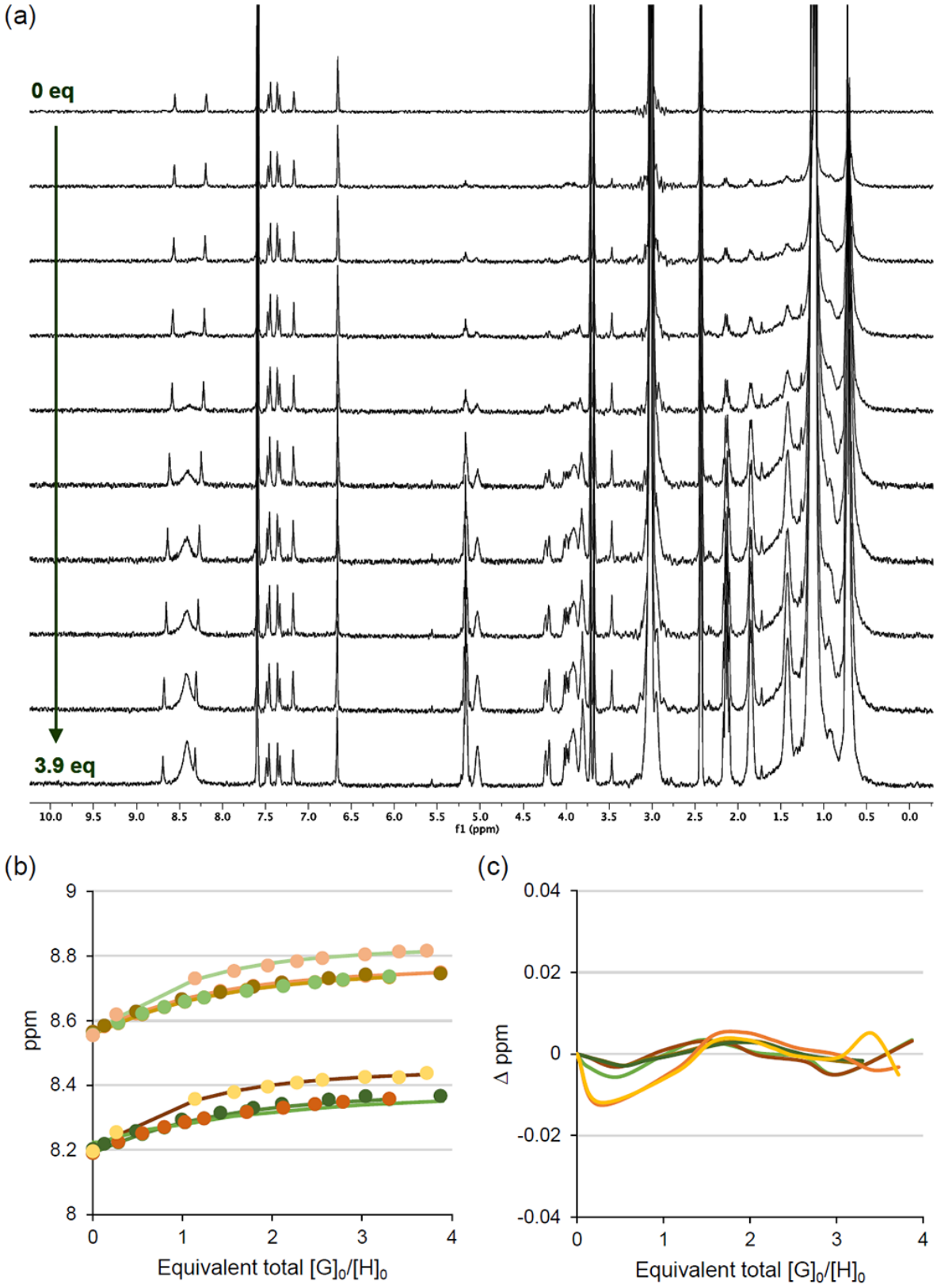

Figure S13. ^{1}H NMR titration of **2a** with POPE in 0.5% Milli-Q H_2O:24.5% DMSO-d_6:75% $CDCl_3$ at 298 K. (a) Stack plot of selected spectra of a representative titration. (b) Fitplot for the urea NHs at δ_A = 8.20 ppm and δ_B= 8.56 ppm using global analysis and 1:1 binding stoichiometry. Data from 3 independent repeats are overlaid. (c) Plot of the residuals for urea NHs at δ_A = 8.20 ppm and δ_B= 8.56 ppm using global analysis and 1:1 binding stoichiometry. Data from 3 independent repeats are overlaid.

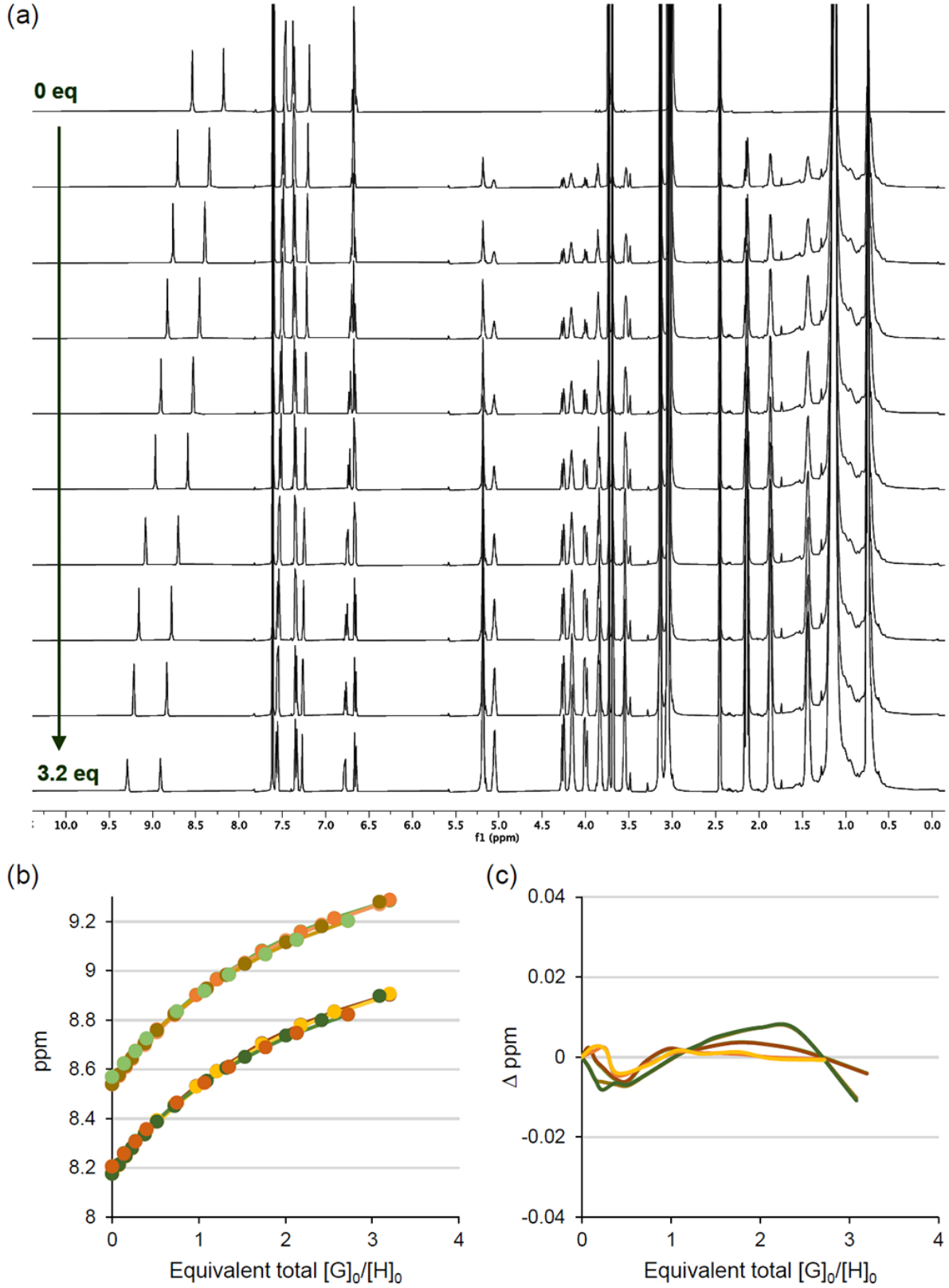

Figure S14. ^{1}H NMR titration of **2a** with POPC in 0.5% Milli-Q H_2O:24.5% DMSO-d_6:75% $CDCl_3$ at 298 K. (a) Stack plot of selected spectra of a representative titration. (b) Fitplot for the urea NHs at δ_A = 8.20 ppm and δ_B= 8.56 ppm using global analysis and 1:1 binding stoichiometry. Data from 3 independent repeats are overlaid. (c) Plot of the residuals for urea NHs at δ_A = 8.20 ppm and δ_B= 8.56 ppm using global analysis and 1:1 binding stoichiometry. Data from 3 independent repeats are overlaid.

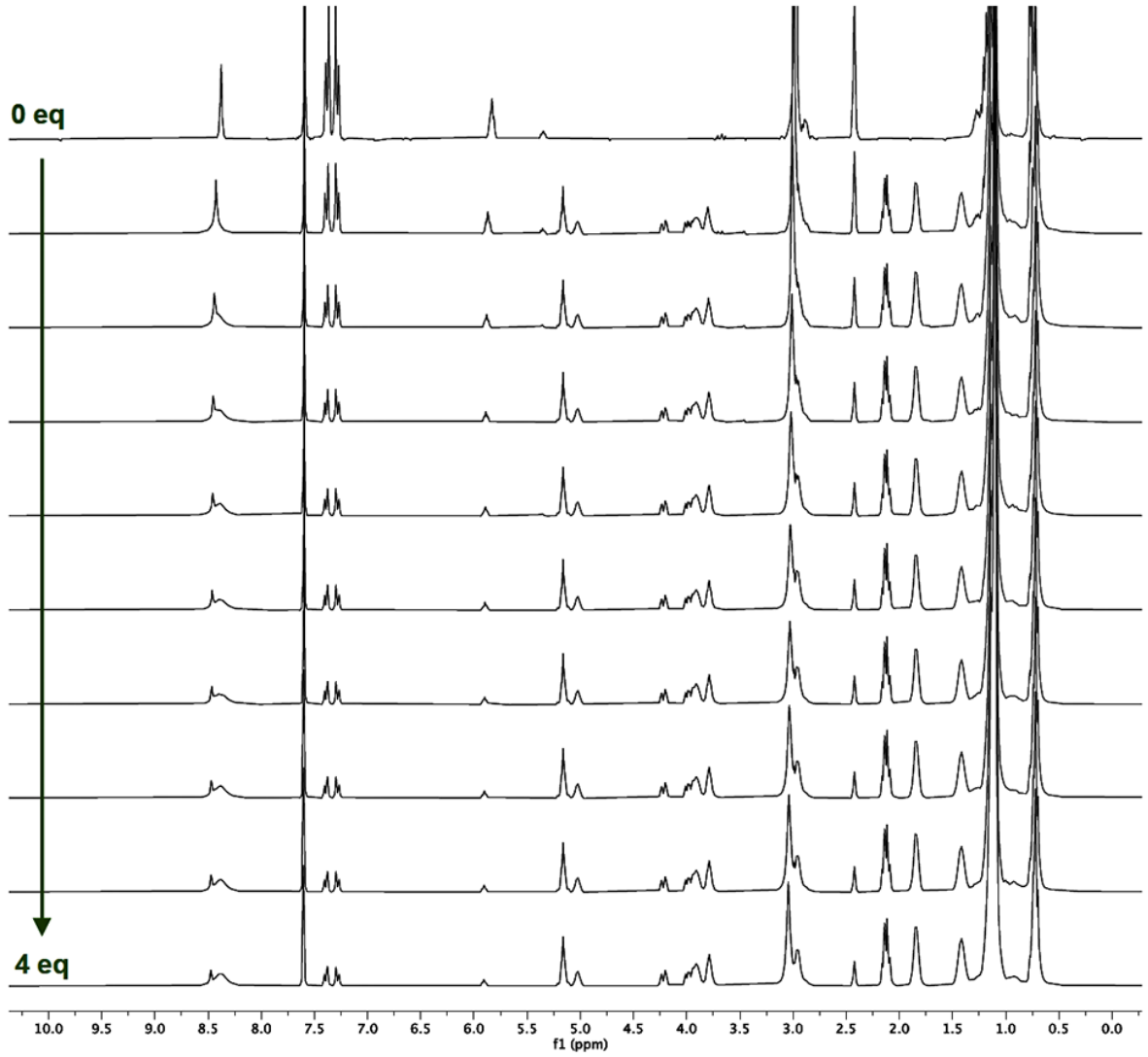

Figure S15. Stack plot of the ^{1}H NMR titration of **2b** with POPE in 0.5% Milli-Q H_2O:24.5% DMSO-d_6:75% $CDCl_3$ at 298 K. The change in chemical shift for the urea NHs is < 0.1 ppm, and we assume no binding event takes place (K_a < 10 M^{-1}).

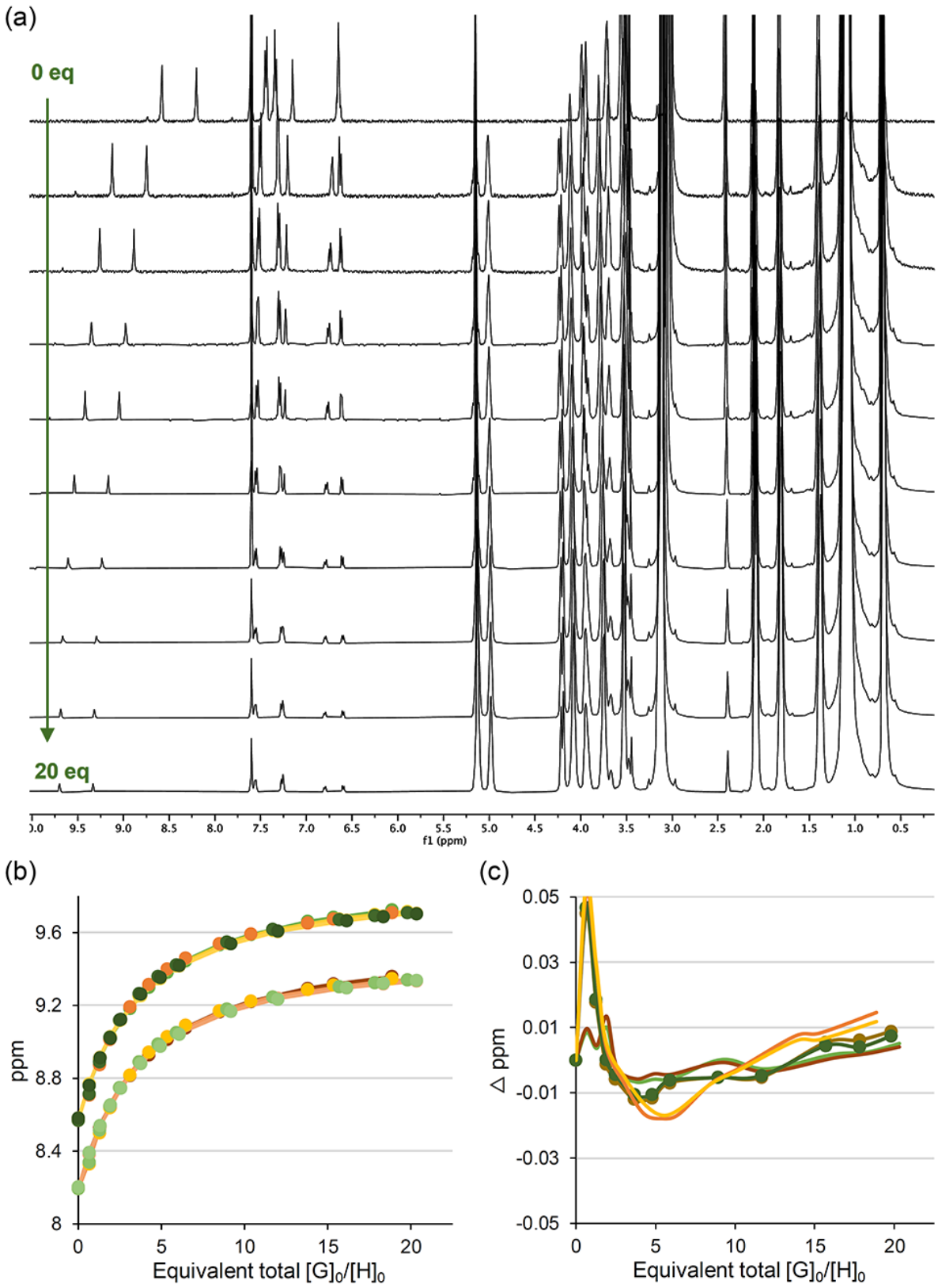

Figure S16. ^{1}H NMR titration of **2b** with POPC in 0.5% Milli-Q H_2O:24.5% DMSO-d_6:75% $CDCl_3$ at 298 K. (a) Stack plot of selected spectra of a representative titration. (b) Fitplot for the urea NHs at δ_A = 5.90 ppm and δ_B= 8.48 ppm using global analysis and 1:1 binding stoichiometry. Data from 3 independent repeats are overlaid. (c) Plot of the residuals for urea NHs at δ_A = 5.90 ppm and δ_B= 8.48 ppm using global analysis and 1:1 binding stoichiometry. Data from 3 independent repeats are overlaid.

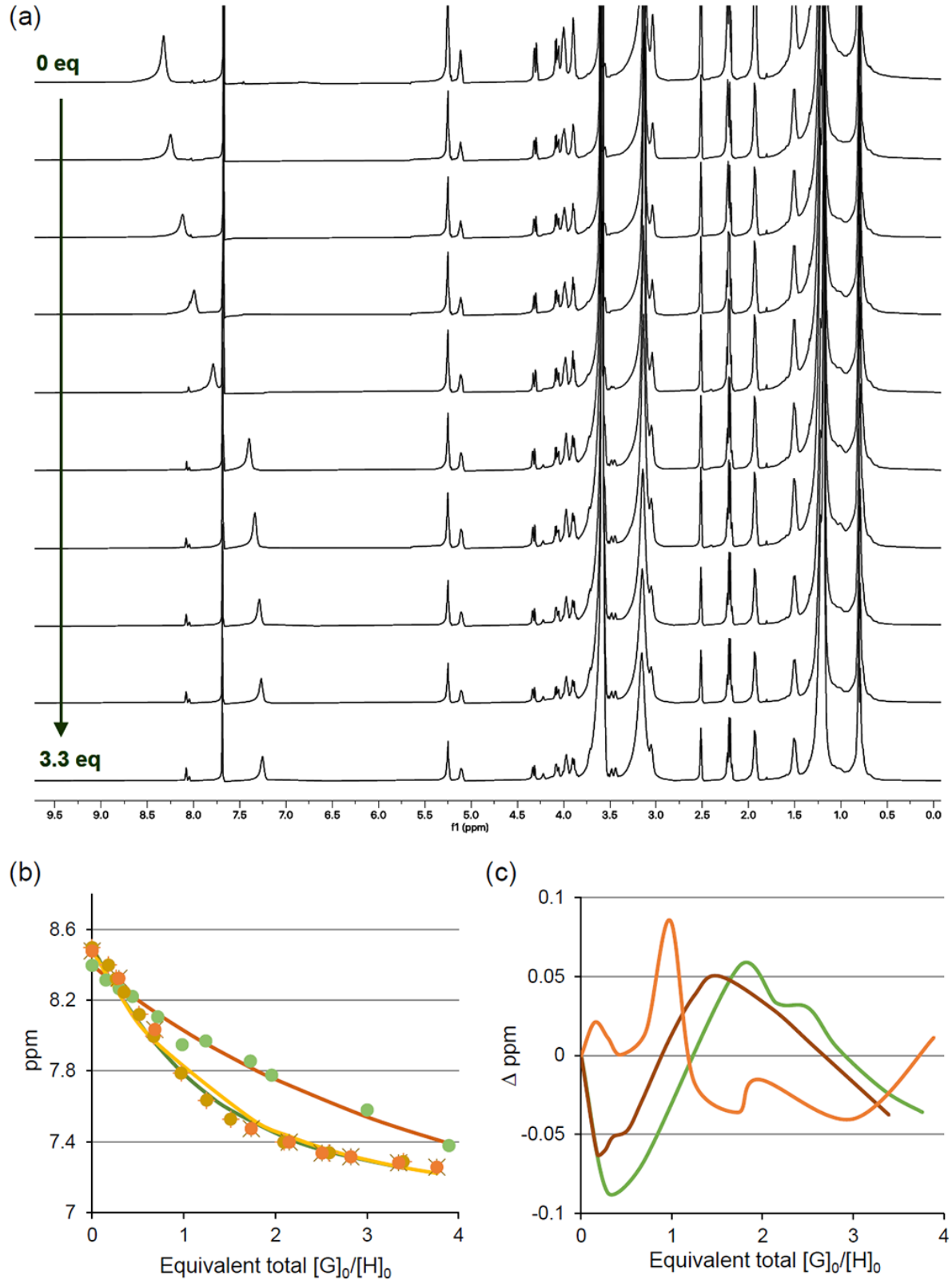

Figure S17. ^{1}H NMR titration of POPE with **18-crown-6** in 0.5% Milli-Q H_2O:24.5% DMSO-d_6:75% $CDCl_3$ at 298 K. (a) Stack plot of selected spectra of a representative titration. (b) Fitplot for the ammonium group of POPE at δ_A = 8.40 ppm using 1:1 binding stoichiometry. Data from 3 independent repeats are overlaid. (c) Plot of the residuals for the ammonium group of POPE at δ_A = 8.40 ppm. Data from 3 independent repeats are overlaid.

S4. Computational modelling

To explain why compound **1b** cannot bind to the headgroups of POPE and POPC, we determined the most stable conformation of **1a** and **1b** using computational modelling. All computer modelling was performed using Molecular Operating Environment™ version 2018:01 (MOE) and conformational analysis employed an MMFF94x force field with an implicit 75:25 chloroform:DMSO solvent model to mimic the conditions used during the ^{1}H NMR titrations (generalized Born solvation model, dielectric constant exterior 15.28 (4.81 for chloroform and 46.7 for DMSO, so approximately 0.75*4.81+0.25*46.7=15.28)). Structures were first generally energy minimized, followed by a LowModeMD conformational search of various possible low-energy conformers (Rejection Limit: 100, Iteration Limit: 10,000, RMS Gradient: 0.005, MM Iteration Limit: 500, RMSD Limit: 0.25, Energy Window: 7, Conformation Limit: 10,000, enforce chair conformation and do not allow amide bond rotation). The lowest energy conforms for **1a** and **1b** are shown in **Figure S18**. It is clear that the flexible linker in **1b** allows the formation of intramolecular hydrogen bonds between the crown ether and urea moieties. This conformation prevents binding to lipid headgroups, as the intramolecular hydrogen bonds compete with hydrogen bonding to the headgroups of the lipids.

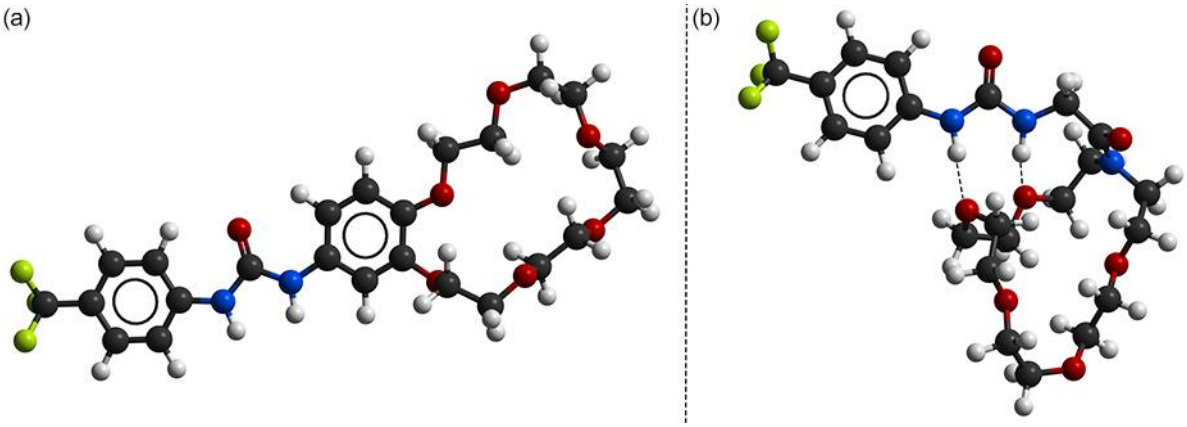

Figure S18. Lowest energy conformation of (a) compound **1a**, and (b) compound **1b** obtained using the Molecular Operating Environment software (MMFF94x force field, Born solvation model).

S5. Fluorescence titrations with POPC and POPE

To determine the interaction between the hosts and PE lipids that are part of a bilayer (membrane), we performed fluorescence titrations whereby aliquots of the hosts in DMSO were added to an aqueous solution of 100 nm large unilamellar vesicles (LUVs) containing NBD-labelled lipids (*Avanti Polar Lipids*, #810130 for NBD-PE and # 810153 for NBD-PC). Due to the inability of pure POPE to form stable liposomes, a mixture of 1:1 POPE:POPC was used. The titrations were thus performed with either 100 nm POPC LUVs containing 1 mol% NBD-PC, or 100 nm 1:1 POPE:POPC LUVs containing 1 mol% NBD-PE.

To prepare the LUVs, the unlabeled lipids were weighed out in a small (25 mL) round bottom flask, and 1 mol% NBD-labelled lipid was added from a 1 mg/mL stock in chloroform (mol% with respect to total unlabeled lipid). The lipids were subsequently dissolved in chloroform to generate a homogenous mixture. The chloroform was removed via a rotary evaporator and the lipid mixture was further dried overnight under high vacuum. The lipid film was hydrated with Tris buffer (10 mM Tris, 150 mM NaCl, pH 7.4) and vortexed until all lipid was in suspension. The resulting suspension was subjected to 11 freeze-thaw cycles, alternating between submersion in liquid nitrogen followed by thawing in mildly warm water. The lipid suspension was allowed to rest at room temperature for 30 minutes before extruding 35 times through a 100 nm polycarbonate membrane (*Nucleopore*) using the Avanti mini extruder set (*Avanti Polar Lipids, Inc*.).

For each titration, the lipid stock solution was diluted with Tris buffer to obtain 2.5 mL of a 25 µM lipid solution in a fluorescence cuvette. The emission spectrum was measured using an Agilent Cary Eclipse fluorescence spectrophotometer (excitation wavelength = 470 nm). Aliquots of the hosts in DMSO (10 mM stock) were added and the emission spectrum was obtained upon each addition. A cuvette stir bar was added to achieve adequate mixing upon each addition. The final addition corresponded to 105-120 µM hosts and a total volume of 25-30 µL DMSO. A control experiment where the same volume of neat DMSO was added was also performed. Fluorescence intensity was normalized by dividing the fluorescence intensity at every wavelength by the fluorescence intensity at 530 nm prior to the addition of compound (maximum fluorescence).

Where there was a significant change in fluorescence intensity, a Stern-Volmer analysis was performed. F_0/F values, whereby F_0 is the intensity at 530 nm before the addition of host and F is the intensity at 530 nm upon each addition, were plotted against the concentration of host and a linear fit was performed using OriginPro 2018. It was found that the data was only linear for the interaction of lipids with compound **1a**. Compounds **1b** and **18-crown-6** showed only a small change in fluorescence that was comparable to the addition of DMSO alone, and the change was not linearly correlated with concentration. Compounds **2a** and **2b** crashed out of solution immediately and could therefore not be analyzed accurately. The results are shown in **Figure S19** - **Figure S25**. The titrations were repeated a minimum of 3 times (independent repeats), and the Stern-Volmer constant was calculated for each repeat and subsequently averaged.

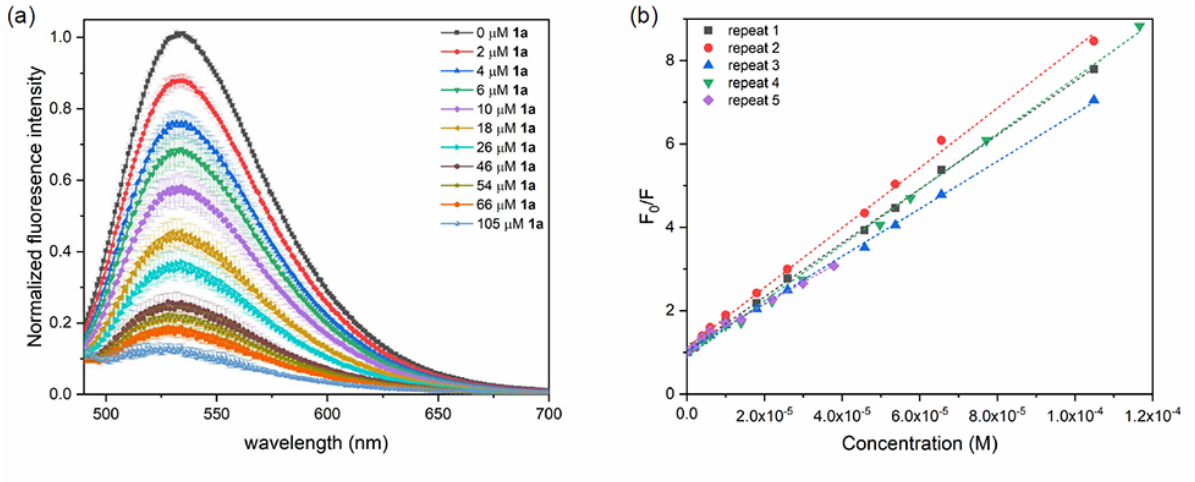

(c)

Plot	Repeat 1	Repeat 2	Repeat 3	Repeat 4	Repeat 5
Intercept	1.03815 ± 0.02487	1.11656 ± 0.05272	1.02743 ± 0.02242	0.90689 ± 0.05096	1.10197 ± 0.03456
Slope	64651.86507	71807.44395	56965.75224	66709.412	52619.40468
Slope error	563.48398	1194.426	507.90632	1072.74673	1843.95668
Residual Sum of Squares	0.03195	0.14355	0.02596	0.16653	0.03346
Pearson's r	0.99966	0.99876	0.99964	0.99871	0.99573
R-Square (COD)	0.99932	0.99752	0.99929	0.99742	0.99148
Adj. R-Square	0.99924	0.99724	0.99921	0.99716	0.99026

Figure S19. Fluorescence titration of **1a** (10 mM stock in DMSO) into a solution of 100 nm LUVs (1:1 POPC:POPE liposomes containing 1 mol% NBD-PE). Excitation wavelength = 470 nm. (a) Normalized fluorescence spectra, average of at least 2 repeats. (b) Stern-Volmer plots for all individual repeats. (c) Results of the linear fit of the Stern-Volmer plots. The slope corresponds to the Stern-Volmer constant K_{SV}.

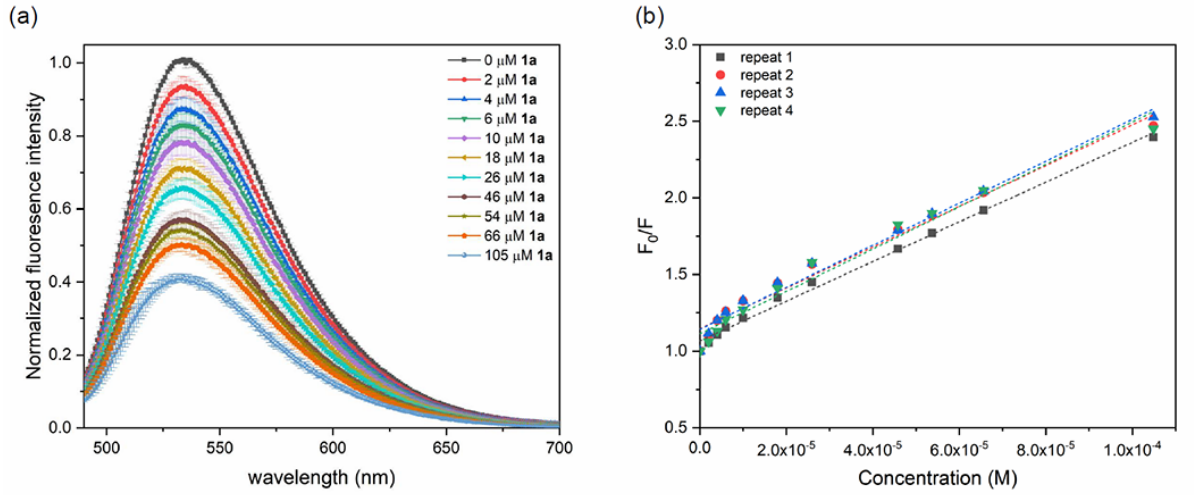

(c)

Plot	Repeat 1	Repeat 2	Repeat 3	Repeat 4
Intercept	1.06594 ± 0.01545	1.14593 ± 0.02991	1.14249 ± 0.0275	1.11287 ± 0.03304
Slope	12959.93317	13305.88363	13699.42182	13817.41219
Slope error	349.97592	677.62794	623.09847	48.42826
Residual Sum of Squares	0.01232	0.0462	0.03906	0.05636
Pearson's r	0.99673	0.98853	0.99082	0.98705
R-Square (COD)	0.99348	0.97719	0.98172	0.97427
Adj. R-Square	0.99276	0.97466	0.97969	0.97142

Figure S20. Fluorescence titration of **1a** (10 mM stock in DMSO) into a solution of 100 nm LUVs (POPC liposomes containing 1 mol% NBD-PC). Excitation wavelength = 470 nm. (a) Normalized fluorescence spectra, average of at least 2 repeats. (b) Stern-Volmer plots for all individual repeats. (c) Results of the linear fit of the Stern-Volmer plots. The slope corresponds to the Stern-Volmer constant K_{SV}.

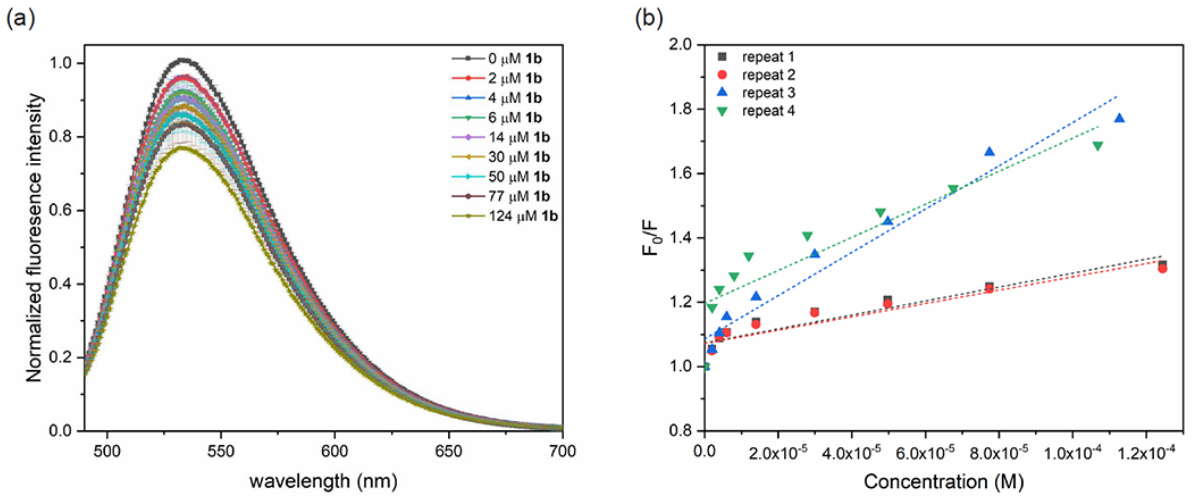

Figure S21. Fluorescence titration of **1b** (10 mM stock in DMSO) into a solution of 100 nm LUVs (1:1 POPC:POPE liposomes containing 1 mol% NBD-PE). Excitation wavelength = 470 nm. (a) Normalized fluorescence spectra, average of at least 2 repeats. (b) Stern-Volmer plots for all individual repeats. Linear fit resulted in R^2 values < 0.75 (no linear correlation).

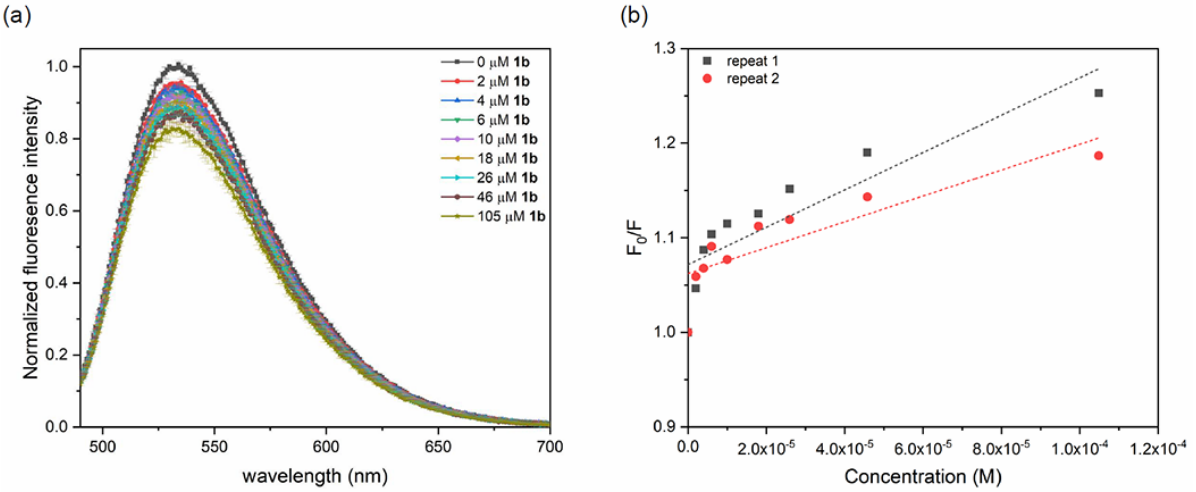

Figure S22. Fluorescence titration of **1b** (10 mM stock in DMSO) into a solution of 100 nm LUVs (POPC liposomes containing 1 mol% NBD-PC). Excitation wavelength = 470 nm. (a) Normalized fluorescence spectra, average of at least 2 repeats. (b) Stern-Volmer plots for all individual repeats. Linear fit resulted in R^2 values < 0.75 (no linear correlation).

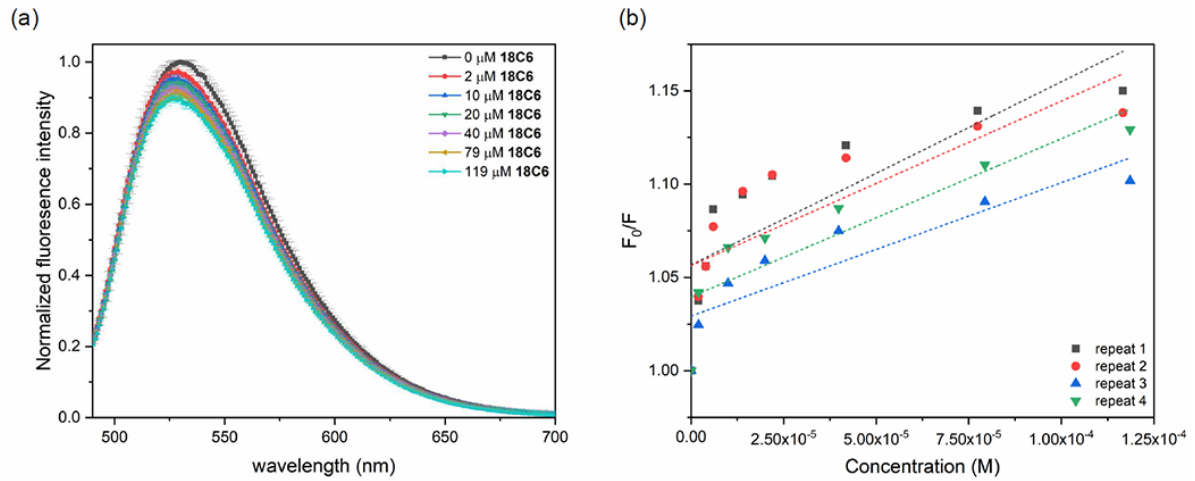

Figure S23. Fluorescence titration of **18-crown-6** (10 mM stock in DMSO) into a solution of 100 nm LUVs (1:1 POPC:POPE liposomes containing 1 mol% NBD-PE). Excitation wavelength = 470 nm. (a) Normalized fluorescence spectra, average of at least 2 repeats. (b) Stern-Volmer plots for all individual repeats. Linear fit resulted in R^2 values < 0.75 (no linear correlation).

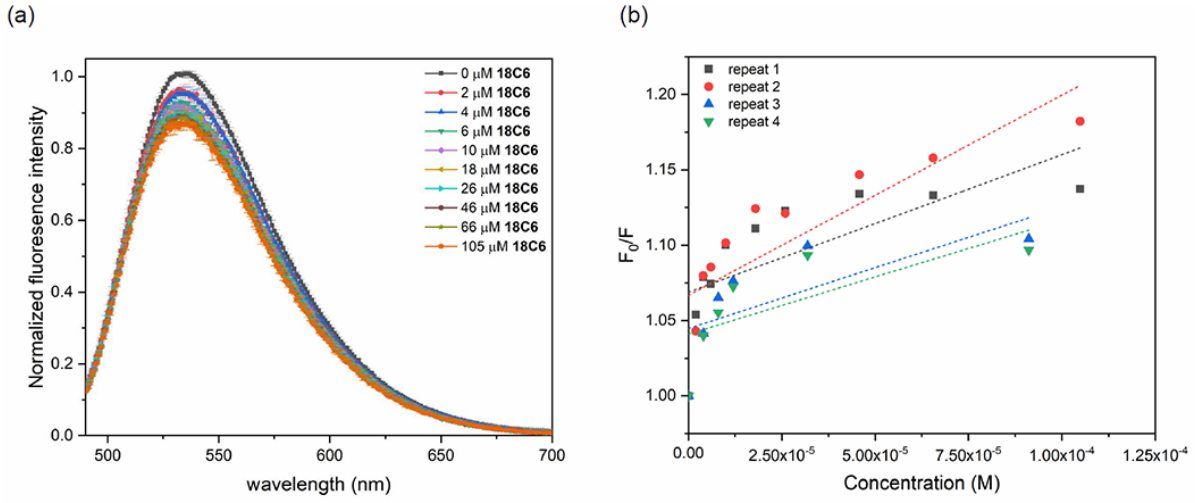

Figure S24. Fluorescence titration of **18-crown-6** (10 mM stock in DMSO) into a solution of 100 nm LUVs (POPC liposomes containing 1 mol% NBD-PC). Excitation wavelength = 470 nm. (a) Normalized fluorescence spectra, average of at least 2 repeats. (b) Stern-Volmer plots for all individual repeats. Linear fit resulted in R^2 values < 0.75 (no linear correlation).

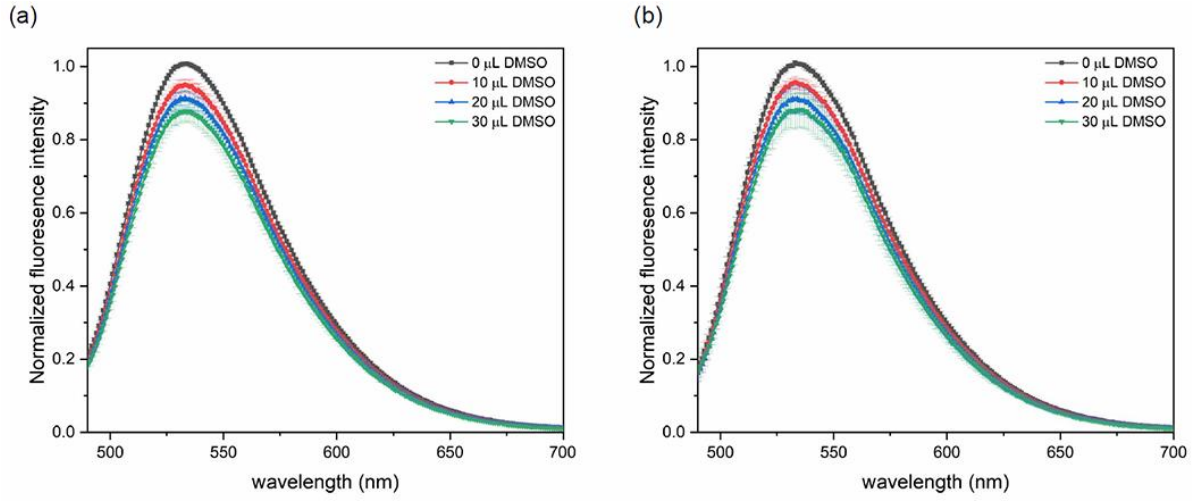

Figure S25. Fluorescence titration of **DMSO** into a solution of 100 nm LUVs. Excitation wavelength = 470 nm. (a) 1:1 POPC:POPE liposomes containing 1 mol% NBD-PE. (b) POPC liposomes containing 1 mol% NBD-PC.

S6. Lipid flip-flop

To obtain additional evidence for the interaction of the hosts with PE lipids in membranes, we performed lipid flip-flop experiments.[3] The experiments measure the ability of the hosts to facilitate the translocation of lipids in the outer leaflet of the lipid bilayer to the inner leaflet of the bilayer. The experiments were performed using DOPC liposomes containing either NBD-PE or NBD-PC in the outer leaflet. To mimic bacterial membranes,[4] we also performed the experiments using 7:3 DOPE:DOPG liposomes containing either NBD-PE or NBD-PC. However the significant quenching of the fluorescence of NBD-labelled lipids by the hosts in PE liposomes (see section above), led to interference with the flip-flop assay in the case of DOPE:DOPG liposomes.

To prepare the liposomes (100 nm LUVs, large unilamellar vesicles), aliquots of the appropriate lipid stock solution in chloroform (DOPC or 7:3 DOPE:DOPG) was transferred to a small round bottom flask and dried via rotary evaporation. The lipid film was dried further on high vacuum for at least 5 hours prior to use. The lipid film was hydrated with buffer (5 mM HEPES, 100 mM NaCl, pH 7.4) and vortexed until all the lipid was removed from the round bottom flask. The resulting suspension was subjected to 9 freeze-thaw cycles, alternating between submersion in liquid nitrogen followed by thawing in mildly warm water. The lipid suspension was allowed to rest at room temperature for 30 minutes before extruding 25 times through a 100 nm polycarbonate membrane (*Nucleopore*) using the Avanti mini extruder set (*Avanti Polar Lipids, Inc.*) to create a stock lipid solution.

For the flip-flop assay, the lipid solution was diluted in buffer (5 mM HEPES, 100 mM NaCl, pH 7.4) to achieve 35 mL of 25 μM lipid in a small glass beaker with stir bar. An ethanol solution of NBD-labelled PE or PC lipid was added to achieve a final concentration of 0.25 μM NBD-PE or NBD-PC (1 mol%) in the outer leaflet of the membrane (exo lipid). After 1 minute of stirring, 3 mL of the solution was transferred to measure the initial percentage of exo NBD-lipid. To the remaining 32 mL

solution was added 32 µL of a DMSO solution of the host and a timer was started. At certain time intervals, 3 mL of the solution was transferred to a cuvette to determine the percentage of exo NBD-labelled lipid. To determine %exo NBD-lipid, a 200 s kinetic fluorescence experiment was performed on the 3 mL samples using an Agilent Cary Eclipse fluorescence spectrophotometer (excitation wavelength = 470 nm, emission wavelength = 530 nm). In this kinetic assay, 180 µL of a dithionite solution (1 M sodium dithionite, 10 mM Tris, pH 10) was added to reduce the nitro group of the NBD-labelled lipid after 50 s, and 180 µL of 10% Triton X-100 was added to lyse the liposomes after 150 s. We found that the dithionite solution degraded rapidly and was therefore prepared fresh every hour. The %exo NBD-lipid is then given by (where F_i is the fluorescence intensity just before the addition of dithionite and F_f is the intensity just before the addition of Triton X-100):

$$\%\ exo\ lipid = \frac{F_i - F_f}{F_i}$$

The data at each time point was further converted to % lipid flipped, by subtracting the %exo lipid at any given time, by the %exo lipid at time t = 0 min (before addition of host). The results are shown in **Figure S26** - **Figure S31**, and clearly show that only host **1a** is able to facilitate the translocation of PE lipids (but not PC lipids). All other compounds could not facilitate flip-flop of either PE or PC.

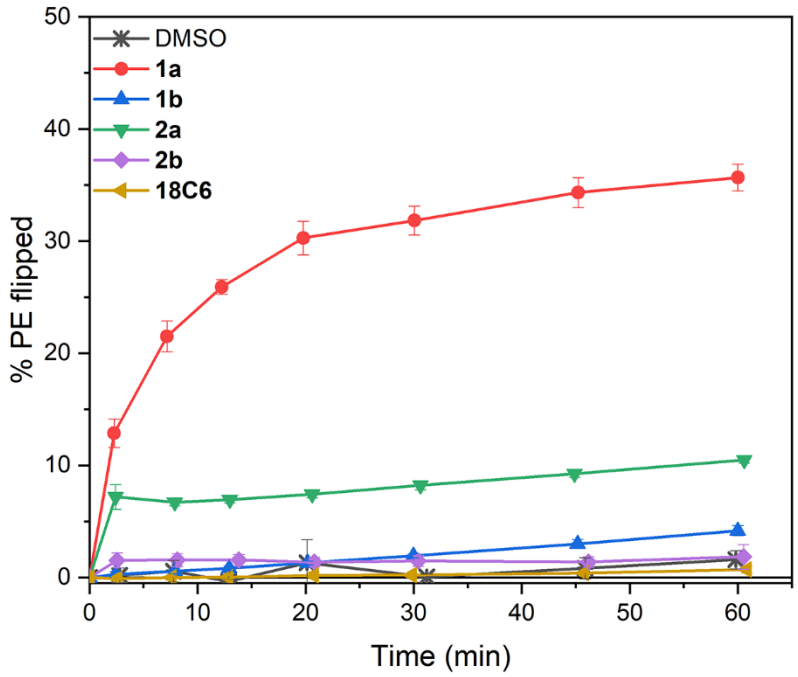

Figure S26. Flip-flop of exo NBD-PE (1 mol%) in 100 nm DOPC large unilamellar vesicles (25 µM) mediated by 25 µM hosts **1a**, **1b**, **2a**, **2b** and **18C6**. DMSO was used as a negative control. The results are the average of 2 biological x 2 technical repeats and the error bars represent standard deviations.

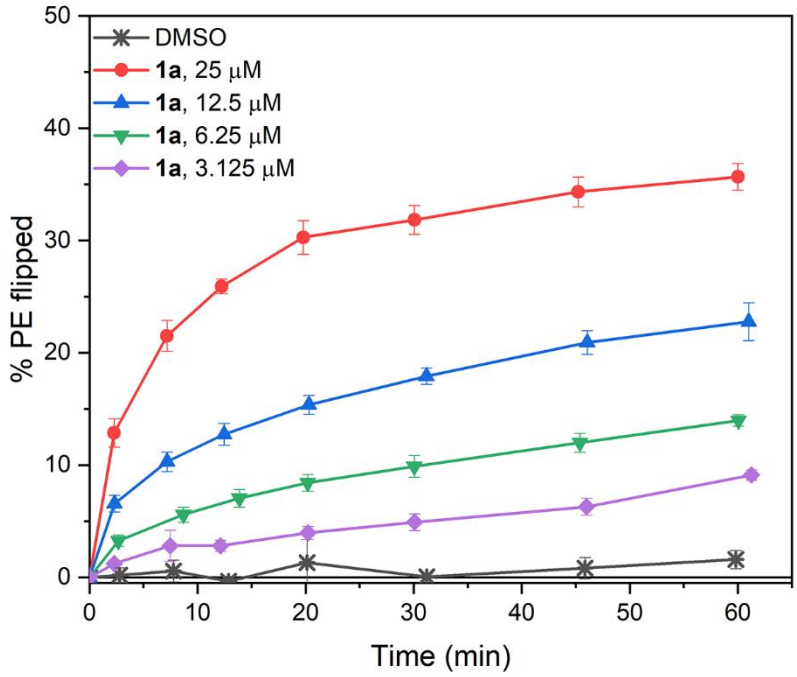

Figure S27. Flip-flop of exo NBD-PE (1 mol%) in 100 nm DOPC large unilamellar vesicles (25 μM) mediated by various concentrations of host **1a**. DMSO was used as a negative control. The results are the average of 2 biological x 2 technical repeats and the error bars represent standard deviations.

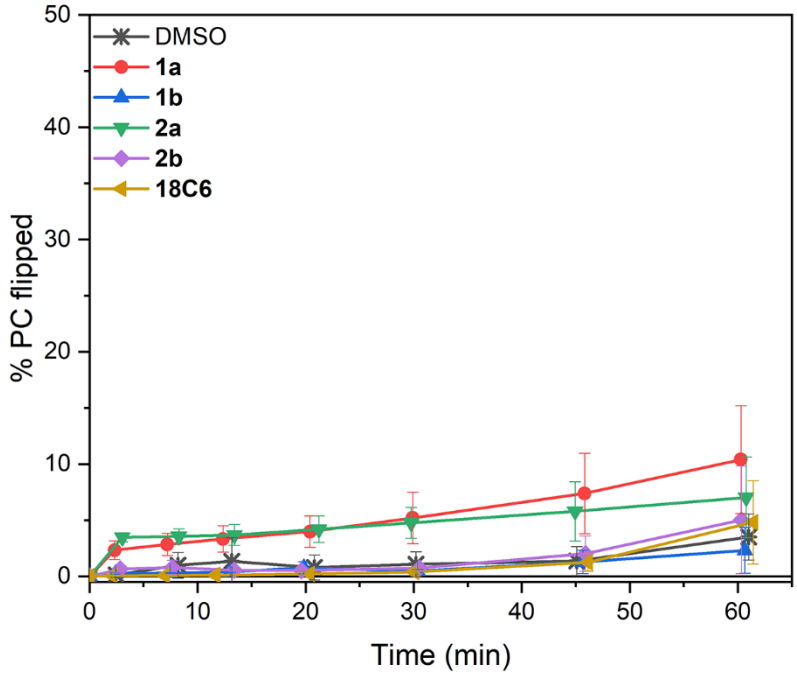

Figure S28. Flip-flop of exo NBD-PC (1 mol%) in 100 nm DOPC large unilamellar vesicles (25 μM) mediated by 25 μM hosts **1a**, **1b**, **2a**, **2b** and **18C6**. DMSO was used as a negative control. The results are the average of 2 biological x 2 technical repeats and the error bars represent standard deviations.

Figure S29. Flip-flop of exo NBD-PE (1 mol%) in 100 nm 7:3 DOPE:DOPG large unilamellar vesicles (25 μM) mediated by 25

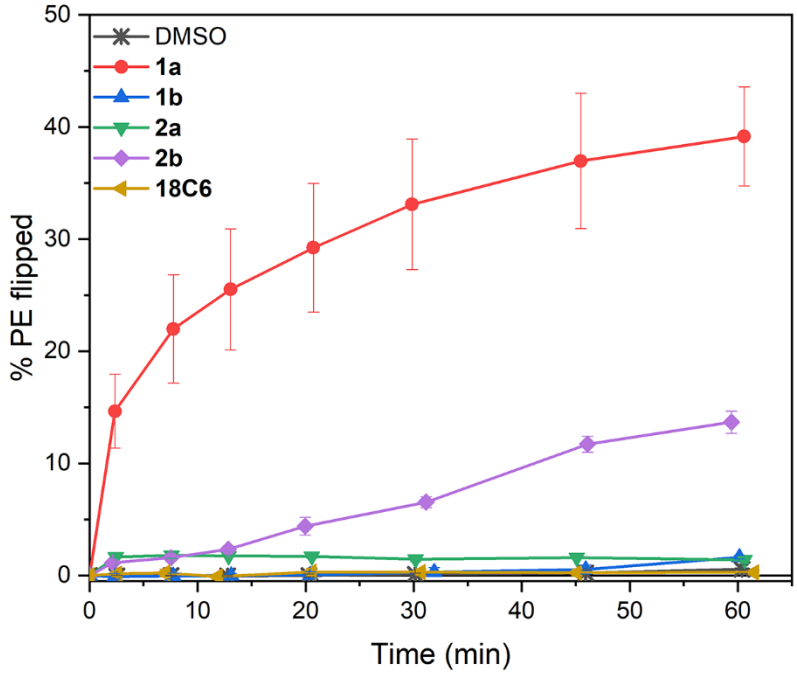

μM hosts **1a**, **1b**, **2a**, **2b** and **18C6**. DMSO was used as a negative control. The results are the average of 2 biological x 2 technical repeats and the error bars represent standard deviations.

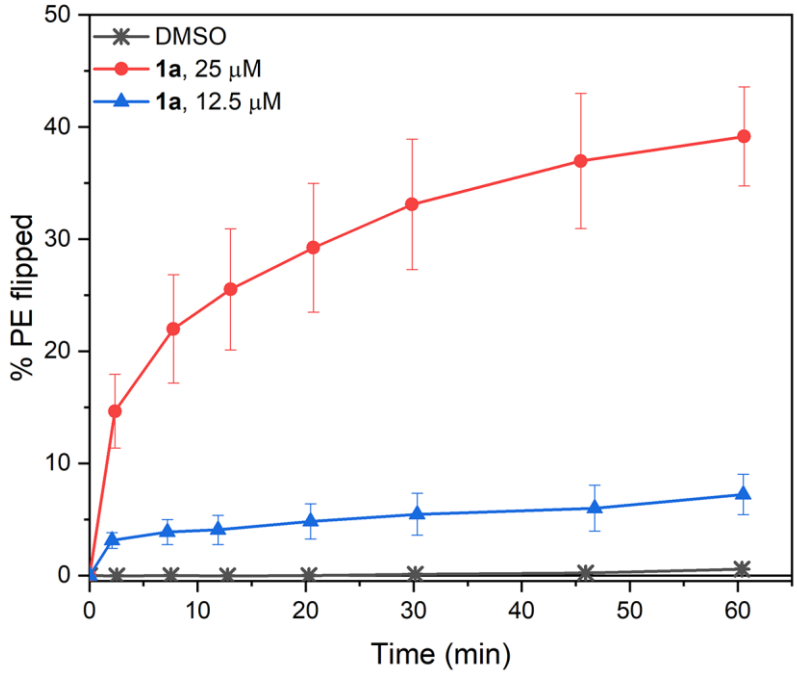

Figure S30. Flip-flop of exo NBD-PE (1 mol%) in 100 nm 7:3 DOPE:DOPG large unilamellar vesicles (25 μM) mediated by various concentrations of hosts **1a**. DMSO was used as a negative control. The results are the average of 2 biological x 2 technical repeats and the error bars represent standard deviations.

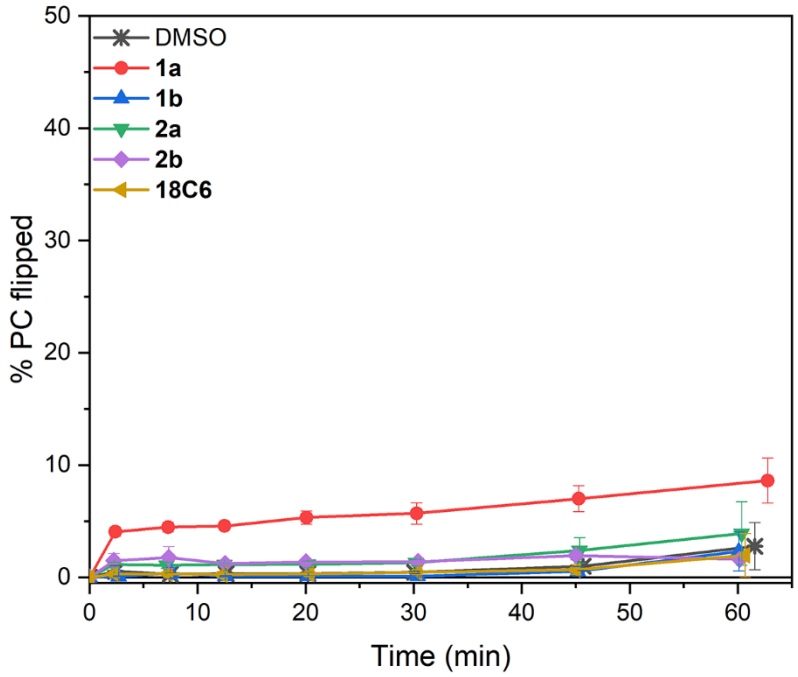

Figure S31. Flip-flop of exo NBD-PC (1 mol%) in 100 nm 7:3 DOPE:DOPG large unilamellar vesicles (25 µM) mediated by 25 µM hosts **1a**, **1b**, **2a**, **2b** and **18C6**. DMSO was used as a negative control. The results are the average of 2 biological x 2 technical repeats and the error bars represent standard deviations.

S7. Calcein leakage

To investigate whether the hosts can cause major disruptions in PE-containing membranes, a standard calcein assay was performed.[5] Due to the inability of POPE to form stable unilamellar liposomes, a 1:1 mixture of POPC:POPE was used. Thus, 100 nm 1:1 POPE:POPC large unilamellar vesicles (LUVs) were formed by transferring an aliquot of the lipid stock solution in chloroform to a small round bottom flask. A lipid film was formed by removal of the chloroform solvent on a rotary evaporator and dried further on high vacuum for at least 5 hours prior to use. The lipid film was hydrated with the internal solution (70 mM calcein, 150 mM NaCl, 10 mM Tris buffer, pH 7.4) and vortexed until all lipid was removed from the glass walls of the round bottom flask. The resulting suspension was subjected to 9 freeze-thaw cycles, alternating between submersion in liquid nitrogen followed by thawing in mildly warm water. The lipid suspension was allowed to rest at room temperature for 30 minutes before extruding 25 times through a 100 nm polycarbonate membrane (*Nucleopore*) using the Avanti mini extruder set (*Avanti Polar Lipids, Inc*.). The resulting uniform LUVs were separated from the unencapsulated calcein by size exclusion chromatography using a Sephadex column (G-50, medium).

For each measurement, the obtained concentrated stock liposome solution was diluted in external buffer (150 mM NaCl, 10 mM Tris buffer, pH 7.4) to afford 3 mL of a final lipid concentration of 10 µM in a cuvette. A cuvette stir bar was added and a 14-minute kinetic fluorescence experiment was

performed using an Agilent Cary Eclipse fluorescence spectrophotometer (excitation wavelength = 490 nm, emission wavelength = 520 nm). In this kinetic assay, 30 µL of a 10 mM DMSO stock solution of the host was added after 1.5 min (resulting in a final host concentration of 100 µM), and 30 µL of 10% Triton X-100 was added to lyse the liposomes after 11.5 min. The percent calcein release is then given by (where F_0 is the fluorescence intensity before the addition of host (t = 0 min), F is the intensity at any given time and F_F is the intensity after the addition of Triton X-100 (final data point)):

$$\%\ calcein\ release = \frac{F - F_0}{F_F - F_0} \cdot 100\%$$

The results are shown in **Figure S32**. No significant calcein leakage is observed for any of the hosts.

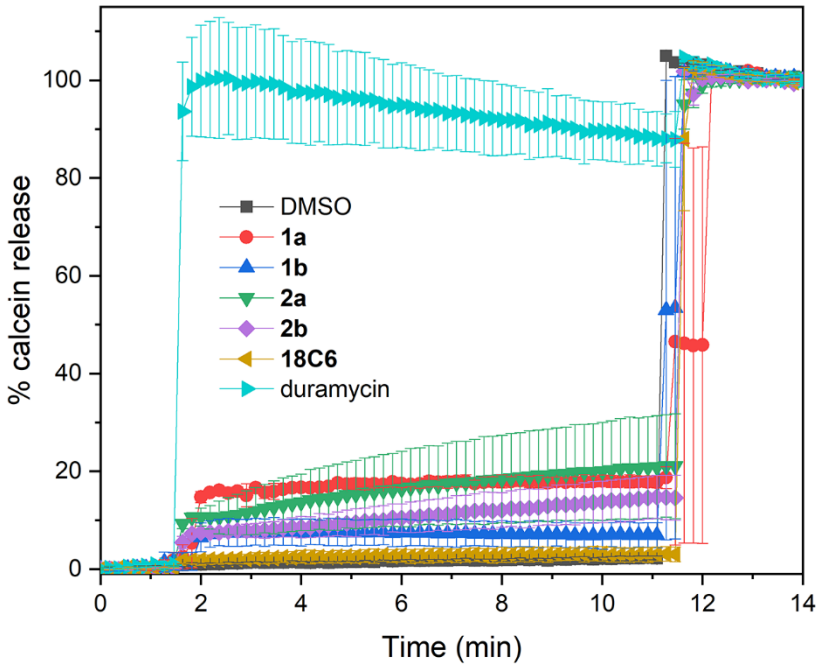

Figure S32. Calcein leakage mediated by 100 µM hosts **1a**, **1b**, **2a**, **2b** and **18C6** from 100 nm 1:1 POPE:POPC large unilamellar vesicles (10 µM) loaded with 70 mM calcein, 150 mM NaCl, 10 mM Tris buffer at pH 7.4. DMSO was used as a negative control and duramycin was used as a positive control. The results are the average of 2 biological x 2 technical repeats and the error bars represent standard deviations.

S8. Bacterial studies

S8.1. Selectivity of antibacterial activity between S. simulans, B. subtilis and B. cereus

S. simulans (ATCC 27848), *B. subtilis* (ATCC 6051) and *B. cereus* (ATCC 117781) were obtained from the American Type Culture Collection and stored in glycerol stocks at -80 °C. For each experiment, a small amount of the glycerol stock was streaked onto a Müller-Hinton agar plate (Sigma-Aldrich #70191) and the agar plate was incubated for 18-24 hours at 35 °C. The obtained colonies were aseptically transferred into sterile cation-adjusted Müller-Hinton broth (Sigma-Aldrich #90922) and vortex briefly. Colonies were added until the inoculum solution achieved an OD_{600} value corresponding to 1×10^8 CFU/mL (determined using a Biowave CO8000 Cell Density meter and 17x100 mm polystyrene culture tubes).

To 30 mL of molten Müller-Hinton agar was added 50 µL of a 25 mM DMSO stock of compounds 1a, 1b, 2a, 2b or 18C6 and 250 µL DMSO for solubility (the blank sample contained 300 µL DMSO), and the mixture was homogenized. The molten agar was transferred to a sterile **100x**15 mm petri dish and allowed to solidify. When the agar was solidified, the agar plate was divided into 3 zones and each zone was inoculated with 10 µL of the 1×10^8 CFU/mL solution of either *S. simulans*, *B. subtilis* or *B. cereus.* The agar plates were subsequently incubated at 35 °C for 48 hours. Photographs of the plates were taken after 18 h, 24 h, 30 h and 48 h incubation at 35 °C. The experiment was performed in duplicate and the results are shown in Figure S33 - Figure S34. Compounds 1b, 2a and 18C6 did not inhibit the growth of any of the bacteria, consistent with their lack of activity in the assays described above. In contrast, 2b showed antibacterial activity against all bacteria tested, regardless of their PE content. This indicates that 2b exerts its antibacterial activity through a mechanism that does not involve PE binding, consistent with its lack of PE binding observed in the ^{1}H NMR titrations and flip-flop assays. More interestingly, compound 1a had no effect on the growth of *S. simulans*, caused a significant delay in the growth of *B. subtilis* and complete inhibition of bacterial growth of *B. cereus*. This appears to be a correlation with the PE-content of these bacterial species (*S. simulans* (0% PE),[6] *B. subtilis* (20-30% PE),[7-8] and *B. cereus* (40-50% PE)[9]) and suggests that the mechanism of 1a involves binding to PE lipids.

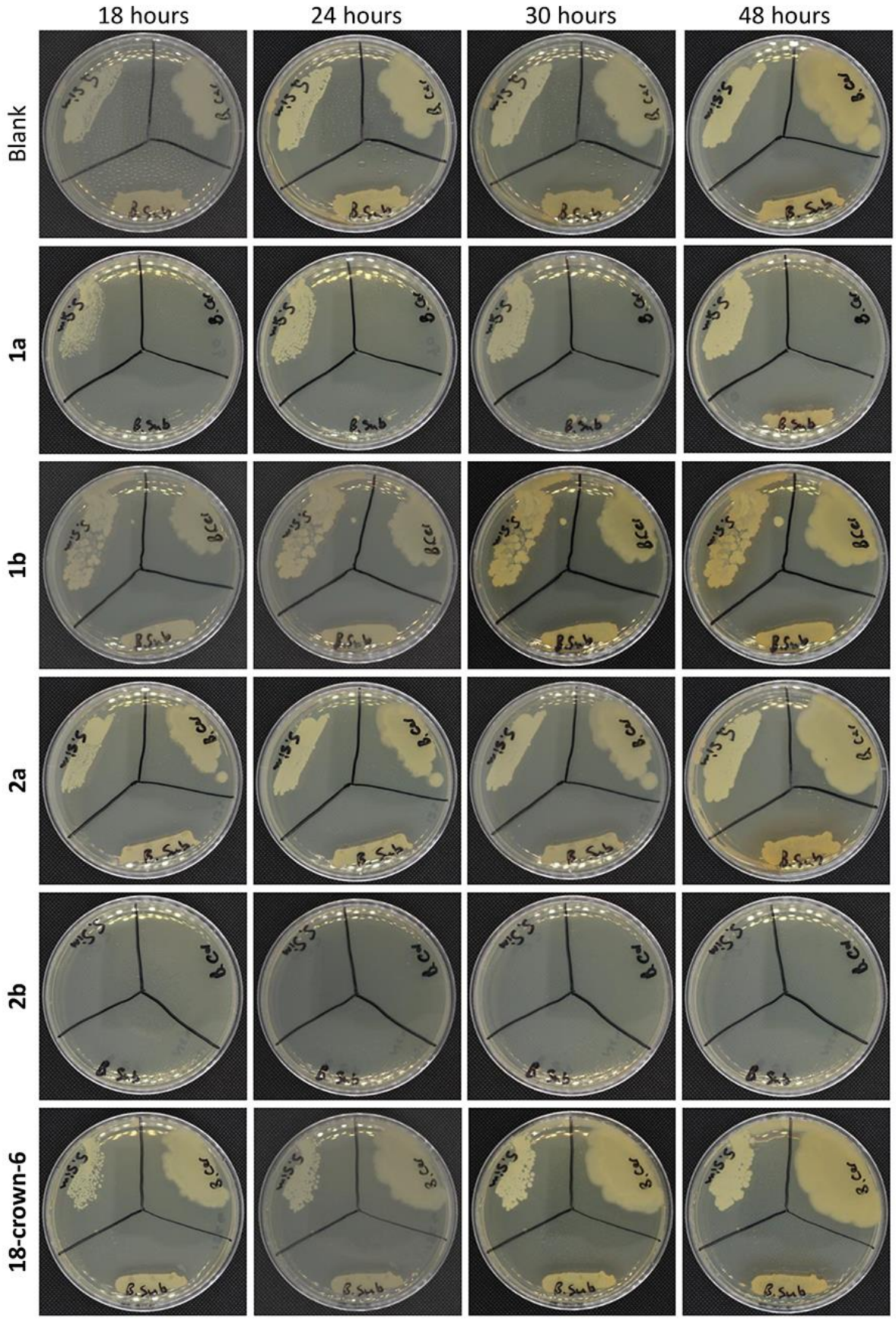

Figure S33. Bacterial selectivity of **1a**-**2b** and 18-crown-6 (biological repeat 1). Bacterial growth was monitored for 24 h at 35 °C on a Müller-Hinton agar plate containing 50 µL of a 25 mM DMSO stock of **1a**, **1b**, **2a**, **2b** and 18-crown-6. Blank contained 300 µL DMSO in the agar plate. All plates are photographed so that the *B. cereus* section is on the right, the *B. subtilis* section is on the bottom, and the *S. simulans* section is on the left of the agar plate.

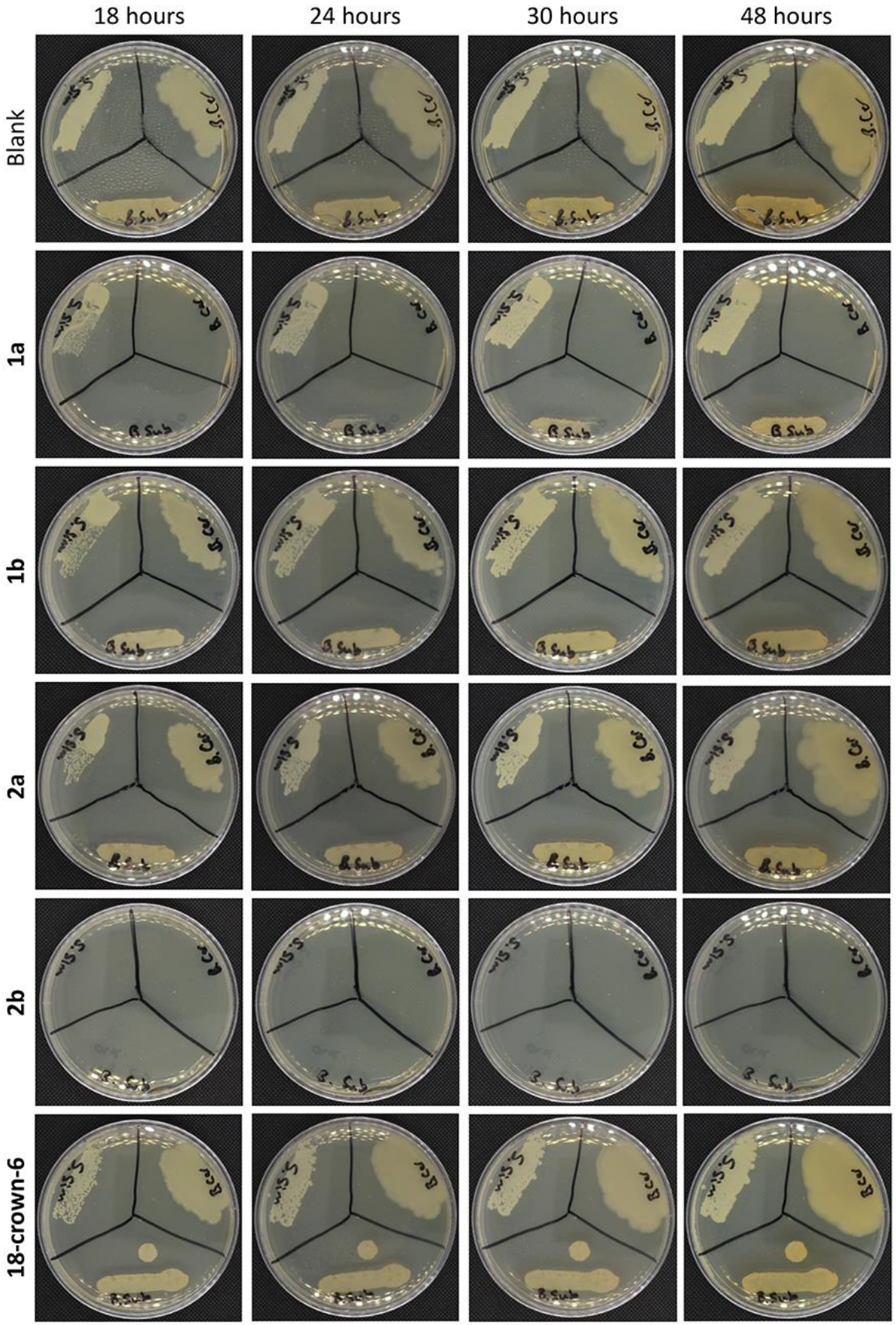

Figure S34. Bacterial selectivity of **1a**-**2b** and 18-crown-6 (biological repeat 2). Bacterial growth was monitored for 24 h at 35 °C on a Müller-Hinton agar plate containing 50 µL of a 25 mM DMSO stock of **1a**, **1b**, **2a**, **2b** and 18-crown-6. Blank contained 300 µL DMSO in the agar plate. All plates are photographed so that the *B. cereus* section is on the right, the *B. subtilis* section is on the bottom, and the *S. simulans* section is on the left of the agar plate.

S8.2. MIC determination

The minimum inhibitory concentration (MIC) against the Gram-positive bacterium *B. cereus* was determined using the broth microdilution method recommended by the Clinical and Laboratory Standards Institute.[10] *B. cereus* was obtained from the American Type Culture Collection (ATCC 117781) and stored in glycerol stocks at -80 °C. For each experiment, a small amount of the glycerol stock was streaked onto a Müller-Hinton agar plate (Sigma-Aldrich #70191) and the agar plate was incubated for 18-24 hours at 35 °C. The obtained colonies were aseptically transferred into sterile cation-adjusted Müller-Hinton broth (Sigma-Aldrich #90922) and vortex briefly. Colonies were added until the inoculum solution achieved an OD_{600} value corresponding to 1 x 10^8 CFU/mL (typically OD_{600} 1.1-1.3 for *B. cereus*). OD_{600} values were determined using a Biowave CO8000 Cell Density meter and 17x100 mm polystyrene culture tubes (VWR #60818-703). The inoculum was subsequently diluted to 5 x 10^5 CFU/mL in sterile cation-adjusted Müller-Hinton broth. 192 µL of this inoculum was transferred to the wells of a sterile flat-bottom polystyrene non-tissue culture treated 96-well plate (Falcon #351172) and 8 µL of a DMSO stock solution of compounds **1a**, **1b**, **2a**, **2b** or **18C6** was added to each well (final DMSO concentration 4%) and the 96-well plate was covered with a Breathe-Easy sealing membrane (Sigma-Aldrich # Z380059). The optical density at 600 nm (OD_{600}) was subsequently measured for 24 hours using a BioTek Cytation 5 Cell Imaging Multi-Mode Reader (35 °C, absorbance measurement at 600 nm, orbital shaking (shaking every 10 minutes, for 1 min at 548 rpm (2 mm)). The MIC value was defined as the minimum concentration of compound that resulted in complete inhibition of bacterial growth over the full 24 hours. Clindamycin was used for quality control reasons (MIC of clindamycin of ~0.75 µg/mL was considered a valid experiment). The results are shown in **Figure S35** - **Figure S40**. Compound **1a** has an MIC value of 25-30 µM (sometimes 25 µM **1a** led to slow growth of *B. cereus* after 20 h), compound **2b** has an MIC value of 6.25 µM, and all other compounds did not have any effect on *B. cereus* growth at the maximum concentration tested (100 µM). We also tried to obtain an MIC value against *B. cereus* for the known PE-binding antibiotic duramycin,[11-12] but faced problems with repeatability. For all concentrations investigated, duramycin caused a delay in bacterial growth. However, full inhibition off bacterial growth was only seen for most repeats at 32 µM and 64 µM and all repeats at 128 µM duramycin.

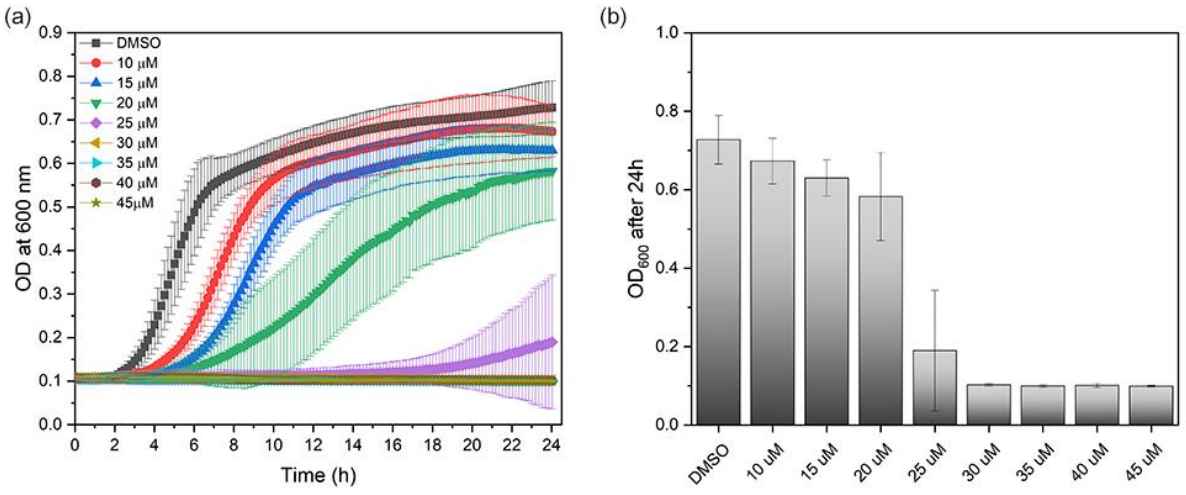

Figure S35. MIC determination for compound **1a**. The change in optical density at 600 nm was measured for 24 h at 35 °C to monitor the growth of *B. cereus* (starting point 5 x 10^5 CFU/mL) in Müller-Hinton broth containing 4% DMSO and various concentrations of compound **1a**. DMSO was used as a negative control. The results are the average of minimum 2 biological x 2 technical repeats and the error bars represent standard deviations. (a) full growth curves. (b) Optical density (600 nm) after 24 hours incubation with various concentrations of **1a**.

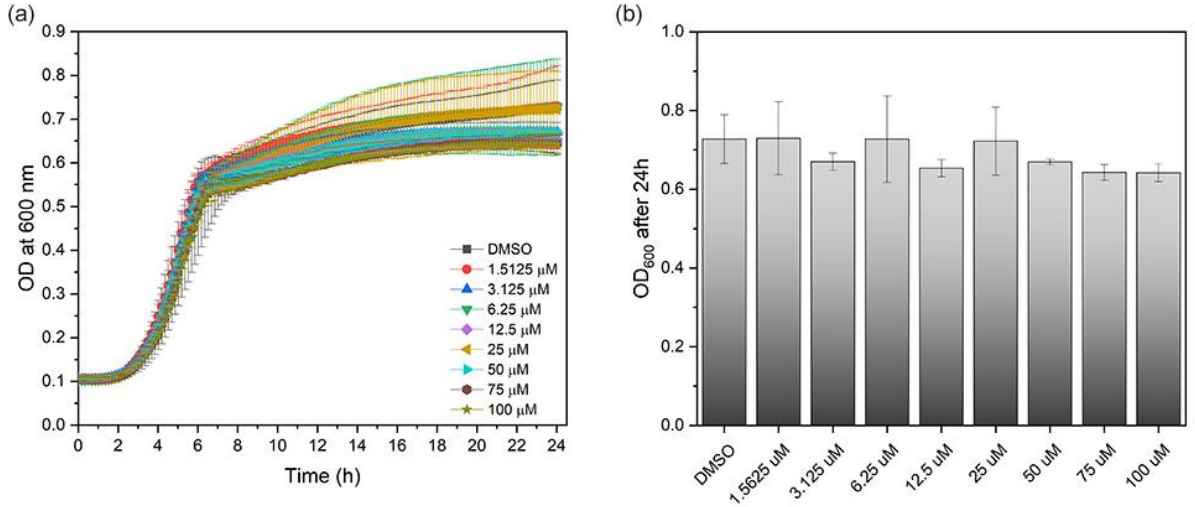

Figure S36. MIC determination for compound **1b**. The change in optical density at 600 nm was measured for 24 h at 35 °C to monitor the growth of *B. cereus* (starting point 5 x 10^5 CFU/mL) in Müller-Hinton broth containing 4% DMSO and various concentrations of compound **1b**. DMSO was used as a negative control. The results are the average of minimum 2 biological x 2 technical repeats and the error bars represent standard deviations. (a) full growth curves. (b) Optical density (600 nm) after 24 hours incubation with various concentrations of **1b**.

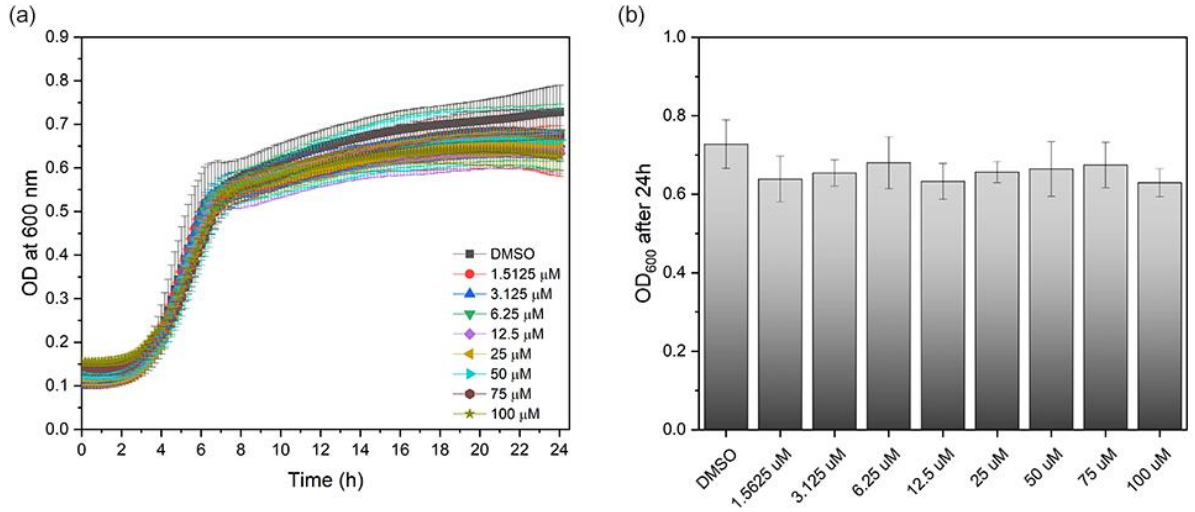

Figure S37. MIC determination for compound **2a**. The change in optical density at 600 nm was measured for 24 h at 35 °C to monitor the growth of *B. cereus* (starting point 5 x 10^5 CFU/mL) in Müller-Hinton broth containing 4% DMSO and various concentrations of compound **2a**. DMSO was used as a negative control. The results are the average of minimum 2 biological x 2 technical repeats and the error bars represent standard deviations. (a) full growth curves. (b) Optical density (600 nm) after 24 hours incubation with various concentrations of **2a**.

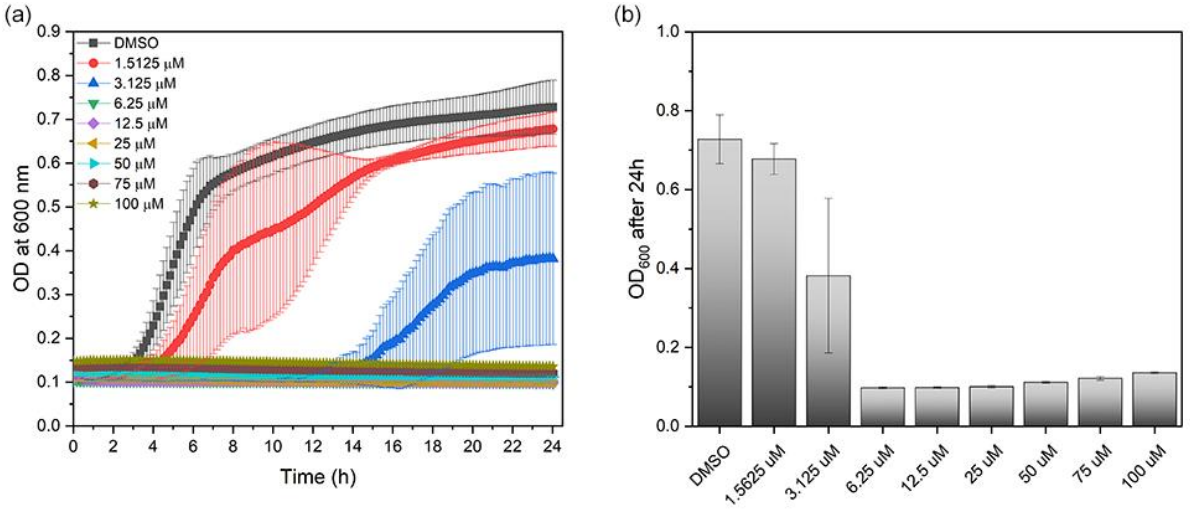

Figure S38. MIC determination for compound **2b**. The change in optical density at 600 nm was measured for 24 h at 35 °C to monitor the growth of *B. cereus* (starting point 5 x 10^5 CFU/mL) in Müller-Hinton broth containing 4% DMSO and various concentrations of compound **2b**. DMSO was used as a negative control. The results are the average of minimum 2 biological x 2 technical repeats and the error bars represent standard deviations. (a) full growth curves. (b) Optical density (600 nm) after 24 hours incubation with various concentrations of **2b**.

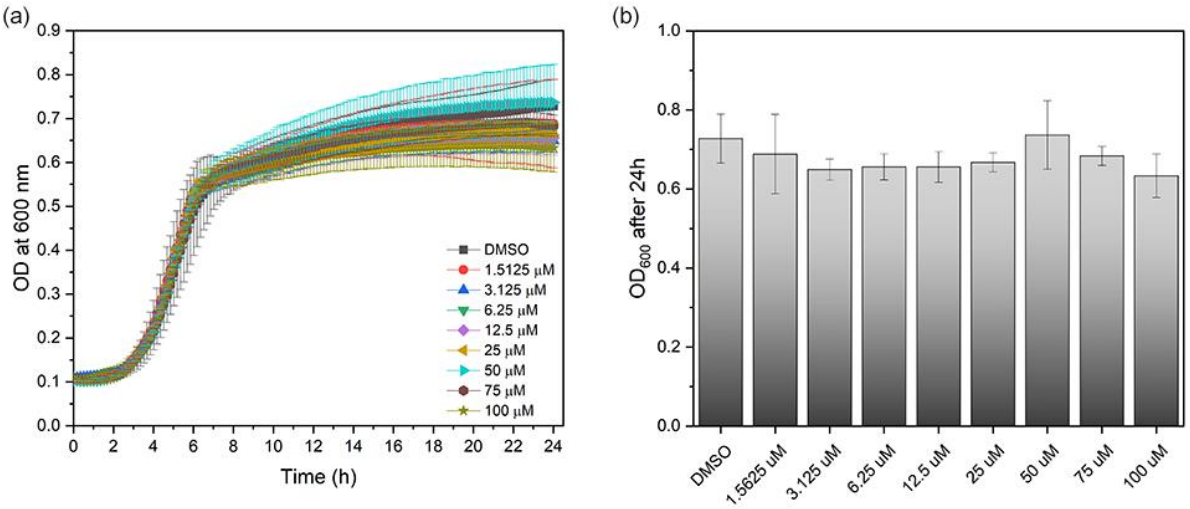

Figure S39. MIC determination for compound **18C6**. The change in optical density at 600 nm was measured for 24 h at 35 °C to monitor the growth of *B. cereus* (starting point 5 x 10^5 CFU/mL) in Müller-Hinton broth containing 4% DMSO and various concentrations of compound **18C6**. DMSO was used as a negative control. The results are the average of minimum 2 biological x 2 technical repeats and the error bars represent standard deviations. (a) full growth curves. (b) Optical density (600 nm) after 24 hours incubation with various concentrations of **18C6**.

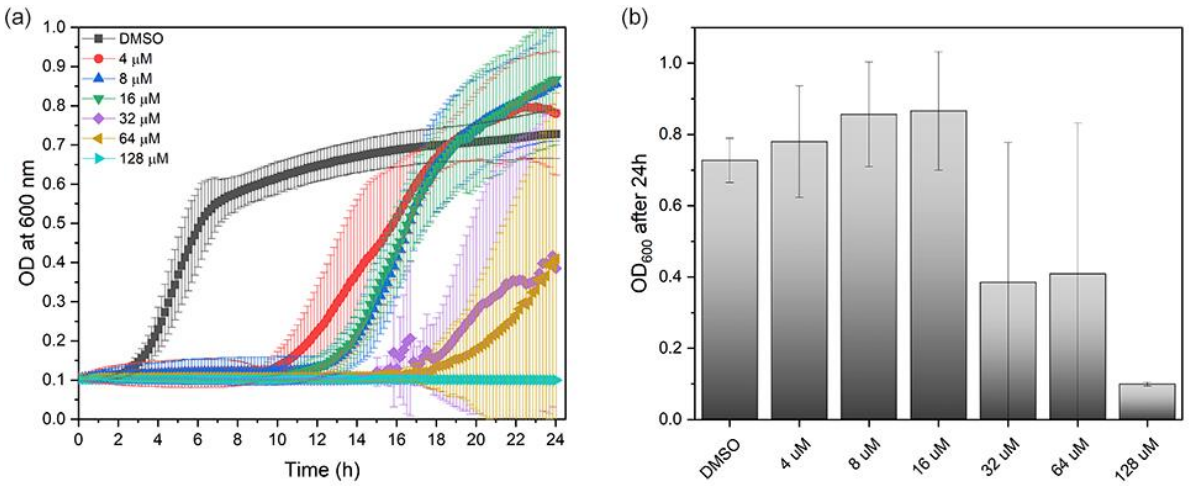

Figure S40. MIC determination for **duramycin**. The change in optical density at 600 nm was measured for 24 h at 35 °C to monitor the growth of *B. cereus* (starting point 5 x 10^5 CFU/mL) in Müller-Hinton broth containing 4% DMSO and various concentrations of **duramycin**. DMSO was used as a negative control. The results are the average of minimum 2 biological x 2 technical repeats and the error bars represent standard deviations. (a) full growth curves. (b) Optical density (600 nm) after 24 hours incubation with various concentrations of **duramycin**.

S8.3. Bactericidal activity

Membrane-active antibiotics are normally bactericidal rather than bacteriostatic.[13-14] The minimum bactericidal concentration (MBC) was therefore determined using the method suggested by the Clinical and Laboratory Standards Institute.[15] In brief, at the end of the MIC determination (see above), 100 µL of the *B. cereus* culture obtained by 24 h incubation with various concentrations of compound **1a** was streaked onto a Müller-Hinton agar plate (Sigma-Aldrich #70191) and the agar plate was incubated for 18-24 hours at 35 °C. The formed colonies were counted to determine the final CFU/mL after 24 h incubation. This final CFU/mL was compared with the initial CFU/mL at the start of the 24 h incubation (typically 5 x 10^5 CFU/mL, but this was determined experimentally each time) to calculate the percentage of bacteria that were killed. The results are shown in **Table S1**. Bactericidal activity is defined as the ability to kill 99.9% of bacteria, and therefore the MBC value for **1a** is 35-40 µM, which is close to the MIC value for **1a** (25-30 µM). We thus suggest that **1a** has bactericidal activity.

Table S1. Bactericidal activity of compound **1a** after 24 h incubation with *B.cereus*.

Concentration **1a**	**% bacteria killed**					
	Repeat 1	Repeat 2	Repeat 3	Repeat 4	Repeat 5	Repeat 6
45 µM	100	99.9	99.8	99.9	100	100
40 µM	100	99.9	99.8	99.9	99.8	100
35 µM	99.9	99.7	99.3	99.7	Overgrown[a]	Overgrown[a]
30 µM	99.9	Overgrown[a]	99.3	Overgrown[a]	Overgrown[a]	Overgrown[a]
25 µM	n.d.[b]	Overgrown[a]	Overgrown[a]	Overgrown[a]	Overgrown[a]	Overgrown[a]

[a] Colonies were too numerous to count. [b] n.d. = not determined.

S8.4. Microscopy studies

To investigate morphological changes in *B. cereus* induced by compounds **1a**, we performed live imaging and Gram staining. For the live imaging, 10 µL of the *B. cereus* cultures obtained by 24 h incubation with various concentrations of compound **1a, 1b, 2a, 2b** and **18C6** was transferred to a 96-well plate with glass bottom suitable for microscopy (Greiner Bio-one #655892) and diluted with 90 µL Müller-Hinton broth. The 96-well plate was subsequently centrifuged for 1 minute at 3000 rpm using an Eppendorf Centrifuge 5810 to ensure that all bacteria are in a single optical plane at the bottom of the 96-well plate. The bacteria were than imaged using a BioTek Cytation 5 Cell Imaging Multi-Mode Reader (40x or 60x objective, Brightfield).

For the Gram-staining, 5 µL of the *B. cereus* culture obtained by 24 h incubation with various concentrations of compound **1a, 1b, 2a, 2b** and **18C6** was transferred onto a Polysine microscope adhesion slide (ThermoScientific #P4981-001) and stained using a Gram stain kit (Azer Scientific #ES800). The slides were subsequently visualized using a BioTek Cytation 5 Cell Imaging Multi-Mode Reader (40x or 60x objective, Brightfield) or an Amscope Quintuple Plan Infinity Kohler Laboratory

Trinocular Compound Microscope (100x oil objective, Brightfield). The results are shown in **Figure S41** - **Figure S50**.

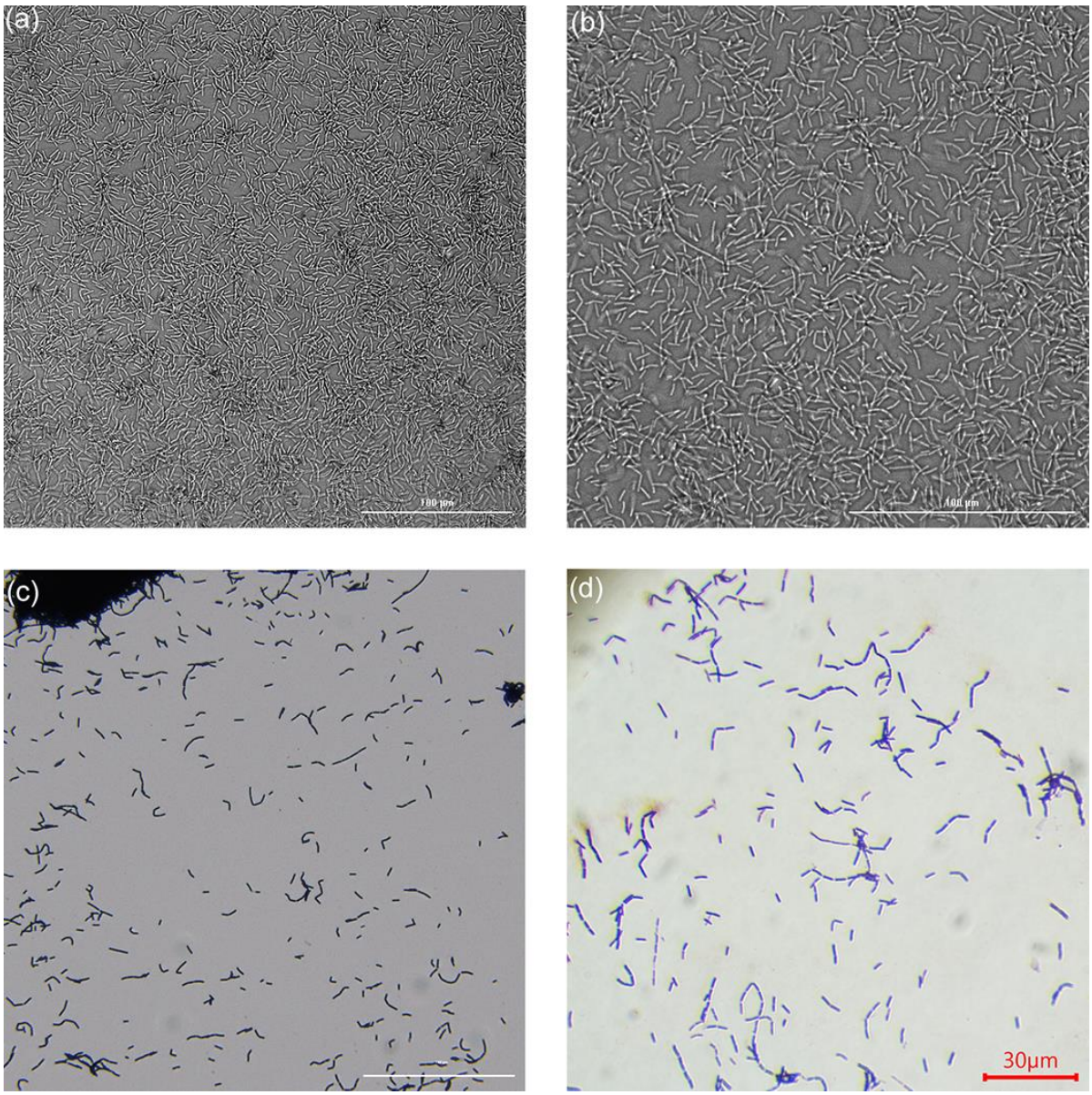

Figure S41. Images of untreated *B. cereus* after 24 h incubation at 35 °C in Müller-Hinton broth (starting point 5 x 10^5 CFU/mL). (a) Image obtained after 1:10 dilution in in Müller-Hinton broth using a BioTek Cytation 5 Cell Imaging Multi-Mode Reader (40x objective, Brightfield). Scale bar represents 100 µm. (b) Image obtained after 1:10 dilution in in Müller-Hinton broth using a BioTek Cytation 5 Cell Imaging Multi-Mode Reader (60x objective, Brightfield). Scale bar represents 100 µm. (c) Image obtained after Gram staining using a BioTek Cytation 5 Cell Imaging Multi-Mode Reader (40x objective, Brightfield). Scale bar represents 100 µm. (d) Image obtained after Gram staining using an Amscope Quintuple Plan Infinity Kohler Laboratory Trinocular Compound Microscope (100x oil objective, Brightfield). Scale bar represents 30 µm.

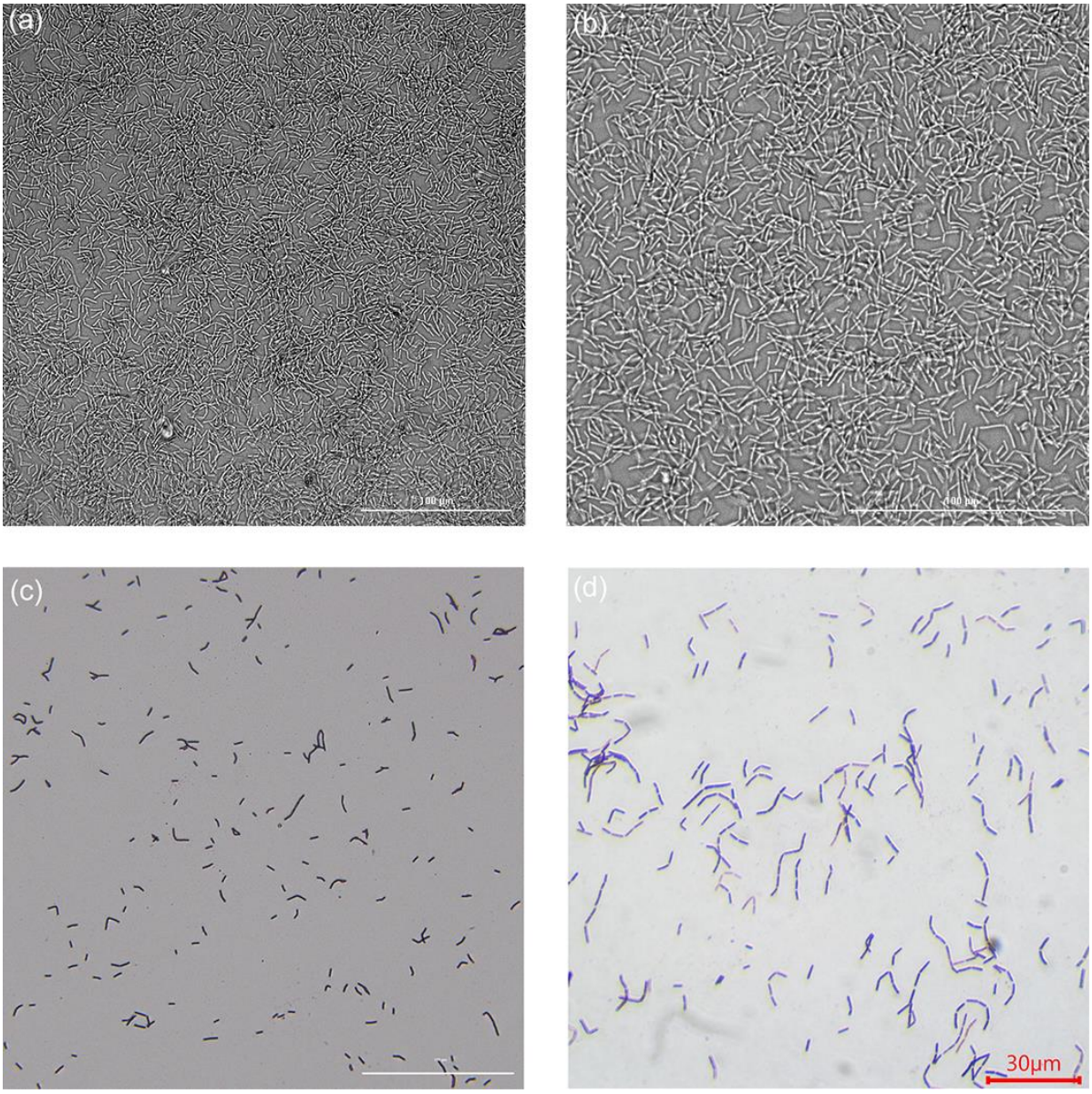

Figure S42. Images of *B. cereus* after 24 h incubation at 35 °C in Müller-Hinton broth containing 4% DMSO (starting point 5 x 10^5 CFU/mL). (a) Image obtained after 1:10 dilution in in Müller-Hinton broth using a BioTek Cytation 5 Cell Imaging Multi-Mode Reader (40x objective, Brightfield). Scale bar represents 100 µm. (b) Image obtained after 1:10 dilution in in Müller-Hinton broth using a BioTek Cytation 5 Cell Imaging Multi-Mode Reader (60x objective, Brightfield). Scale bar represents 100 µm. (c) Image obtained after Gram staining using a BioTek Cytation 5 Cell Imaging Multi-Mode Reader (40x objective, Brightfield). Scale bar represents 100 µm. (d) Image obtained after Gram staining using an Amscope Quintuple Plan Infinity Kohler Laboratory Trinocular Compound Microscope (100x oil objective, Brightfield). Scale bar represents 30 µm.

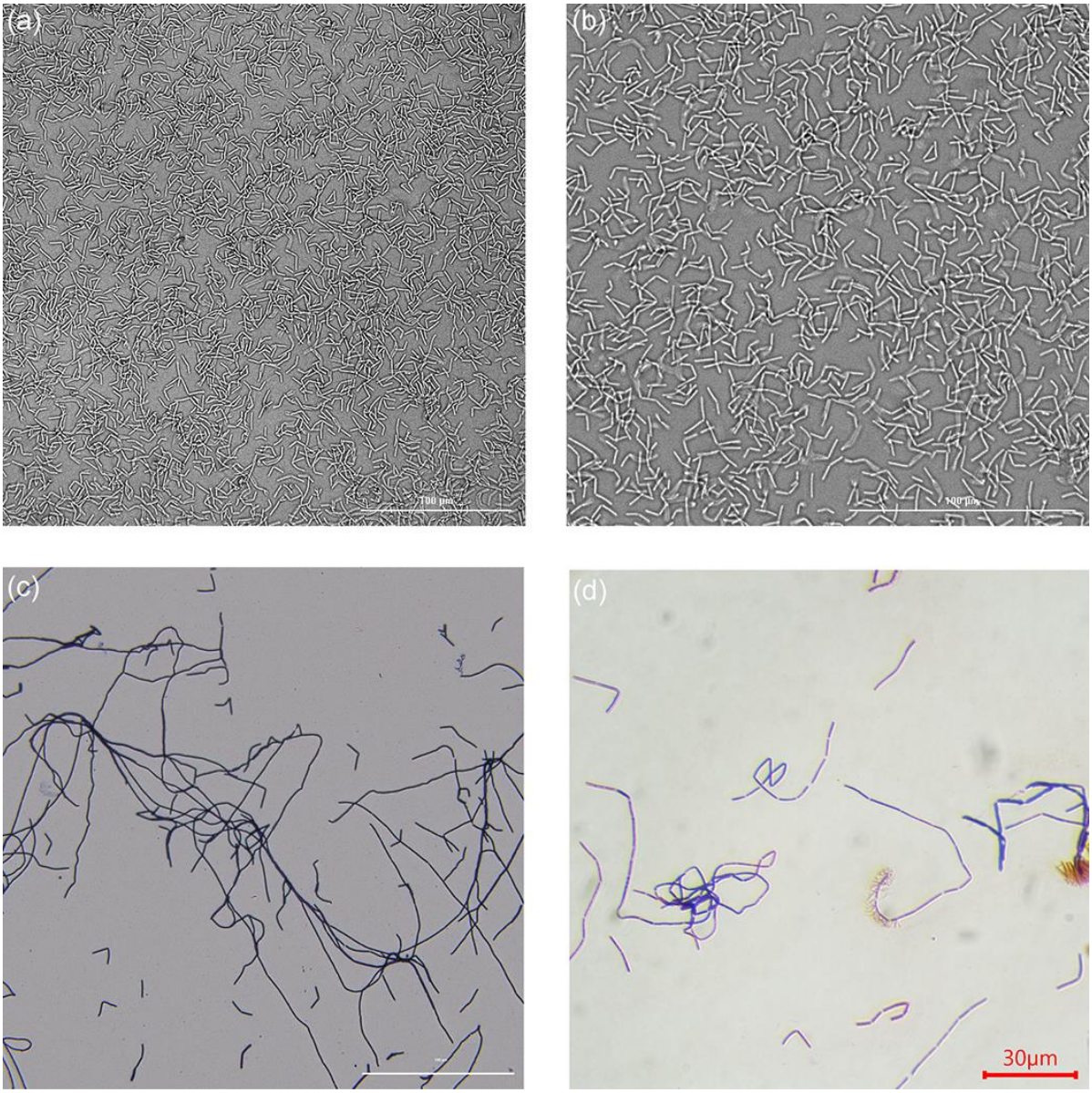

Figure S43. Images of *B. cereus* after 24 h incubation at 35 °C in Müller-Hinton broth containing 4% DMSO and **20 µM 1a** (<MIC) (starting point 5 x 10^5 CFU/mL). (a) Image obtained after 1:10 dilution in in Müller-Hinton broth using a BioTek Cytation 5 Cell Imaging Multi-Mode Reader (40x objective, Brightfield). Scale bar represents 100 µm. (b) Image obtained after 1:10 dilution in in Müller-Hinton broth using a BioTek Cytation 5 Cell Imaging Multi-Mode Reader (60x objective, Brightfield). Scale bar represents 100 µm. (c) Image obtained after Gram staining using a BioTek Cytation 5 Cell Imaging Multi-Mode Reader (40x objective, Brightfield). Scale bar represents 100 µm. (d) Image obtained after Gram staining using an Amscope Quintuple Plan Infinity Kohler Laboratory Trinocular Compound Microscope (100x oil objective, Brightfield). Scale bar represents 30 µm.

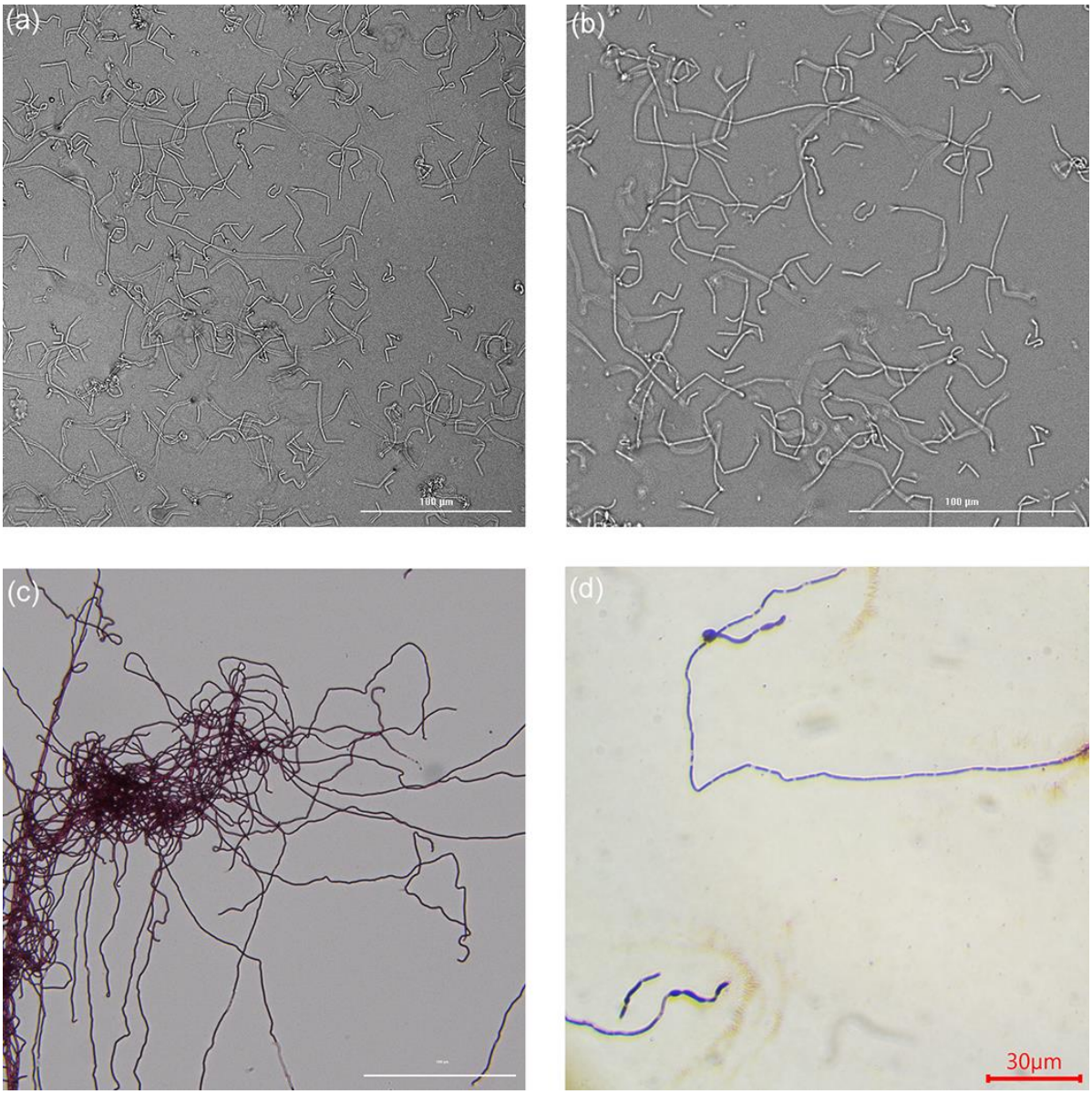

Figure S44. Images of *B. cereus* after 24 h incubation at 35 °C in Müller-Hinton broth containing 4% DMSO and **25 µM 1a** (=MIC) (starting point 5 x 10^5 CFU/mL). (a) Image obtained after 1:10 dilution in in Müller-Hinton broth using a BioTek Cytation 5 Cell Imaging Multi-Mode Reader (40x objective, Brightfield). Scale bar represents 100 µm. (b) Image obtained after 1:10 dilution in in Müller-Hinton broth using a BioTek Cytation 5 Cell Imaging Multi-Mode Reader (60x objective, Brightfield). Scale bar represents 100 µm. (c) Image obtained after Gram staining using a BioTek Cytation 5 Cell Imaging Multi-Mode Reader (40x objective, Brightfield). Scale bar represents 100 µm. (d) Image obtained after Gram staining using an Amscope Quintuple Plan Infinity Kohler Laboratory Trinocular Compound Microscope (100x oil objective, Brightfield). Scale bar represents 30 µm.

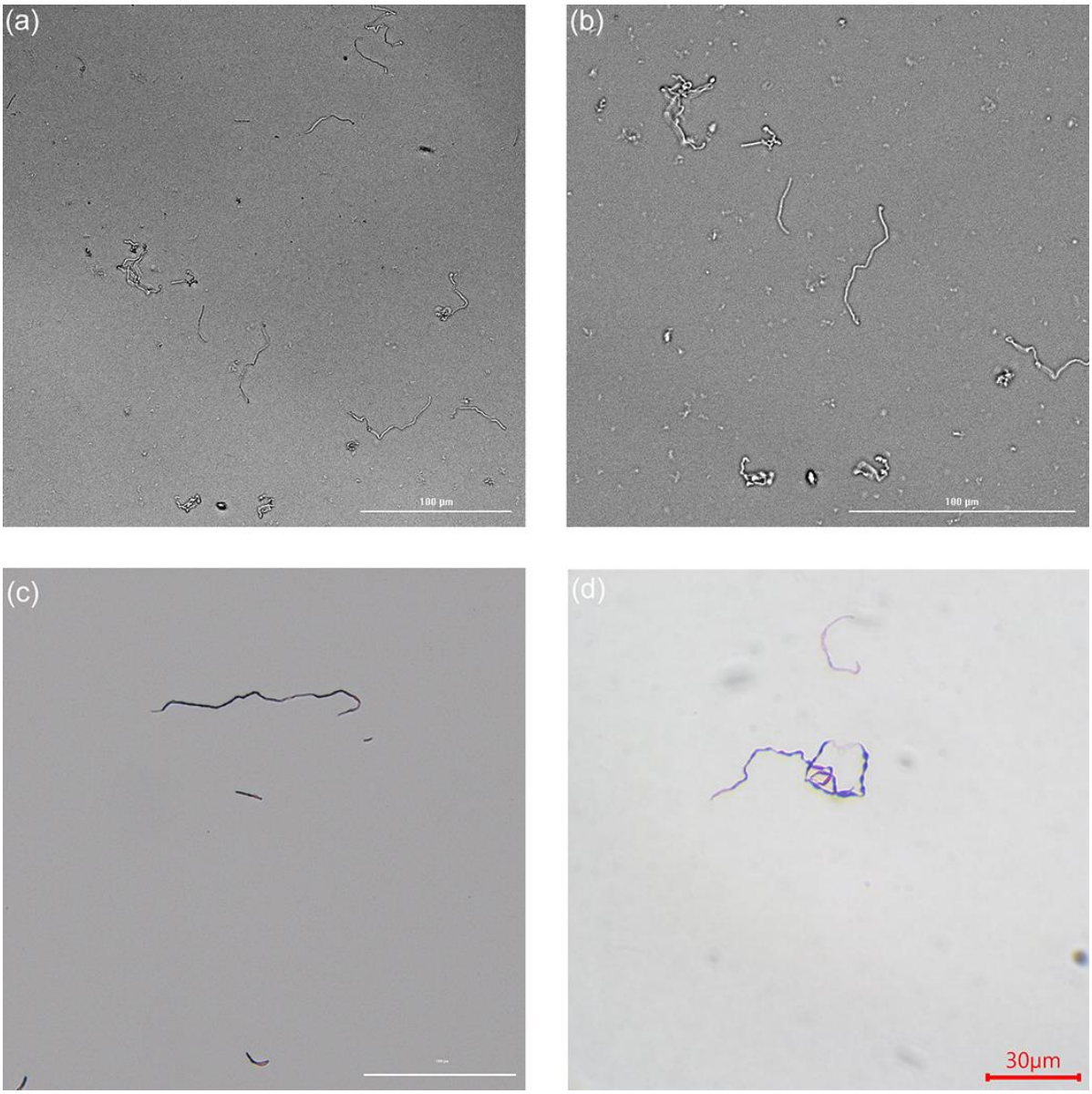

Figure S45. Images of *B. cereus* after 24 h incubation at 35 °C in Müller-Hinton broth containing 4% DMSO and **30 µM 1a** (>MIC) (starting point 5 x 10^5 CFU/mL). (a) Image obtained after 1:10 dilution in in Müller-Hinton broth using a BioTek Cytation 5 Cell Imaging Multi-Mode Reader (40x objective, Brightfield). Scale bar represents 100 µm. (b) Image obtained after 1:10 dilution in in Müller-Hinton broth using a BioTek Cytation 5 Cell Imaging Multi-Mode Reader (60x objective, Brightfield). Scale bar represents 100 µm. (c) Image obtained after Gram staining using a BioTek Cytation 5 Cell Imaging Multi-Mode Reader (40x objective, Brightfield). Scale bar represents 100 µm. (d) Image obtained after Gram staining using an Amscope Quintuple Plan Infinity Kohler Laboratory Trinocular Compound Microscope (100x oil objective, Brightfield). Scale bar represents 30 µm.

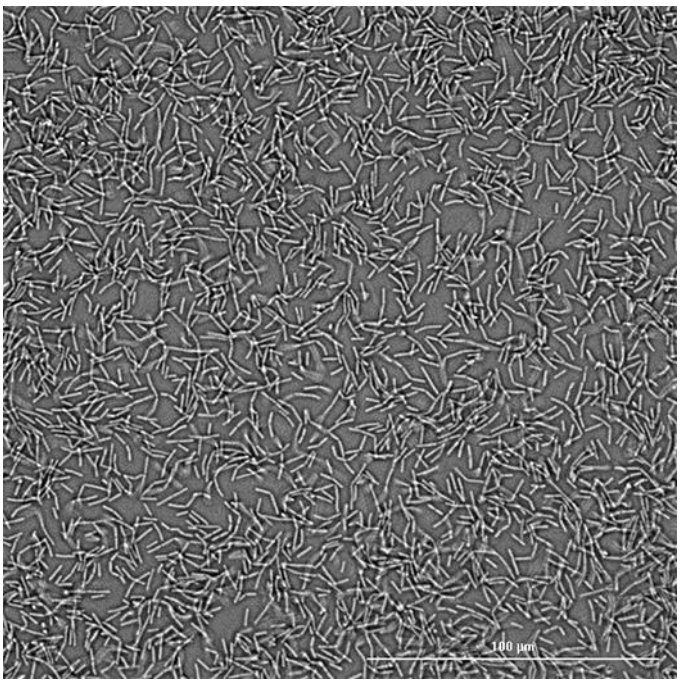

Figure S46. Images of *B. cereus* after 24 h incubation at 35 °C in Müller-Hinton broth containing 4% DMSO and **100 µM 1b** (starting point 5 x 10^5 CFU/mL). Image obtained after 1:10 dilution in in Müller-Hinton broth using a BioTek Cytation 5 Cell Imaging Multi-Mode Reader (60x objective, Brightfield). Scale bar represents 100 µm.

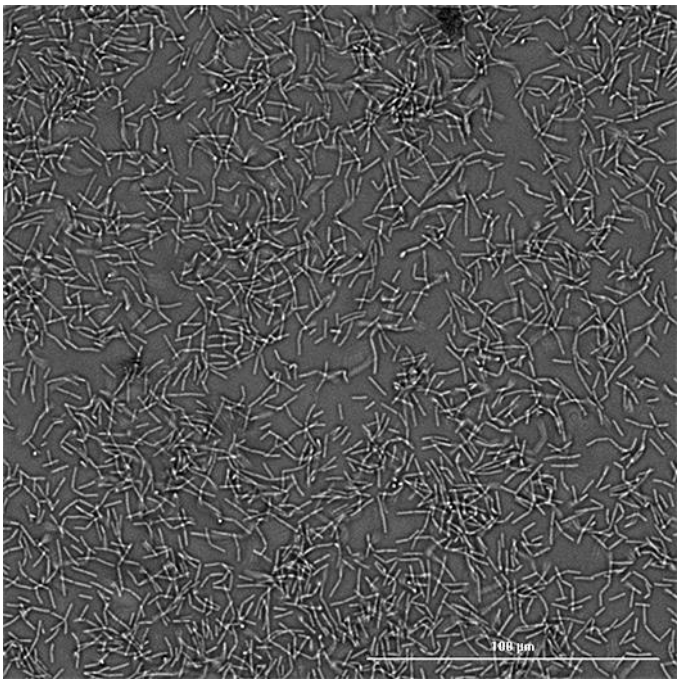

Figure S47. Images of *B. cereus* after 24 h incubation at 35 °C in Müller-Hinton broth containing 4% DMSO and **100 µM 2a** (starting point 5 x 10^5 CFU/mL). Image obtained after 1:10 dilution in in Müller-Hinton broth using a BioTek Cytation 5 Cell Imaging Multi-Mode Reader (60x objective, Brightfield). Scale bar represents 100 µm.

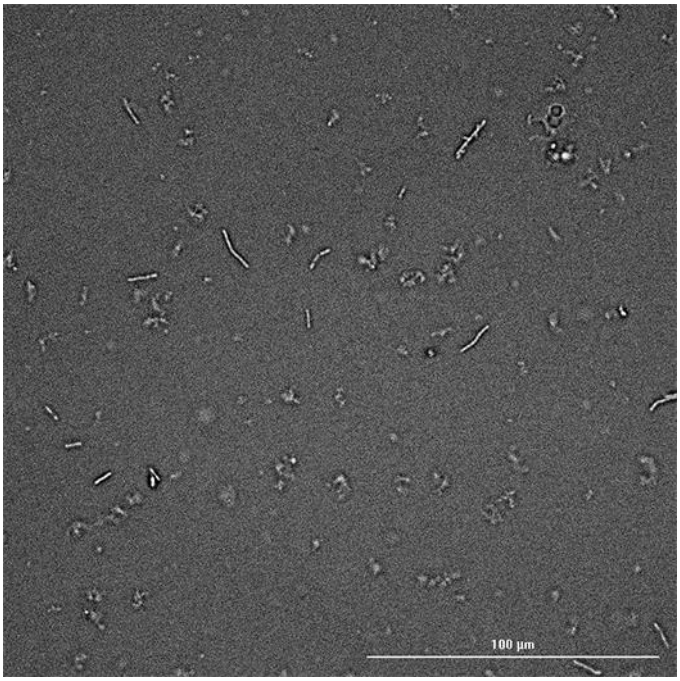

Figure S48. Images of *B. cereus* after 24 h incubation at 35 °C in Müller-Hinton broth containing 4% DMSO and **6.25 µM 2b** (starting point 5 x 10^5 CFU/mL). Image obtained after 1:10 dilution in in Müller-Hinton broth using a BioTek Cytation 5 Cell Imaging Multi-Mode Reader (60x objective, Brightfield). Scale bar represents 100 µm.

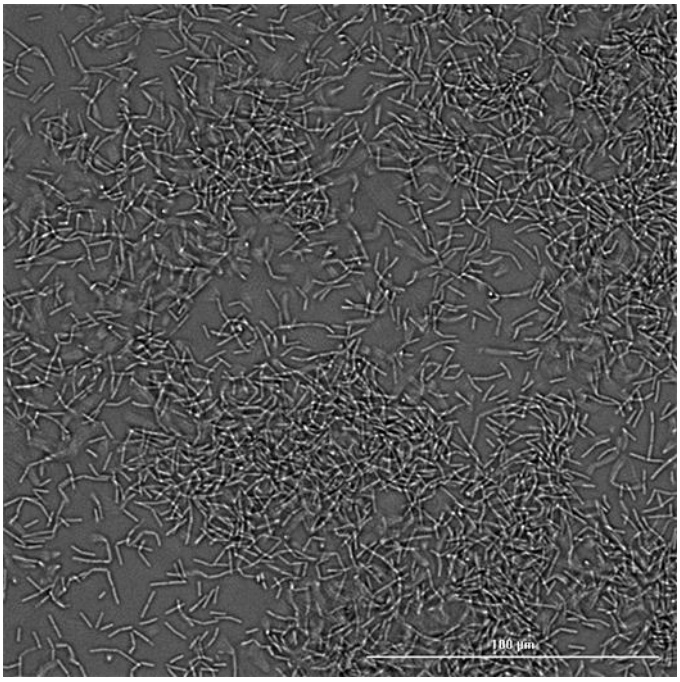

Figure S49. Images of *B. cereus* after 24 h incubation at 35 °C in Müller-Hinton broth containing 4% DMSO and **100 µM 18-crown-6** (starting point 5 x 10^5 CFU/mL). Image obtained after 1:10 dilution in in Müller-Hinton broth using a BioTek Cytation 5 Cell Imaging Multi-Mode Reader (60x objective, Brightfield). Scale bar represents 100 µm.

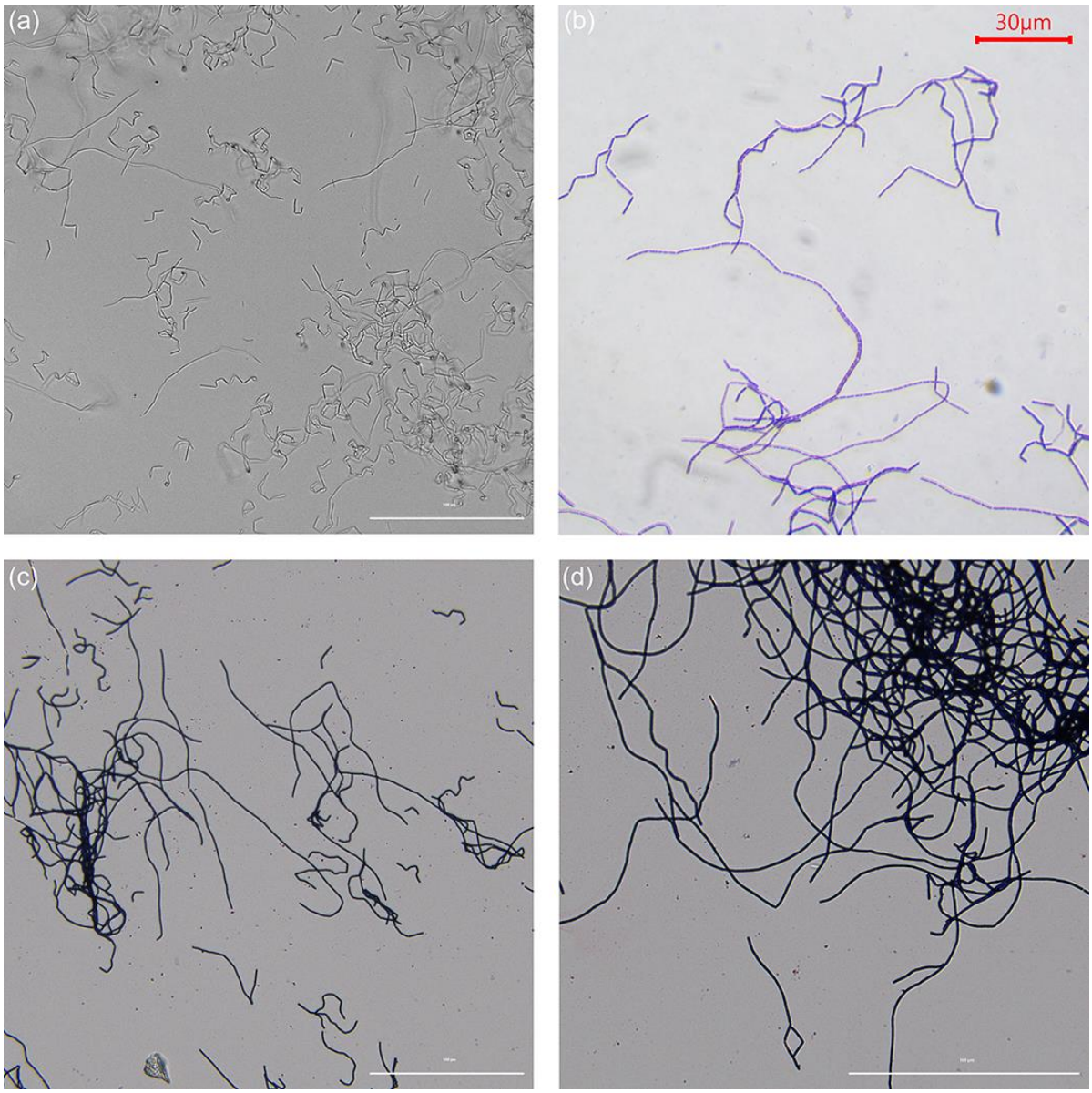

Figure S50. Images of *B. cereus* after 24 h incubation at 35 °C in Müller-Hinton broth containing 4% DMSO and **64 µM duramycin** (=MIC) (starting point 5 x 10^5 CFU/mL). (a) Image obtained after 1:10 dilution in in Müller-Hinton broth using a BioTek Cytation 5 Cell Imaging Multi-Mode Reader (40x objective, Brightfield). Scale bar represents 100 µm. (b) Image obtained after Gram staining using an Amscope Quintuple Plan Infinity Kohler Laboratory Trinocular Compound Microscope (100x oil objective, Brightfield). Scale bar represents 30 µm. (c) Image obtained after Gram staining using a BioTek Cytation 5 Cell Imaging Multi-Mode Reader (40x objective, Brightfield). Scale bar represents 100 µm. (d) Image obtained after Gram staining using a BioTek Cytation 5 Cell Imaging Multi-Mode Reader (60x objective, Brightfield). Scale bar represents 100 µm.

S8.5. Membrane depolarization assay

A membrane depolarization assay was performed using the dye $Disc_3(5)$ (3,3'-dipropylthiadicarbocyanine iodide), according to the method by te Winkel et al.[16] optimized for *B. cereus*. The MIC values for the negative control clindamycin (1 μg/mL) and positive control gramicidin (1.25 μM) against *B. cereus* were initially determined, as described above for the other compounds.

For each experiment, a small amount of the *B. cereus* glycerol stock was streaked onto a Müller-Hinton agar plate (Sigma-Aldrich #70191) and the agar plate was incubated for 18-24 hours at 35 ^{o}C. The obtained colonies were aseptically transferred into sterile cation-adjusted Müller-Hinton broth (Sigma-Aldrich #90922) and diluted to OD_{600} of 0.1. The bacteria were subsequently incubated at 35 ^{o}C until they reached mid-logarithmic phase (typically OD_{600} of 0.5-0.6). The cultures were then centrifuged at 3000 rpm for 5 mins and the pellets were re-suspended and diluted in Müller-Hinton broth supplemented with 0.5 mg/mL BSA (bovine serum albumin) to an OD_{600} of 0.1.

For the measurements at 1xMIC and 1.6xMIC, 172 μL of the diluted cells were transferred to a fluorescence 96-well plate (sterile, black, flat-bottom, polystyrene microplate from Brand #7816668) and the fluorescence was followed for 3 minutes to obtain values for background fluorescence. After obtaining a baseline, 8 μL $DiSC_3(5)$ dissolved in DMSO was added to each well to a final concentration of 1 μM $DiSC_3(5)$ and 4% DMSO, and the fluorescence intensity was measured for another 15 minutes. At this point, 20 μL of stock solutions **1a** and control antibiotics (dissolved to 10x the desired concentration in Müller-Hinton broth with 4% DMSO) were added and the fluorescence was measured for 1 hour. All fluorescence measurements were preformed using a BioTek Cytation 5 Cell Imaging Multi-Mode Reader (35 °C, excitation at 610 nm and emission at 660 nm, time intervals of 23 seconds, orbital shaking (5 seconds at 548 rpm (2 mm) before each measurement). As a control, the measurements were also conducted on Müller-Hinton broth supplemented with 0.5 mg/mL BSA (bovine serum albumin) that did not contain any bacteria.

For the measurements at 10xMIC, the procedure was altered due to the limited solubility of the crown ether compounds. In this case, 193 μL of the diluted cells were transferred to a fluorescence 96-well plate (sterile, black, flat-bottom, polystyrene microplate from Brand #7816668) and the fluorescence was followed for 3 minutes to obtain values for background fluorescence. After obtaining a baseline, 2 μL $DiSC_3(5)$ dissolved in DMSO was added to each well to a final concentration of 1 μM $DiSC_3(5)$ and 1% DMSO, and the fluorescence intensity was measured for another 15 minutes. At this point, 5 μL of stock DMSO solutions of **1a** and control antibiotics were added and the fluorescence was measured for 1 hour. All fluorescence measurements were preformed using a BioTek Cytation 5 Cell Imaging Multi-Mode Reader (35 °C, excitation at 610 nm and emission at 660 nm, time intervals of 23 seconds, orbital shaking (5 seconds at 548 rpm (2 mm) before each measurement). As a control, the measurements were also conducted on Müller-Hinton broth supplemented with 0.5 mg/mL BSA (bovine serum albumin) that did not contain any bacteria.

To convert the raw fluorescence data to fraction of $Disc_3(5)$ released, we used the fact that $Disc_3(5)$ accumulates into polarized cells and self-quenches. Therefore, the highest possible fluorescence that can be measured, should correspond to the values obtained for the control experiments without bacteria. In these control experiment, the procedure described above (3 minutes background fluorescence, followed by addition of $Disc_3(5)$, followed by the addition of compound) was repeated using Müller-Hinton broth supplemented with 0.5 mg/mL BSA (bovine serum albumin) that did not contain any bacteria. By calculating the fraction Disc3(5) release this way, any potential artifacts due to differences in DMSO content, slow stirring or other interferences can be removed. Full

depolarization should correspond to a fraction $Disc_3(5)$ release of 1.0, as is seen for the positive control gramicidin. Results are shown in **Figure S51** - **Figure S53**.

$$fraction\ \ Disc_3(5)\ \ release = \frac{Fluorescence\ intensity\ in\ the\ presence\ of\ B.cereus}{Fluorescence\ intensity\ in\ the\ absence\ of\ B.cereus}$$

For the imaging, the membrane depolarization assay described above was stopped after 15 minutes or 1 hour, and 2 µL of the bacterial solution was transferred to a microscopy cover glass and a 1% agarose gel was put on top of the solution to immobilize the bacteria. Images were taken using a BioTek Cytation 5 Cell Imaging Multi-Mode Reader, with the Texas Red filter set for fluorescence images. All fluorescence images were taken using the same exposure settings (LED intensity = 7, Shutter Speed MS = 1206, Camera Gain = 18). Overlays were generated using the software accompanying the BioTek Cytation 5 Cell Imaging Multi-Mode Reader. Results are shown in **Figure S54** - **Figure S59**.

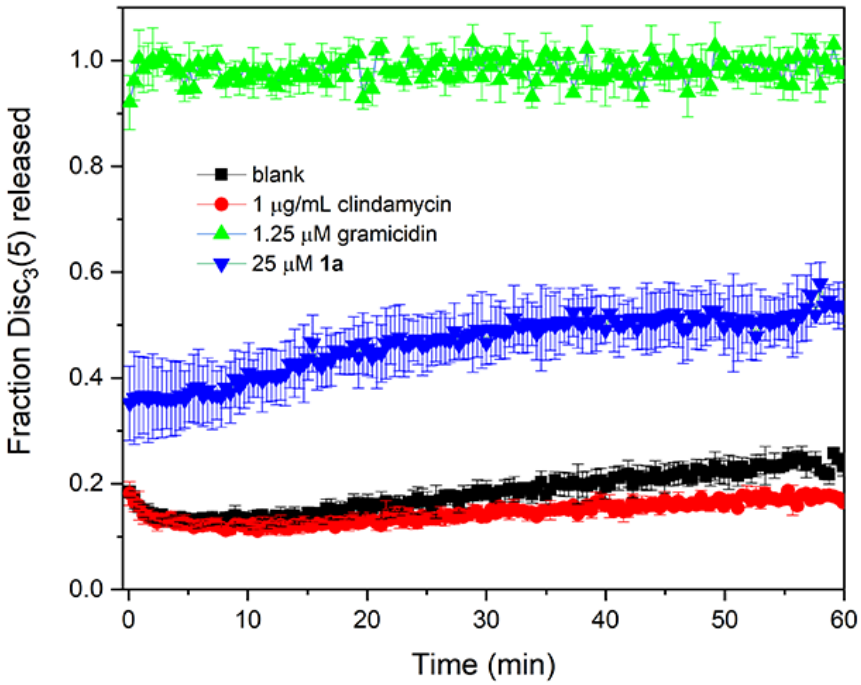

Figure S51. Kinetic trace of the membrane depolarization of *B. cereus* by 1xMIC of clindamycin (negative control), gramicidin (positive control) and **1a**, using $Disc_3(5)$ as the voltage-dependent fluorophore.

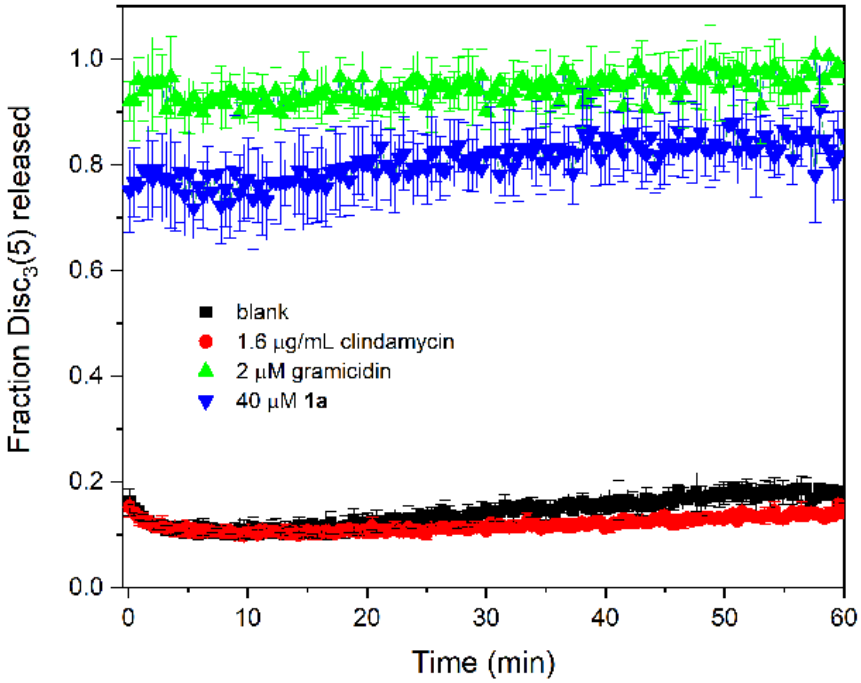

Figure S52. Kinetic trace of the membrane depolarization of *B. cereus* by 1.6xMIC of clindamycin (negative control), gramicidin (positive control) and **1a**, using $Disc_3(5)$ as the voltage-dependent fluorophore.

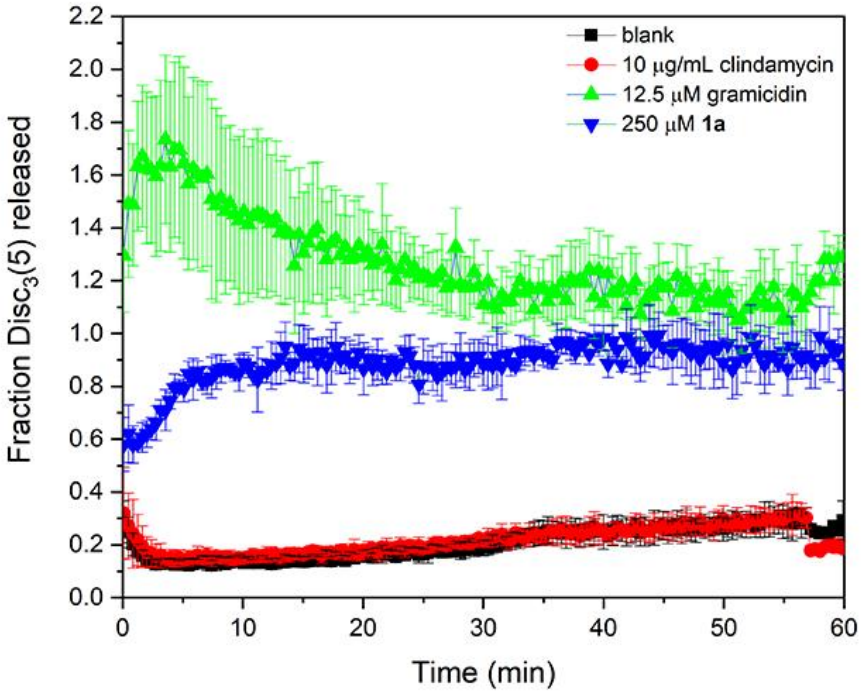

Figure S53. Kinetic trace of the membrane depolarization of *B. cereus* by 10xMIC of clindamycin (negative control), gramicidin (positive control) and **1a**, using $Disc_3(5)$ as the voltage-dependent fluorophore.

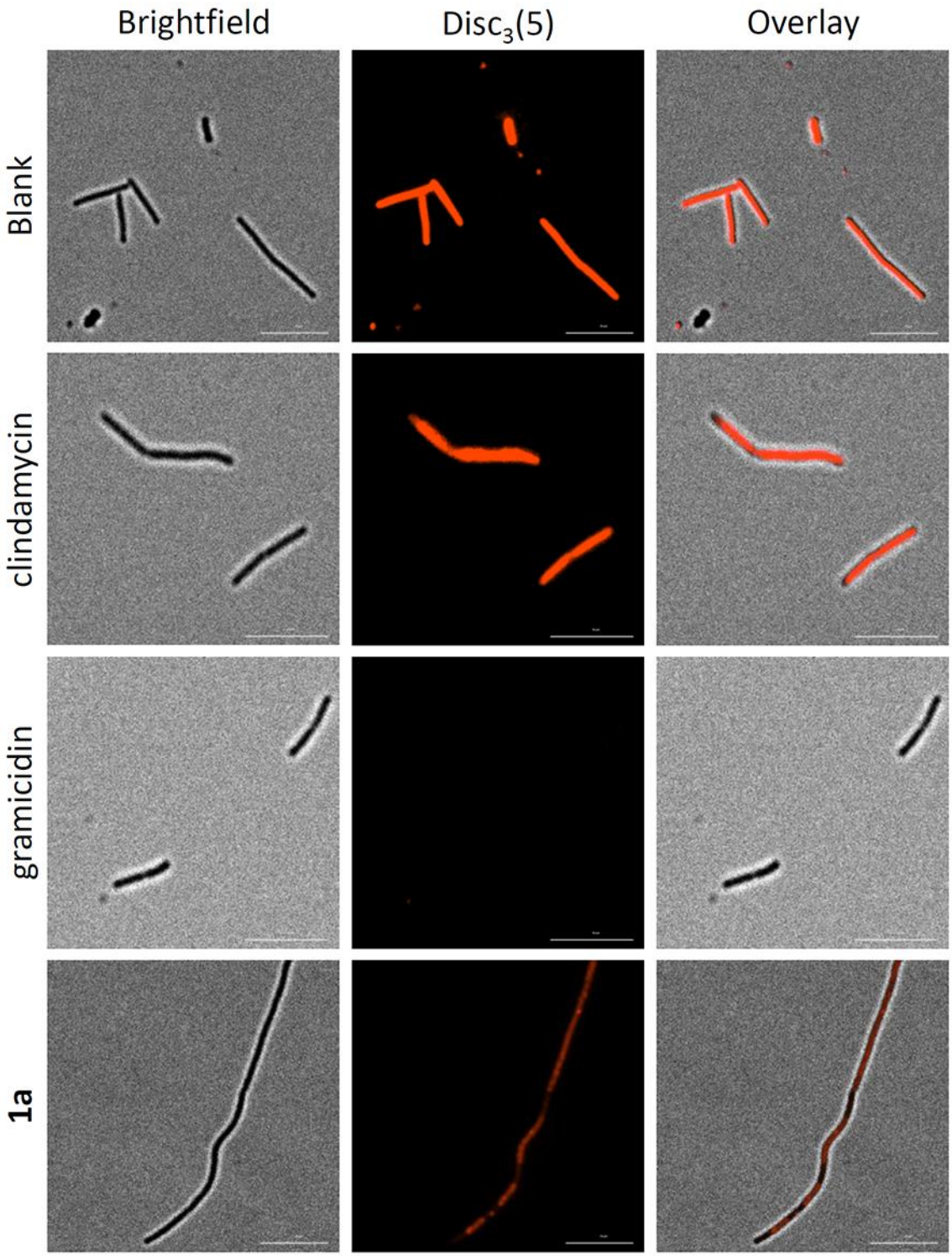

Figure S54. Images of membrane depolarization of *B. cereus* by 1xMIC of clindamycin (negative control), gramicidin (positive control) and **1a**, using $Disc_3(5)$ as the voltage-dependent fluorophore. The *B. cereus* cells were incubated for 15 minutes with 4% DMSO (blank), 1 µg/mL clindamycin, 1.25 µM gramicidin, or 25 µM **1a**. Absence of fluorescence indicates that the cells are depolarized. Scale bars represent 10 µm.

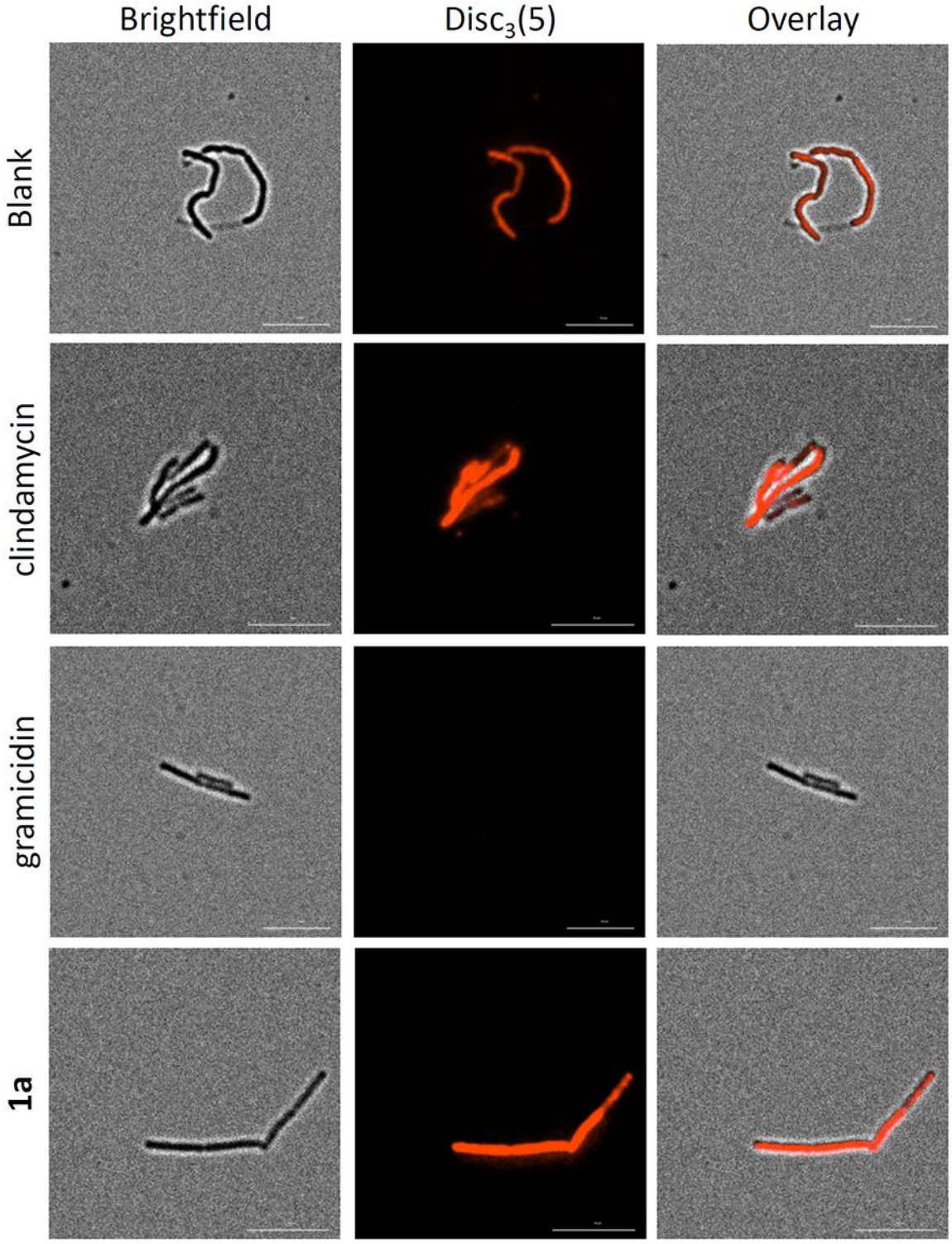

Figure S55. Images of membrane depolarization of *B. cereus* by 1xMIC of clindamycin (negative control), gramicidin (positive control) and **1a**, using $Disc_3(5)$ as the voltage-dependent fluorophore. The *B. cereus* cells were incubated for 1 hour with 4% DMSO (blank), 1 µg/mL clindamycin, 1.25 µM gramicidin, or 25 µM **1a**. Absence of fluorescence indicates that the cells are depolarized. Scale bars represent 10 µm.

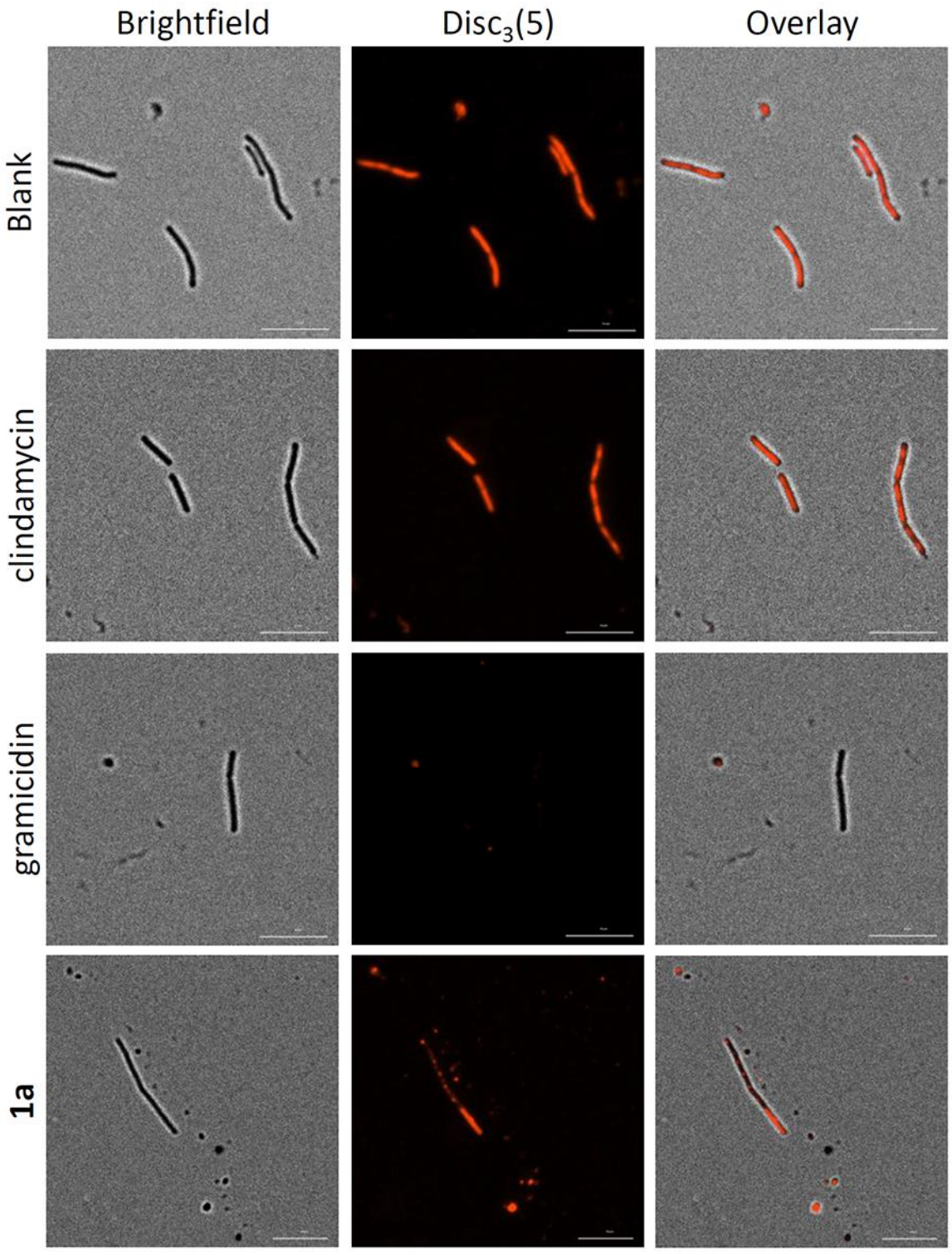

Figure S56. Images of membrane depolarization of *B. cereus* by 1.6xMIC of clindamycin (negative control), gramicidin (positive control) and **1a**, using $Disc_3(5)$ as the voltage-dependent fluorophore. The *B. cereus* cells were incubated for 15 minutes with 4% DMSO (blank), 1.6 µg/mL clindamycin, 2 µM gramicidin, or 40 µM **1a**. Absence of fluorescence indicates that the cells are depolarized. Scale bars represent 10 µm.

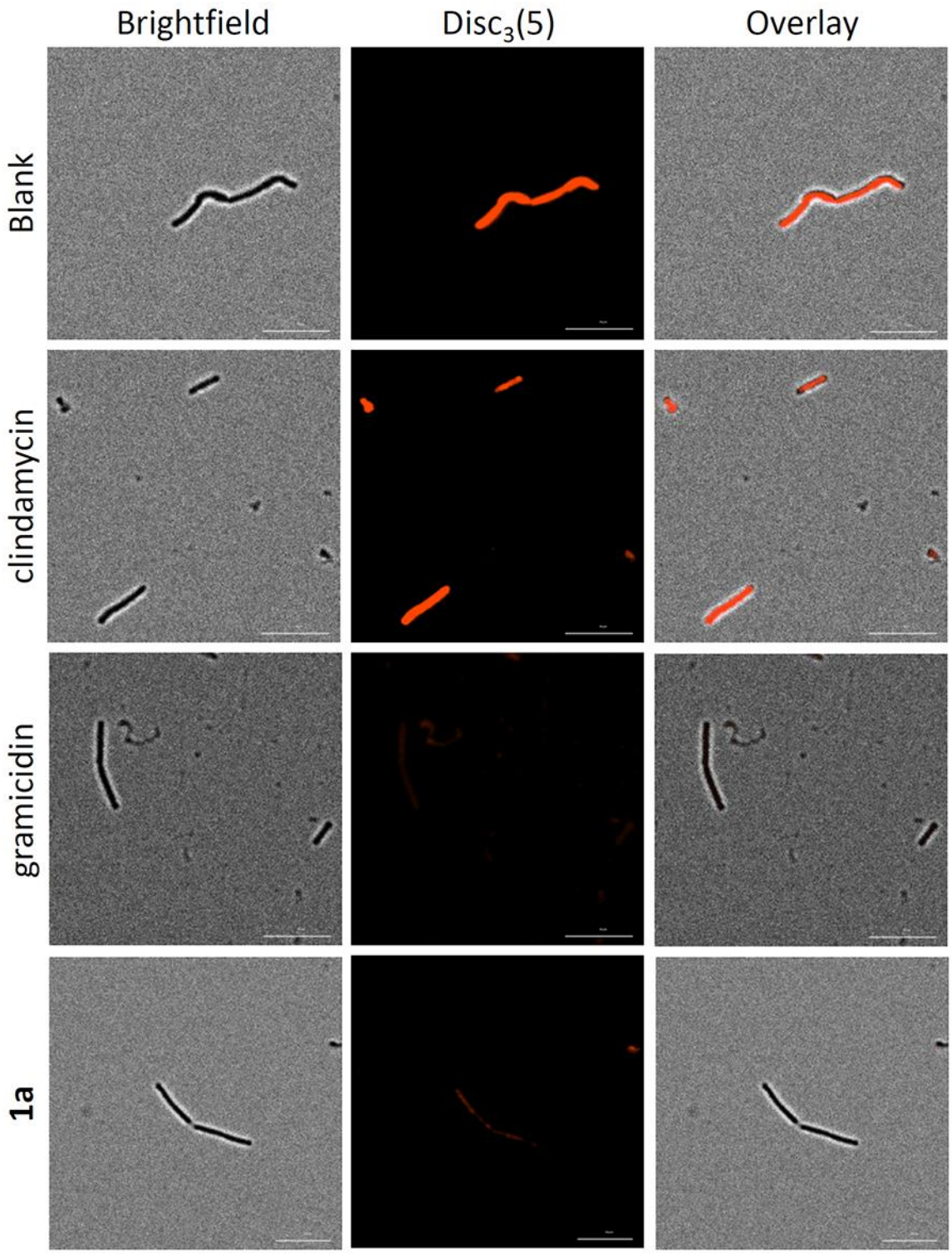

Figure S57. Images of membrane depolarization of *B. cereus* by 1.6xMIC of clindamycin (negative control), gramicidin (positive control) and **1a**, using $Disc_3(5)$ as the voltage-dependent fluorophore. The *B. cereus* cells were incubated for 1 hour with 4% DMSO (blank), 1.6 µg/mL clindamycin, 2 µM gramicidin, or 40 µM **1a**. Absence of fluorescence indicates that the cells are depolarized. Scale bars represent 10 µm.

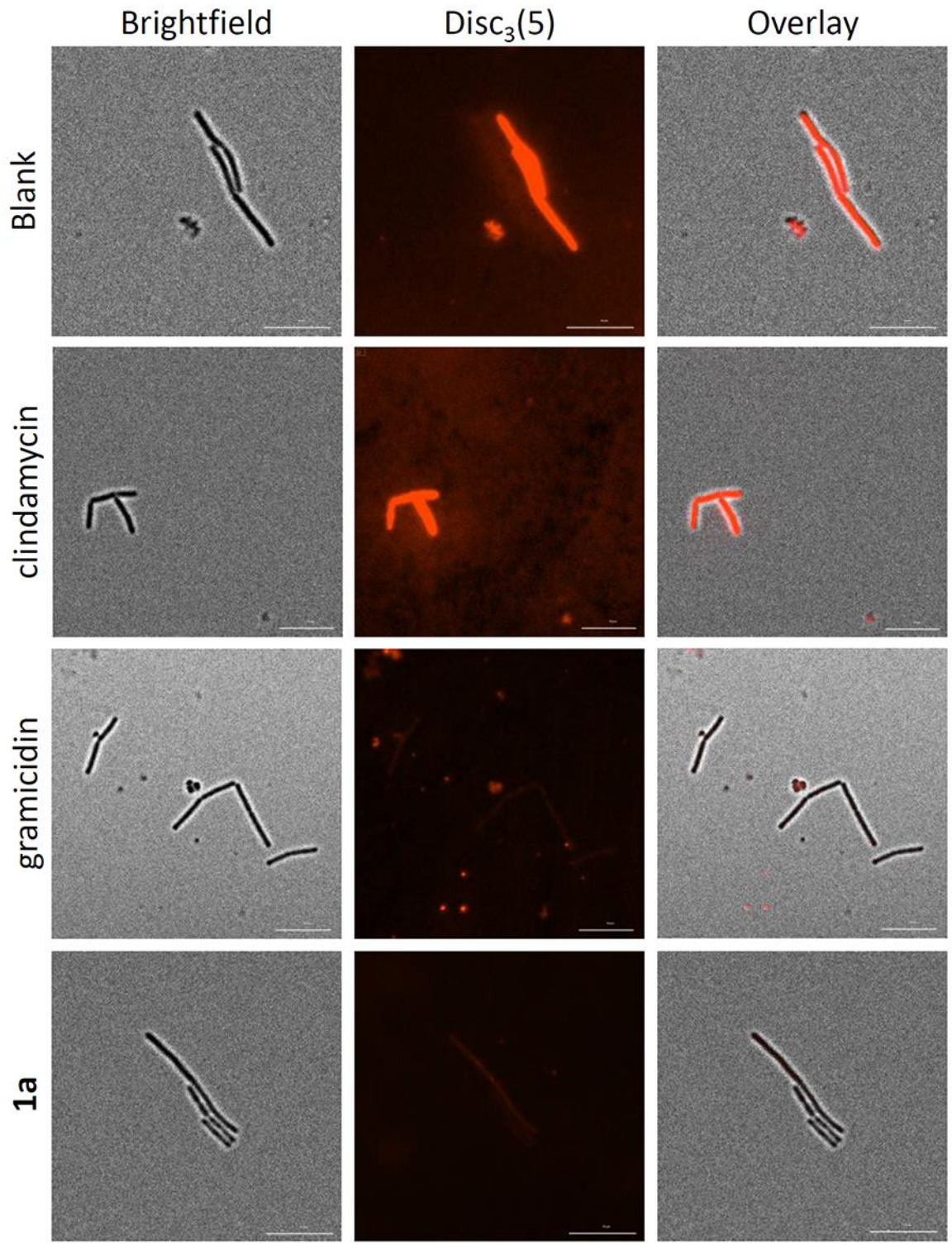

Figure S58. Images of membrane depolarization of *B. cereus* by 10xMIC of clindamycin (negative control), gramicidin (positive control) and **1a**, using $Disc_3(5)$ as the voltage-dependent fluorophore. The *B. cereus* cells were incubated for 15 minutes with 4% DMSO (blank), 10 µg/mL clindamycin, 12.5 µM gramicidin, or 250 µM **1a**. Absence of fluorescence indicates that the cells are depolarized. Scale bars represent 10 µm.

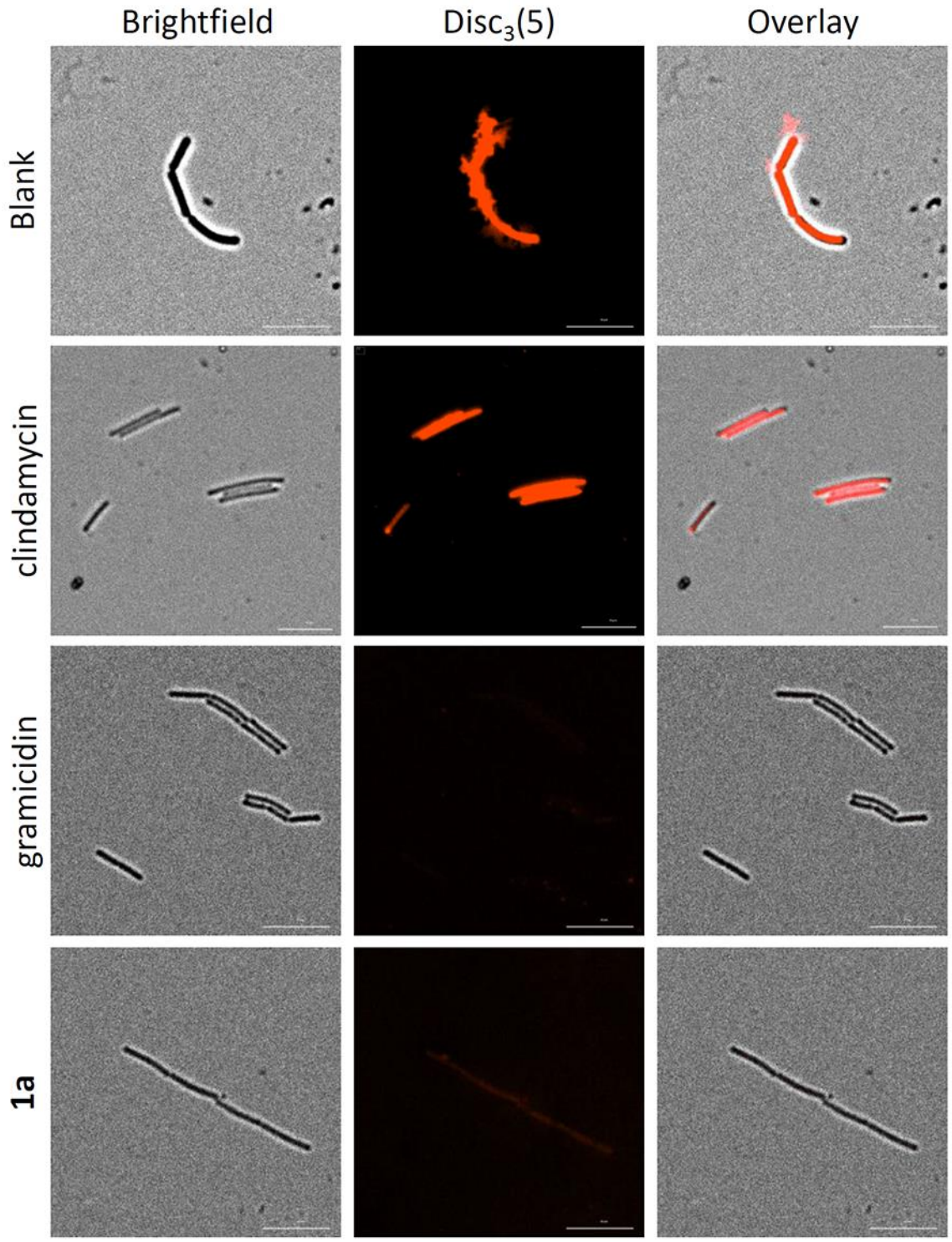

Figure S59. Images of membrane depolarization of *B. cereus* by 10xMIC of clindamycin (negative control), gramicidin (positive control) and **1a**, using $Disc_3(5)$ as the voltage-dependent fluorophore. The *B. cereus* cells were incubated for 1 hour with 4% DMSO (blank), 10 µg/mL clindamycin, 12.5 µM gramicidin, or 250 µM **1a**. Absence of fluorescence indicates that the cells are depolarized. Scale bars represent 10 µm.

S9. References

1. Olsen, G.; Ulstrup, J.; Chi, Q., Crown-Ether Derived Graphene Hybrid Composite for Membrane-Free Potentiometric Sensing of Alkali Metal Ions. *ACS Applied Materials & Interfaces* **2016,** *8* (1), 37-41.
2. Brynn Hibbert, D.; Thordarson, P., The death of the Job plot, transparency, open science and online tools, uncertainty estimation methods and other developments in supramolecular chemistry data analysis. *Chem. Commun.* **2016,** *52* (87), 12792-12805.
3. Boon, J. M.; Smith, B. D., Facilitated Phospholipid Translocation across Vesicle Membranes Using Low-Molecular-Weight Synthetic Flippases. *J. Am. Chem. Soc.* **1999,** *121* (50), 11924-11925.
4. Murzyn, K.; Róg, T.; Pasenkiewicz-Gierula, M., Phosphatidylethanolamine-phosphatidylglycerol bilayer as a model of the inner bacterial membrane. *Biophys. J.* **2005,** *88* (2), 1091-1103.
5. Matsuzaki, K.; Murase, O.; Fujii, N.; Miyajima, K., An Antimicrobial Peptide, Magainin 2, Induced Rapid Flip-Flop of Phospholipids Coupled with Pore Formation and Peptide Translocation. *Biochemistry* **1996,** *35* (35), 11361-11368.
6. Nahaie, M.; Goodfellow, M.; Minnikin, D.; Hajek, V., Polar lipid and isoprenoid quinone composition in the classification of Staphylococcus. *Microbiology* **1984,** *130* (9), 2427-2437.
7. Randle, C. L.; Albro, P. W.; Dittmer, J. C., The phosphoglyceride composition of gram-negative bacteria and the changes in composition during growth. *Biochim. Biophys. Acta, Lipids Lipid Metab.* **1969,** *187* (2), 214-220.
8. Bos, M. P.; Tommassen, J., Biogenesis of the Gram-negative bacterial outer membrane. *Curr. Opin. Microbiol.* **2004,** *7* (6), 610-616.
9. Haque, M. A.; Russell, N. J., Strains of Bacillus cereus vary in the phenotypic adaptation of their membrane lipid composition in response to low water activity, reduced temperature and growth in rice starch. *Microbiology* **2004,** *150* (5), 1397-1404.
10. CLSI, *Methods for dilution antimicrobial susceptibility tests for bacteria that grow aerobically; approved standard*. 11th ed. CLSI standard M07 ed.; Clinical and Laboratory Standards Institute: Wayne, PA, 2018; Vol. 32.
11. Märki, F.; Hänni, E.; Fredenhagen, A.; van Oostrum, J., Mode of action of the lanthionine-containing peptide antibiotics duramycin, duramycin B and C, and cinnamycin as indirect inhibitors of phospholipase A2. *Biochem. Pharmacol.* **1991,** *42* (10), 2027-2035.
12. Iwamoto, K.; Hayakawa, T.; Murate, M.; Makino, A.; Ito, K.; Fujisawa, T.; Kobayashi, T., Curvature-dependent recognition of ethanolamine phospholipids by duramycin and cinnamycin. *Biophys. J.* **2007,** *93* (5), 1608-1619.
13. Baquero, F.; Levin, B. R., Proximate and ultimate causes of the bactericidal action of antibiotics. *Nat. Rev. Microbiol.* **2020,** *19*, 123-132.
14. Mahlapuu, M.; Håkansson, J.; Ringstad, L.; Björn, C., Antimicrobial Peptides: An Emerging Category of Therapeutic Agents. *Front. Cell. Infect. Microbiol.* **2016,** *6* (194).
15. CLSI, *Methods for determining bactericidal activity of antimicrobial agents; approved guideline*. CLSI document M26-A ed.; Clinical and Laboratory Standards Institute: Wayne, PA, 1999; Vol. 32.
16. te Winkel, J. D.; Gray, D. A.; Seistrup, K. H.; Hamoen, L. W.; Strahl, H., Analysis of Antimicrobial-Triggered Membrane Depolarization Using Voltage Sensitive Dyes. *Front. Cell Dev. Biol.* **2016,** *4* (29).